Exploring Urban Air Mobility to Comprehend Urban Air Quality

Xander van Hal

Delft University of Technology

TU Delft Delft University of Technology

Exploring Urban Air Mobility to Comprehend Urban Air Quality

by

Xander van Hal

in partial fulfillment of the requirements for the degree of

Master of Science
in Aerospace Engineering

at the Delft University of Technology,
to be defended publicly on Thursday, 27 June 2024, at 14.30.

Student number:	5598788
Project duration:	4 September 2023 – 27 June 2024
Thesis committee:	
Chair:	Prof. dr. ir. M. Snellen
Supervisor:	Dr. I.C. Dedoussi
External examiner:	Dr. F. De Domenico

TU Delft Delft University of Technology

PREFACE

This MSc thesis marks the end of my master in Aerospace Engineering at TU Delft. Since my childhood, I have been fascinated by the world of aviation. During my bachelor in Advanced Technology at the University of Twente, I followed a minor in aviation and by then I knew I wanted to study Aerospace Engineering. Alongside the courses of my Flight Performance & Propulsion track, I followed some elective courses on the noise & climate effects of aircraft. This intrigued me and therefore I decided to do my MSc thesis at the Aircraft Noise & Climate Effects group in Delft.

During my MSc thesis, I have learned a lot about researching air quality and making it more tangible. Through the ImAFUSA project, developing a framework for Urban Air Mobility in our society, I learned a lot about other aspects of Urban Air Mobility as well. It was great to be part of this project and I sincerely hope it will make a positive impact in the future.

Firstly, I would like to thank my supervisor Irene Dedoussi for her great guidance throughout my thesis. It was a pleasure working with you. I would also like to thank the rest of the Aircraft Noise & Climate Effects group, especially Amy, Mirjam and Marloes, for helping me out with setting up the experiment and processing the results.

Secondly, I would like to thank the project team of ImAFUSA. It was a great pleasure to work with all of you. A special thank you goes to Dimitris and Yiannis from the Municipality of Aigaleo who helped me carry out the experiment successfully. The hospitality in Aigaleo has been amazing.

Finally, I would like to thank all my friends and family. I want to thank my parents and sister for their help and support throughout my study time. Moreover, a big thank you to all my great friends; some still from high school, others who I met during my study time in Enschede and last but not least the ones I met while obtaining my master's degree in Delft.

Xander van Hal
Delft, June 2024

SUMMARY

Breathing in polluted air can lead to several health problems, which is why it should be monitored carefully. Air quality is typically measured using expensive, fixed measurement stations. It is thus hard to monitor the air quality in a certain area both horizontally and vertically. Drones, a type of Urban Air Mobility, can help with this by attaching air quality sensors to them. The overall goal of this research is to find out what additional information Urban Air Mobility can provide to urban air quality monitoring. We first look into the setup of the experiment and how an experiment can be effectively conducted. Hereafter, we look at the results from this experiment. Finally, possible environmental impacts of this application are considered.

We made use of a Sniffer4D Mini 2 air quality sensor box, capable of measuring CO, NO_2, O_3, SO_2, $PM_{2.5}$ and PM_{10}. It has previously been used to measure urban air quality successfully and is adaptable to changing environmental conditions. This sensor box is placed on top of the DJI Mavic 3 Enterprise drone. The setup can fly programmed paths making use of Litchi software. Validation experiments have shown that the sensors respond within 5 seconds to a change in air quality. The temperature profile and wind estimation obtained high correlations with a fixed monitoring station. The absolute values measured do differ with a fixed measurement station due to several environmental factors and because we compare an average with a single measurement.

Experiments have been conducted in a park in Aigaleo (Athens), located adjacent to a busy road. Firstly, point measurements were carried out at five different locations in the park, varying in distance from the busy road. These were purely vertical measurements between 0 and 120 m. Secondly, continuous measurements were executed in which the drone flew along programmed locations and elevations. At each location (separated by 50 m horizontal distance), all elevations between 35 and 120 m were examined. All measurements were carried out on two days in February 2024 between roughly 10.00 and 17.00. The times were chosen based on earlier research showing high variability in air quality; traffic related pollutants increased during the morning and evening rush. In May 2024, a number of extra air quality measurements were taken during a soundwalk experiment on drone noise.

Results showed a variation in air quality relative to time of of day, month of year, altitude and horizontal distance from the busy road. From the continuous measurements, 3D interpolations were created, showing similar results as the fixed measurements. It was found that the temperature had greatly influenced the readings of the sensors. Due to the high number of variables, isolating the effect of the wind speed and its direction proved challenging. We found that the NO_2 and CO concentration are directly determined by the presence of traffic. Although the SO_2 concentration is affected by traffic, others sources also affect this pollutant. The O_3 concentration increases in the afternoon due to the reaction under sunlight. Moreover, there is no specific location where the O_3 concentration is highest because of its indirect formation. Higher concentrations of O_3 where observed in May compared to February. The concentrations of $PM_{2.5}$ and PM_{10} are quite constant throughout the day, but do have a high variability with altitude. Areas with higher concentrations of particulate matter can be found, resulting from its multitude of sources. In May, the measured $PM_{2.5}$ and PM_{10} concentrations were lower than in February as a result of less biomass burning and changing meteorological conditions.

The environmental impact from energy usage of a use case in which the air quality of Aigaleo (6 km^2) would be monitored has been calculated as well. If one would monitor this area with similar parameters to the continuous measurements, twice a day for one year, it would result in an energy usage of 12 260 kWh. Given the energy production in Athens, this results in a total environmental impact of 8 543 kg $CO_{2,e}$ emission.

All in all, this research has shown how air quality can be measured with the use of a drone in vertical and horizontal directions. The time of day, month of year, altitude and horizontal distance from a busy road influenced the pollutant concentrations at the measurement locations. 3D interpolations have been created as well, showing directly where the areas with higher concentrations of air pollutants are located.

CONTENTS

List of Figures

List of Tables

NOMENCLATURE

Abbreviations

Symbol	Description
BC	Black carbon
CH_4	Methane
CO	Carbon monoxide
CO_2	Carbon dioxide
$CO_{2,e}$	Carbon dioxide equivalent
H_2S	Hydrogen sulphide
NH_3	Ammonia
NO_x	Nitrogen oxides (NO & NO_2)
NO	Nitrogen monoxide
NO_2	Nitrogen dioxide
N_2O	Nitrous oxide
OH	Hydroxide
O	Oxide
O_3	Ozone
PM_x	Particulate matter with aerodynamic size smaller than x μm
SO_2	Sulphur dioxide
VOCs	Volatile Organic Compounds
CI	Confidence Interval
CRPS	Continuous Ranked Probability Score
GIS	Geographical Information System
LCA	Life Cycle Assessment
LDSA	Lung-deposited Surface Area
MTOW	Maximum Take-off Weight
R	Pearson Correlation Coefficient
UAM	Urban Air Mobility
UAV	Unmanned Aerial Vehicle

1

INTRODUCTION

1.1. MOTIVATION

Air pollution can cause harm to all living species and the environment worldwide. Presently, air pollution causes approximately seven million people to die prematurely every year [5]. It is therefore important to measure air quality and reduce urban air pollution if the air quality is insufficient.

Monks et al. [6] defined air quality as "*a measure of the concentrations of gaseous pollutants and size or number of particulate matter*". In short, it is the way to measure pollution in the air. By gaseous pollutants, one refers to CO, NO_2, O_3 and SO_2. Particulate matter is defined by size; $PM_{2.5}$ and PM_{10} have aerodynamic sizes of less than than 2.5 and 10 μm, respectively. The combination of gaseous pollutants and particulate matter defines the air quality. They can originate directly from pollution sites or form because of chemical reactions in the atmosphere [7]. NO_2, O_3 and $PM_{2.5}$ have the greatest impact on air quality.

Measuring air pollution can be done in several ways [8]. Firstly, one can use ground-monitoring stations. These stations have good temporal resolution, but are expensive and have limited spatial resolution as only one fixed place can be measured. Secondly, satellites can be used to measure air pollution; however, these often have bad temporal resolution. To gain a better understanding of air quality, Urban Air Mobility (UAM) can be equipped. A drone can fly over urban areas while measuring air quality. Data with good temporal as well as spatial resolution can be generated if the measurements are carried out in an efficient and accurate manner.

Previous research on measuring urban air quality with drones has mainly focused on particulate matter. Typically, lower concentrations of air pollutants are measured when further away from a polluting source. Also, higher concentrations were measured during rush hour in the morning and evening [9] and a higher wind speed led to dispersion of air pollutants [10]. Several research [9, 11–14] focused on the vertical variation of air quality in the first hundreds of meters altitude. Particulate matter concentrations were typically highest near the ground, whereas gaseous pollutants concentrated at higher altitudes. Non-linear variations with altitude of these gaseous pollutants were found as well. Aside from this, a number of environmental and meteorological conditions impact the pollutant concentrations [13, 14].

The consulted research also found that variations in temperature, humidity and wind affect the readings by the sensors resulting in less accurate data. This can partially be counteracted by placing the sensors further away from the downwash of the drone [10, 15]. Commercial air quality sensor boxes, which typically have integrated solutions for these changes in temperature, humidity and wind, will also aid in obtaining more accurate results [9, 13, 14].

Although most UAM concepts nowadays are driven by a fully electric power train, there might still be indirect emissions [16]. For example, the generation of the electricity used will result in emissions. Moreover, one can look at the whole life cycle of a drone (from production to recycling); a life cycle assessment (LCA) can analyse the impact of this [17, 18]. Another factor to look at is noise. Due to the scope of this research, we will only be looking at the environmental impact through electricity usage.

Overall, we want to find out how air quality measurements can be taken using drones and which setup is most suitable for mobile and accurate measurements. Moreover, the goal is to find out what results can be

obtained once measurements have been carried out. Finally we want to look at the environmental impact this application has.

This research has been carried out as part of the ImAFUSA EU project, which focuses on evaluating factors that influence citizens' acceptance of UAM [19]. The monitoring of urban air quality with the use of drones is a use case of UAM and therefore part of this project. Moreover, the environmental impact of UAM is evaluated in the project and therefore touched upon here as well.

1.2. RESEARCH OBJECTIVE AND QUESTIONS

Drones can aid in gaining more information about air quality, as they can constantly monitor air quality in both vertical as well as horizontal direction. However, several challenges are faced.

The sensors to measure air quality are affected by a number of environmental factors such as temperature and wind. Therefore, placing these sensors on a drone, will result in additional challenges to be faced. A setup should thus be selected carefully to accurately measure air pollution.

Aside from this, previous research has shown how that the air quality is influenced by a number of factors, including the presence of sun light, temperature and wind. Mixed conclusions are obtained. More research will thus be needed to find the effect of these environmental factors.

All in all, to test the viability of drones to measure urban air quality, an experiment should be designed carefully to test a new setup. The environmental impact should be touched upon as well, as this is often forgotten in other research.

The main research question is formulated as follows: '**How can Urban Air Mobility provide meaningful information about urban air pollution?**'. To answer this question, several sub-questions have been formulated. These are listed below. Per sub-question a short explanation is given.

1. **Which configuration of drone and air quality sensor box can be used to accurately measure urban air pollution?**
   Based on accuracy, feasibility and budget a configuration will be chosen which can be used to measure urban air pollution in this step.
2. **How can an experiment be effectively conducted to measure urban air pollution given a drone and air quality sensor box configuration?**
   The design of the experiment will be discussed here to accurately measure urban air pollution. Given limited flight time of the drone, measurements will be carried out at several locations and varying elevations to obtain good spatial resolution in vertical and horizontal directions.
3. **Which (additional) information can Urban Air Mobility provide about urban air pollution?**
   Answering this question will aid in how the results from measuring air quality with UAM can be used to gain better understanding of urban air pollution in both vertical as well as horizontal direction. Several environmental factors will impact the recordings, which should be accounted for. Finally, 3D interpolations of the measurements are made to create a better understanding of the dispersion of pollutants.
4. **What is the environmental impact when measuring air quality with Urban Air Mobility?**
   Answering this question will help to better understand how UAM can negatively impact society. Methods on how this environmental impact can be quantified will be looked into, for example through a LCA and noise measurements.

1.3. OUTLINE

Next, chapter 2 about the research article follows, which gives an overview of the whole MSc thesis project. The research article is further elaborated on in a separate chapter on conclusions and recommendations, chapter 3. Finally, a number of supplements is listed in chapter 4 for further clarification on certain parts of the research.

2

RESEARCH ARTICLE

Exploring Urban Air Mobility to Comprehend Urban Air Quality

Abstract — This paper discusses urban air quality measurements carried out in a park in Aigaleo (Athens), located adjacent to a busy road. The measurements were taken using the Sniffer4D Mini 2 sensor box with a drone to investigate how Urban Air Mobility can aid in measuring urban air quality. CO, NO_2, O_3, SO_2, $PM_{2.5}$ and PM_{10} concentrations were recorded through point measurements at varying locations, altitudes and times. Several validation measurements were carried out, showing that temperature heavily influenced the outcome of the recordings. Due to the high number of variables, no conclusion has been found on the wind effect. During rush hour, NO_2 and CO concentrations were highest close to the traffic; however, NO_2 concentration showed non-linear behaviour with increase in altitude when further from the traffic or out of rush hour. SO_2 concentration always decreased with an increase in altitude; highest concentrations were observed further from the busy road. Highest O_3 concentrations were obtained in the afternoon at higher altitudes, due to its reaction under sunlight. $PM_{2.5}$ and PM_{10} concentrations had a high variability due to environmental conditions. Additionally, continuous measurements were carried out, in which the drone flew a path through several locations and altitudes. The results from these were interpolated to enable the detection of areas with higher concentrations of air pollutants.

1. INTRODUCTION

Bad air quality can cause harm to all living species world-wide resulting in seven million premature deaths every year [5]. Air quality further deteriorates due to an increase in traffic, industry and other polluting sources [20]. Furthermore, it is influenced by environmental factors such as temperature and wind which affect the dispersion of the air pollutants [21]. Air pollution becomes trapped in urban environments due to the high density of buildings. This emphasises why air quality is now of great concern in urban areas. This research contributes to better understanding of urban air quality by testing an experimental setup using Urban Air Mobility (UAM), more commonly known as drones. The measurable condition of the air is most often determined by the concentrations of CO, NO_x (NO + NO_2), O_3, SO_2, $PM_{2.5}$ and PM_{10} [22]. Of these, NO_2, $PM_{2.5}$ and O_3 have the greatest impact on human health [20].

CO is produced by the incomplete combustion of fuels including wood, petrol, charcoal, natural gas and kerosene [22]. CO can bind to haemoglobin in the blood where oxygen would usually bind. It therefore reduces the amount of oxygen the blood can carry, which results in adverse health effects [23].

The gaseous pollutants NO_x are formed by the combustion of fossil fuels and typically originate from transport, industry and coal-fired power stations [20]. A reaction can occur between NO and O out of which NO_2 is formed. Inhalation of NO_x can result in a wide range of respiratory and cardiovascular diseases [24].

O_3 is formed by reactions between NO_x and volatile organic compounds (VOCs) [25]. This reaction happens under sunlight and therefore the highest O_3 levels are obtained during summer. O_3 stays in the troposphere for approximately three weeks and is removed by deposition or chemical reactions with hydroxide (OH) or NO_x. Breathing in O_3 can lead to lung diseases and asthma [24].

The toxic, gaseous pollutant SO_2 mainly results from the burning of solid and liquid fuels contaminated with sulphur (e.g. kerosene) [26]. It slowly spreads

through the atmosphere. For people with chronic lung diseases, SO_2 can cause intense breathing problems [24].

Particulate matter is grouped by diameter; $PM_{2.5}$ and PM_{10} are two of the most popularly researched. Inhaling particulate matter deeply into the lungs can result in cardiopulmonary and lung diseases. $PM_{2.5}$ can remain suspended in the air for weeks and be transported over hundreds of kilometres; PM_{10} will only last a few hours because of gravity and washout [25]. Sulphates, nitrates, ammonia, chloride, black carbon and mineral dust are examples of particulate matter [22].

To guarantee a safe living environment, the concentrations of the discussed air pollutants should be monitored. However, since air quality is often measured at fixed, relatively expensive measurement stations, limited information is available about the air quality in an urban area [8]. Moreover, air quality is typically measured near ground level, disregarding the vertical profile of air quality. Efforts should be made to obtain both vertical and higher-resolution horizontal profiles of air pollution. Drones equipped with air quality sensors have the advantage of quickly measuring pollution levels at different locations and altitudes [27]. External influences such as temperature and wind do, however, impact the outcome of the measurements.

Consulted research in which urban air quality is measured using drones showed that higher air pollutant concentrations are measured when moving closer to a polluting source. High wind speeds assisted in dispersion of air pollutants [10]. During rush hour, higher traffic-related air pollutant concentrations (here particulate matter and CO) were measured [9]. Several research papers [9, 11–14] looked into the vertical dispersion in the first several hundred meters of air pollutants; as an example, Cichowicz and Dobrzański [28] showed that different behaviour can be found in concentrations for different gaseous pollutants. Typically, particulate matter concentrations were higher when close to the ground, whereas gaseous air pollutant concentrations can increase with altitude. It has been found that polluting sources and meteorological conditions greatly impact the air pollutant concentrations [13, 14].

For this research, we will be looking at the air quality in Aigaleo (Athens), a typical urban environment with known struggles with air quality. This is caused by a number of variables. Air quality in Athens is worsened due to relatively low wind speeds and temperature inversions. Air quality in Athens has been worsened as a large quantity of biomass was burnt due to the economic crisis (2009) and COVID-19 pandemic (2020) [29, 30]. Mostly during the winter, increased CO and particulate matter concentrations were observed [31].

In Athens, the particulate matter concentration at background sites is typically increased due to central heating and biomass burning [32]. The traffic determined the particulate matter concentration (37% for $PM_{2.5}$ and 44% for PM_{10}) when measuring close to a road. Another source for an increase in particulate matter concentration can be ships, as shown by Haugen et al. [33]. All in all, Athens provides an adequate testing environment for the experimental setup researched in this article.

The overall goal of this research is to investigate how Urban Air Mobility can provide meaningful information on urban air pollution. We will discuss how air quality measurements can effectively be conducted using the chosen drone configuration and shown what conclusions can be drawn from the obtained results. Moreover, we will touch upon the environmental impact from measuring urban air quality via drones.

2. METHODS

This section discusses the methodology of the research which consists of the experimental setup, a description of the field campaign, validation measurements carried out and environmental conditions during the field campaign.

2.1. EXPERIMENTAL SETUP

The experimental setup consists of the Sniffer4D Mini 2 sensor box, capable of measuring the previously discussed air pollutants; CO, NO, NO_2, O_3, SO_2, $PM_{2.5}$ and PM_{10}. These are measured by Alphasense amperometric gas sensors for the gaseous pollutants and a laser scattering dust sensors for the particulate matter [12, 34], which obtained high correlations of 0.81-0.95 with a scientific grade monitoring station [35]. During the measurements the NO sensor malfunctioned and the concentration of CO was often too low to be sensed by its sensor. The Sniffer4D Mini 2 also records several other parameters: temperature (°C), relative humidity (%), latitude, longitude, altitude (m), pressure (Pa) and UTC time. The predecessor of the Sniffer4D Mini 2 has been used to measure urban air quality successfully [13, 14]; polluting sources were identified and the trends of air pollutants with altitude were obtained.

The Sniffer4D Mini 2 tackles changes in temperature through algorithms, which account for changes in sensitivity and zero temperature dependency of the Amperometric gas sensors [36]. These sensors were calibrated at 20 °C. For accurate measurements, the temperature should be stable as quick changes in temperature result in unreliable measurements. Variations in wind speed and direction are tackled by the integrated ventilator in the Sniffer4D Mini 2, which

produces a constant inflow [35].

Figure 2.1: Sniffer4D Mini 2 placed on top of the DJI Mavic 3 Enterprise during the measurements in Aigaleo.

The Sniffer4D Mini 2 is placed on top of the DJI Mavic 3 Enterprise drone as shown in figure 2.1. This combination can fly up to 21 minutes on one battery; the battery powers both the drone and the Sniffer4D Mini 2. The setup weighs 1.2 kg, and thus falls within the C2 drone category [37]. Using Litchi software, it can fly a programmed path to ensure repeatability of the measurements [38].

2.2. DESCRIPTION OF FIELD CAMPAIGN

Measurements were carried out on two consecutive days in a park in Aigaleo (Athens), Greece, located adjacent to a busy road. The experimental site can be seen in figure 2.2, where the busy road has been indicated as well. The measurements were conducted during different hours of the day (roughly 10.00-17.00), in order to see the variability of air pollutants with time of day.

Firstly, point measurements were conducted at five selected locations indicated with A-B-C-D-E in figure 2.3. Measurements were conducted at each of the indicated locations from 0 to 120 m altitude with a vertical flying speed of 0.8 m/s; a maximum set to ensure stable pressure [35].

Secondly, continuous measurements were recorded through flying a programmed path, with movements in horizontal as well as vertical directions, using Litchi software [38]. The route can be seen in figure 2.4. The vertical flying speed was again 0.8 m/s and increased to 3.0 m/s during the diagonal parts (e.g. F-G) of the flight path. Because air quality varies significantly faster vertically [13], we analyse all altitudes at each location. Horizontally, air quality tends to vary less and it can travel over several hundreds of meters. It was therefore deemed appropriate to separate the measurement locations in horizontal direction by 50 m [39].

Figure 2.2: Measurement site in Athens, Greece. The park and busy road have been annotated.

Figure 2.3: Overview of point measurements.

Figure 2.4: Overview of continuous measurements.

2.3. VALIDATION MEASUREMENTS

Firstly, the accuracy of the temperature and estimated wind speed and direction are examined. An experiment was designed and conducted to compare measurements of our setup with measurements from the KNMI Cabauw measurement station, a 213 m high tower measuring environmental conditions at several altitudes [2]. We flew close to this measurement station in an altitude range of 0-120 m at different vertical flying speeds, up to the limit of 0.8 m/s

(set because of atmospheric pressure [35]). Lastly, the response time of the sensors and a comparison of the concentrations measured with the Sniffer4D Mini 2 versus the KNMI measurement station are discussed.

Vertical flying speed [m/s]	R temp [-]	R wind speed [-]	Difference average wind direction [°]
Hover at every 20 m altitude	0.95	0.86	11
0.2	0.90	0.61	7
0.4	0.88	0.62	1
0.8	0.98	0.80	3

Table 2.1: Pearson correlation coefficients for wind speed and temperature (temp) at varying measurement speeds. The differences between the average wind direction from Airdata and the KNMI data have been included as well.

The outcome of the validation exercises is summarised in table 2.1. For the temperature and wind speed, we make use of Pearson correlation coefficients (R), as we expect a linear relationship between the measured values of our setup and the KNMI measurement station. This linear relationship is not expected for the wind direction and, therefore, we look at the difference in value measured. The temperature profile obtained high Pearson correlation coefficients of 0.88 and higher with the KNMI data. It is independent of the examined flying speeds. The wind speed and direction have been estimated with an algorithm developed by Airdata in this research. This algorithm compares the inputs to the motors of the drone with the actual movement of the drone to estimate the wind speed and direction [40]. The estimated wind speed obtained Pearson correlation coefficients of at least 0.6 with data from the KNMI measurement station. It is independent of the flying speeds examined. A maximum difference of 11 ° is found between the measured wind directions by Airdata and the KNMI data. This shows that the Airdata algorithm for the wind can be used to obtain reliable estimates.

The response time of all sensors is less than 5 seconds, which has been tested by placing the Sniffer4D Mini 2 close to the exhaust of a car. After the engine started, the CO, NO_x and SO_2 sensors immediately exhibited a peak. The air pollutant values recorded by the Sniffer4D Mini 2 have also been compared to the KNMI measurement station. The values measured by the Sniffer4D Mini 2 are 2 to 4 times as high as the concentrations measured at the KNMI measurement station. This is due to the KNMI data being an average, with slight variations depending on the specific location measured at.

Several conclusions can be found through the validation. Firstly, the temperature needs to stabilise after the drone has taken off to obtain accurate results. Secondly, the flight speed should be limited to 0.8 m/s in vertical direction to ensure the temperature and atmospheric pressure do not change too rapidly. Finally, all sensors respond well within 5 seconds and it is thus not deemed necessary to stop at certain altitudes as this will limit flight range. The interested reader can find more about the validation exercises in section 4.2.

2.4. ENVIRONMENTAL CONDITIONS

On the first day of the February measurements in Aigaleo, the wind came from northeast direction with an average wind speed of 5 m/s. This can be seen in figure 2.5.

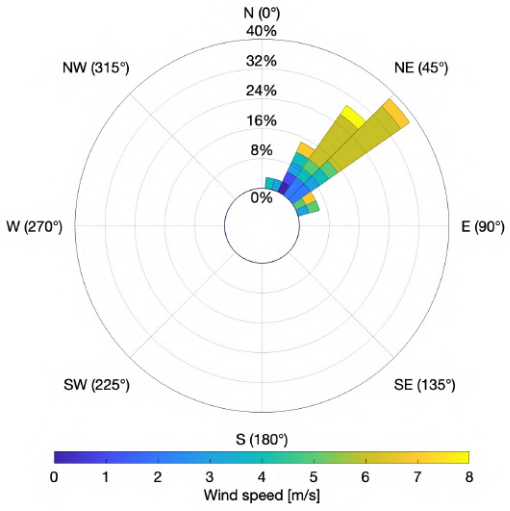

Figure 2.5: Wind rose on first day of measurements at 16.30. Measured at location A.

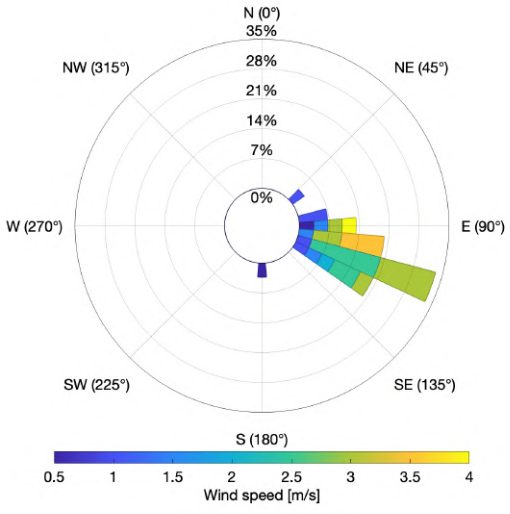

Figure 2.6: Wind rose on second day of measurements at 17.00. Measured at location A.

In the afternoon of the second day, the wind changed

direction and now came from the south with an average wind speed of 2.5 m/s, as shown in figure 2.6.

On both days, the temperature (from the Sniffer4D Mini 2) varied between 7 and 10 °C, which is a relative large difference with the calibration conditions of the Sniffer4D Mini 2 (20 °C). On both days there were some clouds, resulting in periods of sun and overcast.

2.5. DATA PROCESSING

The downward movement of the drone is included in the results for the point measurements, as the temperature was still stabilising during the upward movement of the drone. Temperature shifts are typically found below 5 and above 119 m altitude; we thus only look at the recordings in the 5-119 m altitude range.

In section 3, results are discussed which have the smallest temperature variability (less than 0.5 °C) to make sure the results are minimally influenced by temperature. All other results can be found in subsection 4.3.1. The remaining results are filtered with a moving average filter of the five nearest neighbours on both sides. They are plotted per five points to improve readability of the graphs.

For the continuous measurements, air quality is measured over a path in both horizontal as well as vertical direction. The results have been filtered by only selecting taking measurements at the coordinates as indicated in figure 2.4. These have been imported into ArcGIS software and are interpolated in 3D. We use the Empirical Bayesian Kriging 3D method since good results were obtained in previous research on air quality [41, 42]. In section 3, a measurement is discussed with a temperature variability of 1.0 °C, significantly lower than the other continuous measurements. The latter ones can be found in subsection 4.3.2.

3. RESULTS & DISCUSSION

Firstly, we summarise the expectations of air quality trends from measurement stations in Athens and compare these to our measurements. Next, the variation of air quality with time of day and consequently with altitude are discussed. Both of these results have been obtained through the point measurements. Hereafter, the 3D interpolations of air quality data are presented. We end with a section on the environmental impact of monitoring air quality with the use of drones.

3.1. COMPARISON WITH EXPECTATIONS FROM ATHENS MONITORING STATIONS

Data analysis of air quality at several measurement stations in Athens (see section 4.1) showed that air quality varies significantly during the day. Peaks in NO_2 concentration are found during the morning rush and late afternoon as a result from traffic. CO, $PM_{2.5}$ and PM_{10} concentrations increase in the morning and the evening, where the latter peak partly originates from the burning of biomass. The observed O_3 concentration reaches its maximum during the afternoon as it forms under sunlight. The concentration of SO_2 only shows a slight increase in the morning and is unpredictable during the rest of day. The comparison of these expectations to the results of this research can be found in subsection 3.2.

Furthermore, we compare the data found with the measurement stations of the months February and May. In May, a higher O_3 concentration is observed due to the increased sunlight. The CO, $PM_{2.5}$ and PM_{10} concentrations are lower since there is less heating, which is typically fuelled by burning biomass. The NO_2 and SO_2 concentrations are similar in both months.

These findings are in line with a comparison made between measurements carried out in May and the earlier described measurements in February. During a soundwalk experiment on drone noise in the same park in Aigaleo, several air quality measurements were taken at altitudes ranging from 10 to 30 m. Significantly higher O_3 concentrations were found in May, due to the increase in sunlight. Significantly lower concentrations of $PM_{2.5}$ and PM_{10} were obtained in May, similar to the findings from the local measurement stations. NO_2 and SO_2 concentrations were similar in both months, as expected from the measurement stations. No conclusion could be drawn for the CO concentration due to the limitations of its sensor. More information on this comparison can be found in subsection 4.3.4.

3.2. VARIATION OF AIR QUALITY WITH TIME OF DAY FROM POINT MEASUREMENTS

We look at the obtained average air quality concentrations between 5 and 10 m altitude for the variation of air quality with time of day. This range has been chosen because of its proximity to ground level pollution sources, making it the most impacted area. 95% confidence intervals have been included to illustrate the variations in air quality in the chosen altitude range. Moreover, we compare measurements from location A, C and E, increasing in distance from the road, to evaluate the effect of traffic on air quality. Finally, we exclude the CO concentration here, as this is too often equal to zero on average.

In figure 2.7 the average NO_2 concentration between 5 and 10 m altitude at locations A, C and E can be seen. On the first day, a significant decrease is found during the early afternoon at all measurement stations as traffic decreased. This decrease is in line with the expectation from the local measurement sta-

tions; also here, higher concentrations of NO_2 were observed during rush hour. The found reduction is largest for location A, located closest to the busy road.

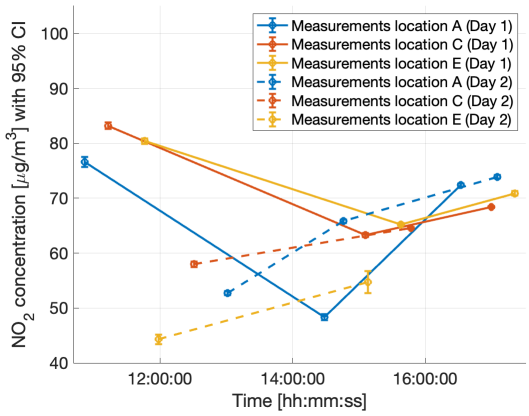

Figure 2.7: Average NO_2 concentrations with 95% confidence interval during different times of day 1 and 2. Measurements from locations A, C and E.

During rush hour on the first day, all observed NO_2 concentrations are within 5 $\mu g/m^3$ of each other. When looking at the measured NO_2 concentrations on the second day, significantly lower concentrations (about -15 $\mu g/m^3$) are observed at location E compared to location A. The wind speed was lower on the second day, indicative of less dispersion of air pollutants; one should however be careful with jumping to conclusions, as other environmental factors changed as well.

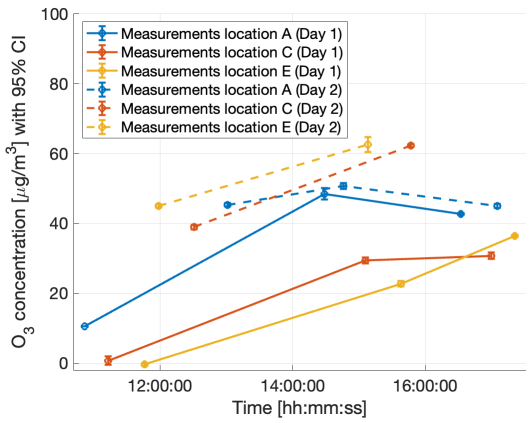

Figure 2.8: Average O_3 concentrations with 95% confidence interval during different times of day 1 and 2. Measurements from locations A, C and E.

The average O_3 concentrations can be seen in figure 2.8. On the first measurement on the first day, the measured concentration at location E was zero due to a problem with the sensor. On both days, highest concentrations are observed early in the afternoon, caused by the presence of more sunlight at this time in comparison to the morning. This is in line with expectations from the local measurement stations. There is not one specific location where the highest O_3 concentration is observed as O_3 is not a directly emitted pollutant.

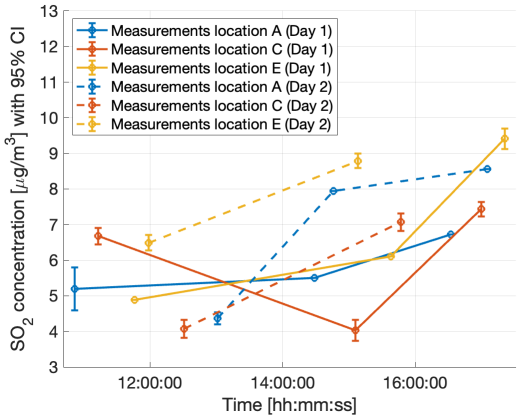

Figure 2.9: Average SO_2 concentrations with 95% confidence interval during different times of day 1 and 2. Measurements from locations A, C and E.

On both days highest SO_2 concentrations are found in the late afternoon, as seen in figure 2.9. We find the highest measured concentrations (9-10 $\mu g/m^3$) at location E, which indicates that traffic is not the main contributor to SO_2 emission. It is likely that the SO_2 concentration results from a mix of external factors, but the higher measurements during rush hour do indicate some influence by traffic.

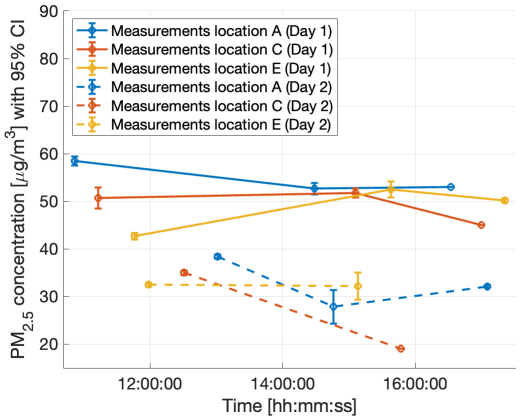

Figure 2.10: Average $PM_{2.5}$ concentrations with 95% confidence interval during different times of day 1 and 2. Measurements from locations A, C and E.

No clear trend with time of day is found for the $PM_{2.5}$ concentrations as can be seen in figure 2.10. The confidence interval is large in comparison to other air pollutants. The concentrations of PM_{10} are also similar with time of day and can be seen in figure 2.11. Although a slight increase of $PM_{2.5}$ and PM_{10} concentrations during rush hour is expected from the Athens monitoring stations, this is not observed in the results. On both days, the $PM_{2.5}$ concentrations are

slightly higher than the PM_{10} concentrations. Around 15.00 on the first day, the $PM_{2.5}$ concentration is 52 $\mu g/m^3$ on average whereas this is 56 $\mu g/m^3$ for the PM_{10} concentration. On the second day, all concentrations are significantly lower. This is not in line with the lower wind speed which is measured on the second day, as this would result in less dispersion and thus higher measured particulate matter concentrations.

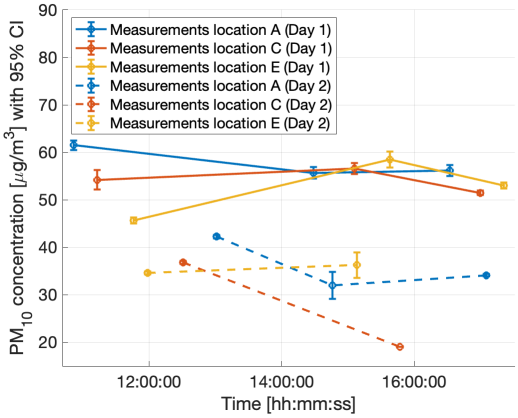

Figure 2.11: Average PM_{10} concentrations with 95% confidence interval during different times of day 1 and 2. Measurements from locations A, C and E.

3.3. VERTICAL VARIATION OF AIR QUALITY WITH ALTITUDE FROM POINT MEASUREMENTS

For the variation of air quality with altitude, we look at measurements which have a temperature variability of less than 0.5 °C to minimise the influence of the temperature on the results. A comparison is made between results from location A, C and E, which are increasingly further away from the main road, at rush hour (17.00) and non rush hour (13.00-15.00).

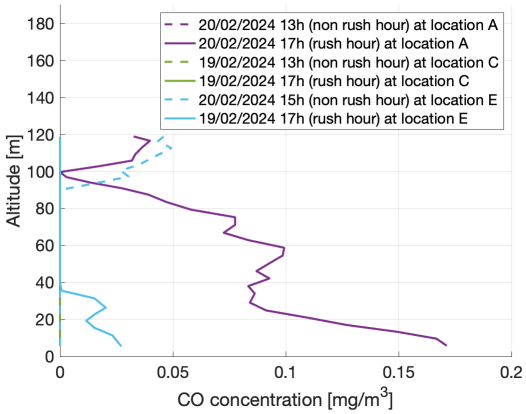

Figure 2.12: CO concentration variation with altitude. Locations A, C and E during and outside of rush hour.

The CO concentrations can be seen in figure 2.12. The measured concentration is only non-zero during rush hour measurements, caused by more exhaust gases of traffic at this time. Higher CO concentrations are measured when closer to the road (at location A) since CO is a direct pollutant of traffic. The CO concentration also decreases with an increase in altitude as it moves further away from the traffic.

In figure 2.13 it is shown how the NO_2 concentration during non rush hour increases with altitude up to 70 m after which it starts to decrease again. At rush hour, an overall decrease with altitude can be found at location A (traffic). This effect origins from the higher number of traffic present at this hour and is not as strong at locations C and E.

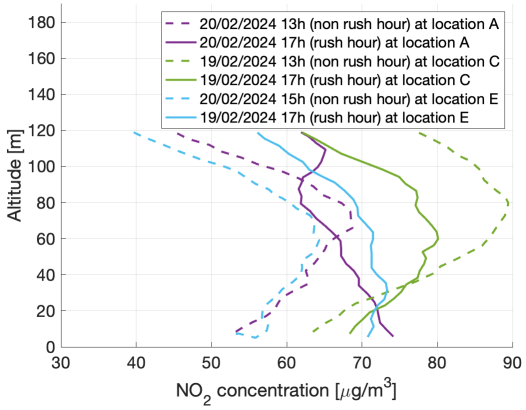

Figure 2.13: NO_2 concentration variation with altitude. Locations A, C and E during and outside rush hour.

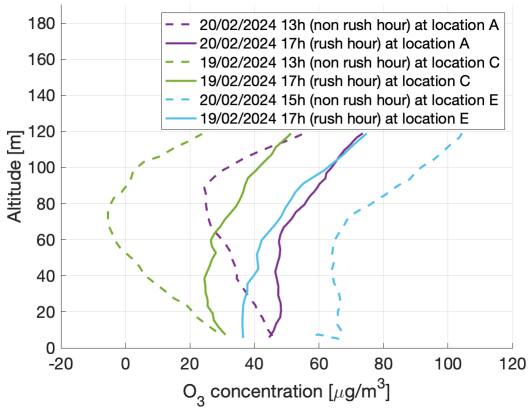

Figure 2.14: O_3 concentration variation with altitude. Locations A, C and E during and outside of rush hour.

The O_3 concentrations are stable up to an altitude of 60 m, after which they increase. They can be found in figure 2.14. The trend is similar during and outside of rush hour, although outside of rush hour the ozone concentrations decreases a little with the first 60 m of altitude. The increase after 60 m altitude could be explained by more sunlight at these altitudes, which could be blocked by obstacles (e.g. trees) at lower

altitudes. The observed trend is similar at all locations, indicating that O_3 is not a directly emitted air pollutant. After 60 m altitude, the NO_2 concentration decreases whereas the O_3 increases, indicative of the non-linear relationship between these two air pollutants.

The measured SO_2 concentrations decrease with altitude which is most noticeable in the lower range of 0 to 35 m altitude. Beyond 35 m altitude, the SO_2 concentration stabilises. This is independent of location and time of day. The SO_2 originates from air pollution sources present close to the ground. We find that the SO_2 concentration changes slowly which is one of its characteristics.

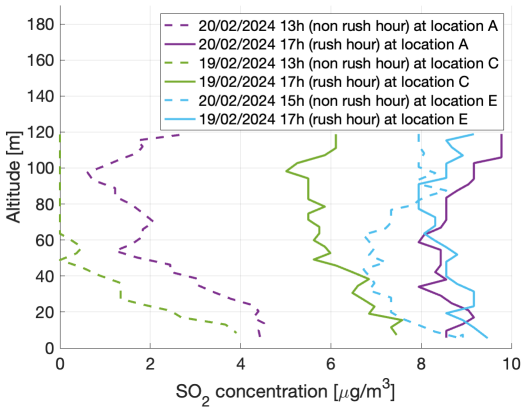

Figure 2.15: SO_2 concentration variation with altitude. Locations A, C and E during and outside of rush hour.

On average, $PM_{2.5}$ and PM_{10} concentrations as shown in figure 2.16 and figure 2.17 are relatively stable with increasing altitude. For some measurements, increases are found whereas other measurements showed decreased concentrations. The particulate matter concentrations have a high variability caused by the multitude of sources.

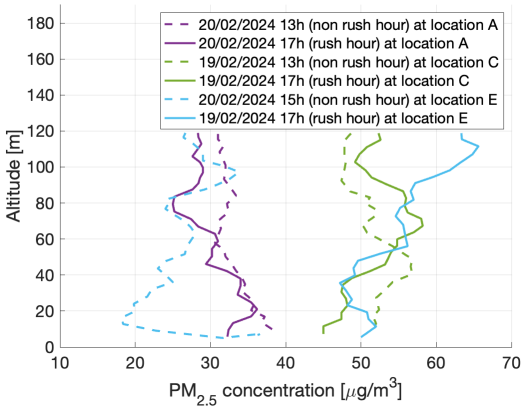

Figure 2.16: $PM_{2.5}$ concentration variation with altitude. Locations A, C and E during and outside of rush hour.

Overall, the non-linear trends of NO_2 and O_3 are in line with previous research [13]. We have seen that the air quality can vary fast with altitude and is dependent on a number of environmental factors such as traffic, temperature and wind. SO_2 and CO are typically highest close to the ground; these are mainly formed close to the ground and do not move in upward direction. The found particulate matter concentrations are slightly increasing or decreasing with altitude; this is in line with research found carried out during different meteorological conditions [14].

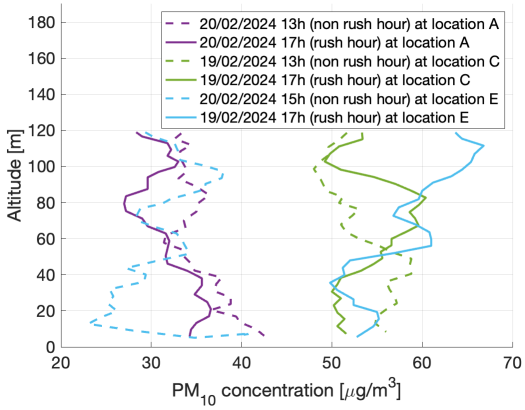

Figure 2.17: PM_{10} concentration variation with altitude. Locations A, C and E during and outside of rush hour.

3.4. 3D INTERPOLATED AIR QUALITY DATA FROM CONTINUOUS MEASUREMENTS

Finally, Empirical Bayesian Kriging 3D interpolations have been created from the continuous measurements. The included measurement was taken on the second day at 16.22 with a relative high average wind speed of 8.4 m/s in northwestern direction. The altitude range of the measurements is 35-120 m. More information on the accuracy of the interpolation and a comparison between the continuous and point measurements can be found in subsection 4.3.2.

Interpolated CO results can be seen in figure 2.18. The highest CO concentrations are obtained at the front of the park, close to the road. They are typically found at lower altitudes, in line with the results from subsection 3.3.

The interpolated results for the NO_2 concentration can be seen in figure 2.19. An increase of the NO_2 concentration is found at the front side of the park. The wind in northwestern direction might have had an effect on this. In line with what was found in the results from subsection 3.3, highest NO_2 concentrations are obtained at an altitude of 70 m.

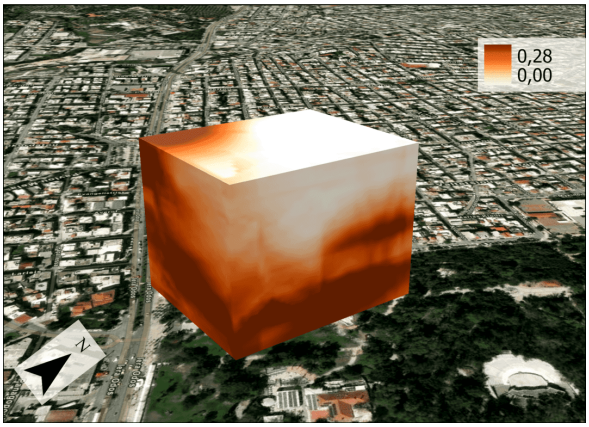

Figure 2.18: Empirical Bayesian Kriging 3D interpolation of CO concentration [mg/m^3]. Data used from second day at 16.22.

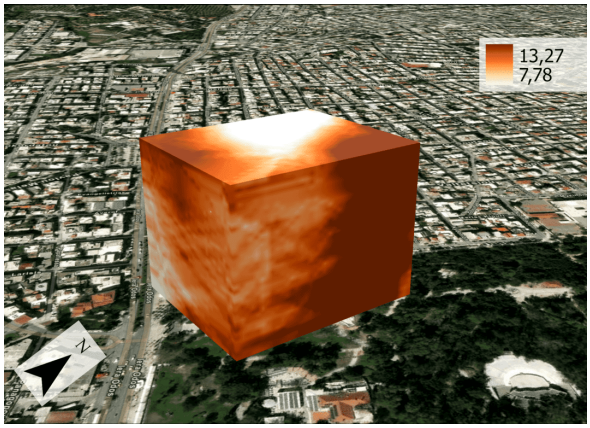

Figure 2.21: Empirical Bayesian Kriging 3D interpolation of SO_2 concentration [µg/m^3]. Data used from second day at 16.22.

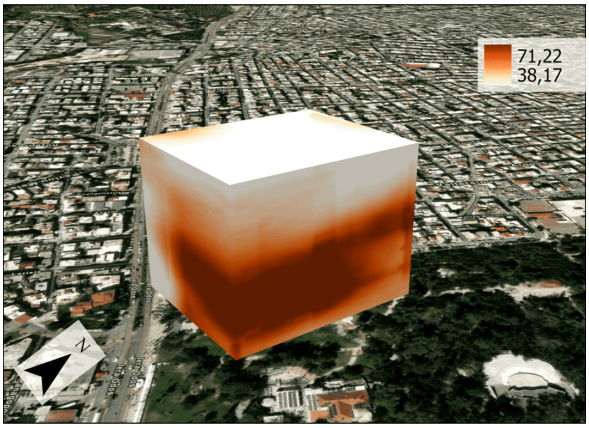

Figure 2.19: Empirical Bayesian Kriging 3D interpolation of NO_2 concentration [µg/m^3]. Data used from second day at 16.22.

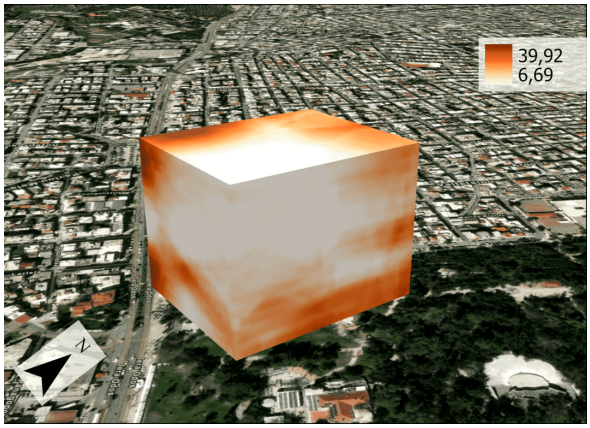

Figure 2.22: Empirical Bayesian Kriging 3D interpolation of $PM_{2.5}$ concentration [µg/m^3]. Data used from second day at 16.22.

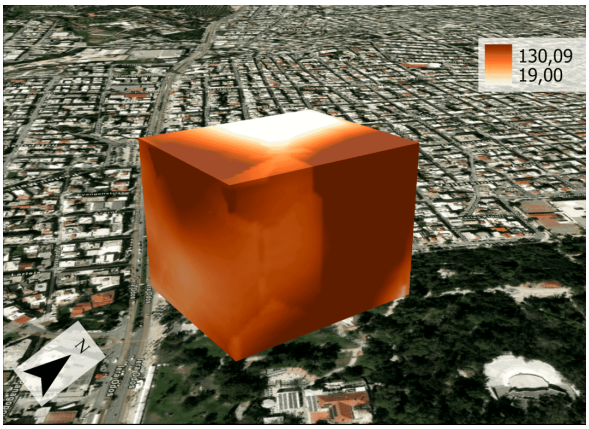

Figure 2.20: Empirical Bayesian Kriging 3D interpolation of O_3 concentration [µg/m^3]. Data used from second day at 16.22.

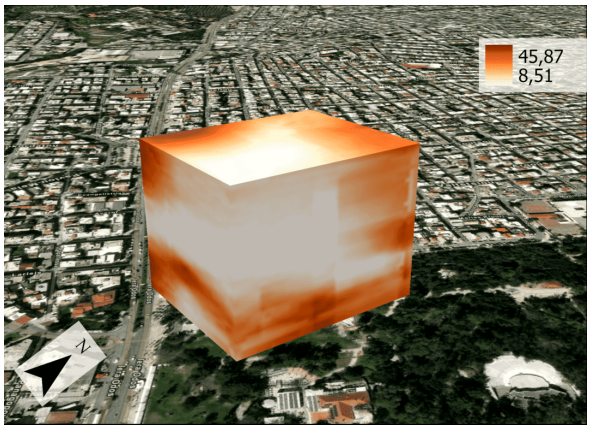

Figure 2.23: Empirical Bayesian Kriging 3D interpolation of PM_{10} concentration [µg/m^3]. Data used from second day at 16.22.

As shown in figure 2.21, highest SO_2 concentrations are found at the rear side of the park, the furthest away from the road. This indicates that traffic is not the main source for SO_2 emission. We find a stable SO_2 concentration with altitude after the first 35 m altitude, which is similar to the results from subsection 3.3.

The results for the O_3 concentration can be seen in figure 2.20. Similar to the results of subsection 3.3, the highest O_3 concentrations are found at an altitude of 120 m and further away from the road, as O_3 is not a primary pollutant of traffic. Due to its indirect formation, we do not find an effect of the wind speed and direction.

No clear trend is found for the $PM_{2.5}$ concentration, similar as to what was found in the results of subsection 3.3. The interpolated results can be seen in figure 2.22. Some areas of higher concentrations of $PM_{2.5}$ can be detected. PM_{10} behaves similar to $PM_{2.5}$, with some areas of higher concentrations and no clear trend found. The interpolated PM_{10} concentration can be seen in figure 2.23. The measured concentrations of PM_{10} are higher than the ones from $PM_{2.5}$.

All in all, it is challenging to distinguish an effect of the wind speed and direction due to the number of variables in measurement conditions. Moreover, there will be fluctuations in the wind field due to gusts; the wind speed and direction are neither uniform in space because of the presence of buildings. For NO_2, CO and SO_2, highest concentrations are observed at the side of the park where the wind is coming from. This result is not found for another continuous measurement at 16.43 on the same day (see subsection 4.3.2), which could result from the lower wind speed at that measurement; however, as indicated earlier, the temperature variability was also higher for this other measurement and it is thus hard to find conclusions on the wind effect. The results from the included continuous measurement are in line with the outcomes of the point measurements.

3.5. ENVIRONMENTAL IMPACT

As mentioned earlier, we will look into the environmental impact of this experimental setup as well. Previous Life Cycle Assessment (LCA) studies have shown that UAM can be more environmentally friendly than its competitors [17], for e.g. delivery purposes [43]. This is dependent on the energy usage and its source [18]. We calculate the air pollution emitted to generate the required electricity for a use case of air quality monitoring.

For the use case, it is assumed that air quality is monitored in Aigaleo (Athens), which covers an area of 6 km^2. Parameters have been taken from the previously discussed continuous measurements; a resolution of 50 m in horizontal direction, a vertical range of 116 m and a flight speed of respectively 3 and 0.8 m/s in horizontal and vertical direction. The drone flies according to an optimised trajectory as designed by Zhao et al. [3]. It is assumed that the flights are carried out twice a day for one year. The combined energy consumption of the tested drone configuration is 3.67 W per minute. The total flight time is circa 4 581 minutes which results in a total energy consumption of 12 260 kWh.

Pei et al. [44] calculated the emission factors for energy production for all European countries. Since results are only available up to 2017, results might have changed due to a changed distribution of electricity sources in Greece. An overview with the emissions per kWh and the total emission for our use case can be seen in table 2.2. A total of 8 543 kg $CO_{2,e}$ is emitted which should be considered before equipping drones to measure air quality. More information on the environmental impact can be found in section 4.4.

	Emission [g/kWh]	**Total emission [kg]**
CO_2	694.3	8512.6
$CO_{2,e}$	696.8	8543.2
CH_4	0.02	0.2
NO_x	1.2	14.9
N_2O	0.007	0.1
SO_2	3.3	41.0
$PM_{2.5}$	0.06	0.7

Table 2.2: Overview with emissions per kWh and total emissions of the use case scenario.

4. CONCLUDING REMARKS

Air pollution can lead to adverse health conditions and should therefore be monitored. Nowadays, this is typically done with the use of fixed, expensive air quality monitoring stations. In order to obtain better spatial resolution in both horizontal as well as vertical direction, drones can be used.

This research showed how drones can be employed to monitor the air quality in a 3D area. Especially in urban areas, air pollution stays trapped close to the ground. Therefore, investigating the air quality at several altitudes will aid in understanding how air pollutants disperse. Moreover, sources of air pollution can be located, as for example is done in this research with traffic. By moving away from this traffic, both in horizontal as well as vertical direction, its impact can be observed on the air quality across a wider area. Utilising these results, adjustments can be made to improve air quality locally. At several altitudes and locations, areas with higher concentrations of air pollutants are found which should be considered when designing urban areas.

The effect of environmental conditions, primarily temperature and wind, could not be identified due to too much changing variables. Therefore, it is recommended to conduct more repetitions of similar research. Due to the influence of the temperature, the actual sensor readings might change. Measuring a specific area over a longer period would be beneficial to better evaluate how these environmental conditions influence air quality.

Overall, Urban Air Mobility can be used to monitor air quality. Although there are still challenges ahead, this research has proven how an experiment can be designed and results can be obtained with a selected setup. These results can be used to find conclusions on urban air quality at different moments, locations and altitudes.

3

CONCLUSIONS AND RECOMMENDATIONS

The goal of this research has been to investigate how Urban Air Mobility, i.e. drones, can provide meaningful information about urban air pollution. This research has been carried out as part of the ImAFUSA EU project.

Firstly, a drone and air quality sensor box were selected in order to measure urban air pollution. The chosen sensor box is the Sniffer4D Mini 2, which has been used in previous research to accurately measure urban air pollution. It is capable of measuring CO, NO_2, O_3, SO_2, $PM_{2.5}$ and PM_{10}. External influences from temperature and wind are tackled by respectively temperature algorithms and a ventilator resulting in a constant inflow. The sensors are, however, still sensitive to changing environmental conditions and thus efforts should be made to keep these as stable as possible.

Secondly, an experiment was set up. As a location, a park in Aigaleo (Athens) was selected, located adjacent to a busy road. The measurement campaign consisted of two parts; firstly, point measurements were taken at five individual locations for an altitude range of 0-120 m. Secondly, continuous measurements were carried out in which the drone flew along a path of locations and altitudes itself. The vertical measurement speed was always limited to 0.8 m/s to limit influences from too rapidly changing atmospheric pressure and temperature. Moreover, measured locations and times were chosen carefully to be able to evaluate the effect of traffic on pollutant densities. As air quality disperses slower in vertical direction, continuous measurements were measured at 50 m intervals horizontally and vertically at all altitudes between 35-120 m. All of the described measurements were carried out in February. Additionally, some air quality measurements were taken during a soundwalk experiment on drone noise in May.

As mentioned earlier, a changing temperature can greatly impact the sensor readings. It should thus be kept as stable as possible. After the drone has taken off, it should hover for some time to let the temperature stabilise. Validation exercises have been carried out for the response time of the sensors, the concentrations measured, the temperature sensor and wind estimations. All sensors respond within 5 seconds to a change in air quality and higher values are typically measured by the Sniffer4D Mini 2 in comparison to a local measurement station, caused by the fact that we compare an average to a single measurement and a difference in location. Temperature and wind estimation provide good correlations with a KNMI measurement station. Due to changing environmental conditions, it is not possible to identify the effect of changes in temperature and wind on the measured air pollutants. However, trends with increasing times of day, month of year, altitude and distance from the traffic have been found.

Highest NO_2 concentrations are observed close to the ground near the road at rush hour. When further away from this road or outside of rush hour, a non-linear trend is found with increasing altitude; a maximum is obtained at about 70 m altitude. The NO_2 concentration is similar in February and May. O_3 concentrations increased in the afternoon due to the increase in sunlight present. For the same reason, higher O_3 concentrations are observed in May compared to February. Typically, a non-linear trend with altitude is found with a minimum at circa 60 m. Since O_3 is an indirect pollutant, no specific location is found where highest concentrations are observed.

The highest SO_2 concentrations were obtained near ground level. In the first 35 m altitude, the SO_2 concentration typically decreases; hereafter, it stays constant up to 120 m. Since rush hour has not had a direct effect on this trend, it is likely that traffic is not the main source for SO_2 pollution. Moreover, the highest values are

observed at the furthest distance from the road. A slight increase is, however, found in the late afternoon, indicative that traffic has some impact. Measured SO_2 concentrations are similar in February and May. The measured CO concentrations are often zero because of the sensor specifications. During rush hour, non-zero readings are measured due to the presence of traffic. These are typically highest at the location closest to the traffic and near the ground.

The $PM_{2.5}$ concentrations are on average stable during the day. Although they vary greatly with altitude, a stable trend is found with increasing altitude. No specific location is found where the $PM_{2.5}$ concentration is highest. For the PM_{10} concentration, the trends are similar to the $PM_{2.5}$ concentration, although significantly higher readings are obtained. Similar to the $PM_{2.5}$ concentrations, the PM_{10} concentrations are on average quite stable with time of day and altitude. In May, the observed $PM_{2.5}$ and PM_{10} concentration were significantly lower than in February, due to a decrease in biomass burning and meteorological conditions.

Although this use case of air quality monitoring has provided useful results, its environmental impact should be discussed as well. As a use case, it has been calculated how much energy would be used if one would monitor the air quality in Aigaleo (6 km^2) for one year twice a day. Parameters have been taken from the continuous part of the measurements. This resulted in an energy usage of 12 260 kWh, which adds up to a total of 8 543 kg $CO_{2,e}$ emitted.

Overall, we have thus been able to accurately measure the air quality with the chosen setup and see what effect the presence of traffic has in both vertical as well as horizontal direction. We touched upon the environmental impact of these measurements as well. This research will help to better understand how air quality can be measured effectively using drones and what conclusions can be drawn from it.

3.1. RECOMMENDATIONS

Although the measurements were successful, some questions have not been answered yet. We are currently not able to find conclusions on the effect of the wind speed and direction, as other environmental factors were changing as well. Efforts should be made to isolate this effect as much as possible, although it will remain challenging.

The sensors are heavily temperature dependent and it was therefore decided to keep the temperature as stable as possible. This limits, however, the conclusions that can be found for the effect from temperature. Since measurements were carried out at a relatively low temperature in comparison to the calibration temperature, it is advised to carry out measurements closer to this calibration temperature. With this approach it can be validated if the recordings of the sensors are in line with e.g. a fixed, accurate measurement station; in this research, we focused mainly on the trends found. Finally, in terms of sensors, efforts should be made to fix the NO sensor, as this gave bad recordings.

Furthermore, it would be useful to carry out measurements over a greater time range. Firstly, measuring early in the morning (6.00-10.00) would be useful to be better able to identify the morning rush in the air quality concentrations. Also measuring in the evening (18.00-24.00) could be useful as previous research has shown that air quality tends to deteriorate during the evening. Secondly, previous research has shown that air quality can differ by the day of week. It would thus be nice to have a larger experiment campaign over several weeks. Finally, air quality differs by month. Therefore, carrying out this experiment more times a year, would be beneficial to expand our knowledge of air quality.

As a final part, the environmental impact was calculated for monitoring air quality using drones. This was done by looking into the air pollution generated during the electricity production. As mentioned earlier, analysis on noise or a LCA study have not been included. These analyses would be useful to better estimate the environmental impact of monitoring air quality using drones. In the current environmental impact, data is used from 2017 as this was the latest available data. Efforts should be made to redo the calculation once newer data is available.

4

SUPPLEMENTS

This chapter provides several supplements to the research article for the interested reader. Firstly, data research on the air quality in Athens is provided. Secondly, supporting material for the validation of the measurements is discussed. Thirdly, all results obtained during the measurement campaigns in Aigaleo (Athens) are shown; in the research paper, a selection of these results has been included. A validation of the 3D interpolations is also part of this. Finally, the environmental impact is explained more extensively than in the research article.

4.1. DATA RESEARCH AIR QUALITY ATHENS

There are several measurement stations located in Athens [45], which are grouped into the categories traffic, industrial and background. The goal is to find which effect effect polluting sources, especially traffic, have on air quality. Therefore, the concentrations found by a background measurement station will be compared to the concentrations found at a traffic measurement station. Since concentrations can differ due to the characteristics of a measurement station, we focus on the differences in trends found. Although traffic is a significant polluting source, other sources such as central heating should not be forgotten [31].

When possible, results from the years 2021 and 2022 for the measurement stations have been taken. Sometimes results are missing at certain measurement stations (e.g. missing years or pollutants). It is mentioned if results have been taken from different years. We ensure that the Covid period (2020) is avoided as this might have detrimental effects on the comparison. A detailed map with the locations of each measurement station can be found below in figure 4.1.

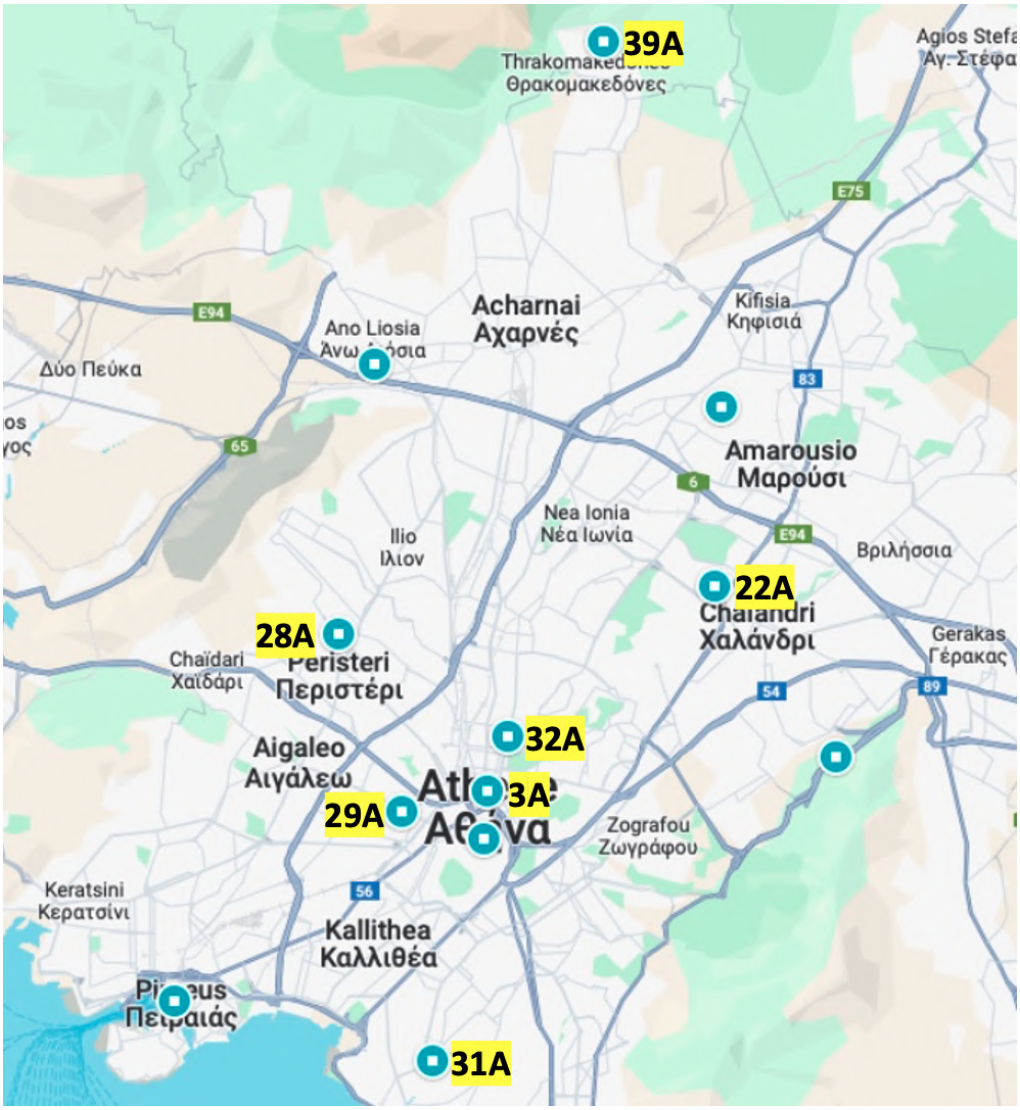

Figure 4.1: Locations of measurement stations in Athens, Greece [1].

Most of the used measurement stations are relatively close to the centre of Athens. Measurement station 39A is an exception which should be considered during the discussion of the results. Below, a list is provided with the type of each measurement station:

- 3A: traffic
- 22A: background
- 28A: background (close to Aigaleo)
- 29A: industrial (at same road park in Aigaleo)
- 32A: traffic
- 39A: background (in a park)

To make a better analysis on which pollutants affect the air quality, an additional comparison is made with measurement stations in the Netherlands [46]. The locations of these can be found in figure 4.2 and these are also grouped into traffic, industry and background measurement stations. Therefore, we analyse them in the same way as we do with the Athens measurement stations.

Figure 4.2: Locations of measurement stations in the Netherlands [1].

The type of each measurement station in the Netherlands can be found in the following list:

- Wijk aan Zee: industry
- Kanaaldijk: industry
- Westerpark: background
- Vondelpark: background
- van Diemenstraat: traffic

The air quality can be assessed according to the European Air Quality Index, shown in table 4.1. It should be noted that the CO concentration is not included in this index.

	Good	**Fair**	**Moderate**	**Poor**	**Very poor**	**Extremely poor**
NO_2 concentration [$\mu g/m^3$]	0-40	40-90	90-120	120-230	230-340	340-1000
O_3 concentration [$\mu g/m^3$]	0-50	50-100	100-130	130-240	240-380	380-800
SO_2 concentration [$\mu g/m^3$]	0-100	100-200	200-350	350-500	500-750	750-1250
$PM_{2.5}$ concentration [$\mu g/m^3$]	0-10	10-20	20-25	25-50	50-75	75-800
PM_{10} concentration [$\mu g/m^3$]	0-20	20-40	40-50	50-100	100-150	150-1200

Table 4.1: European air quality levels for air pollutants [4].

4.1.1. CO CONCENTRATION

The measured CO concentration at a background and traffic measurement location for respectively hour of day, day of week and month of year can be found in figure 4.3, figure 4.4 and figure 4.5. The 95% confidence intervals have been included in grey.

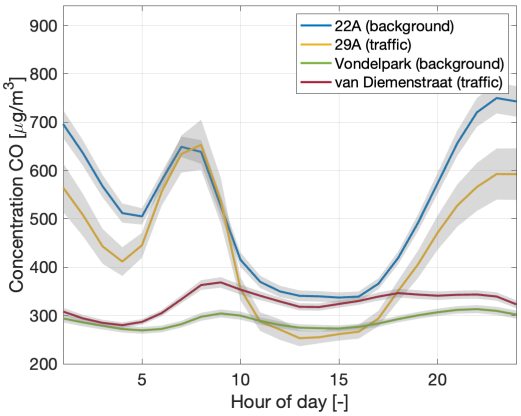

Figure 4.3: Average CO concentration per hour of day. The 95% confidence interval has been annotated in grey.

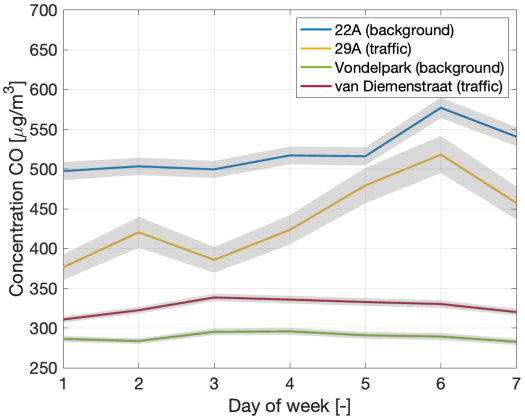

Figure 4.4: Average CO concentration per day of week. The 95% confidence interval has been annotated in grey.

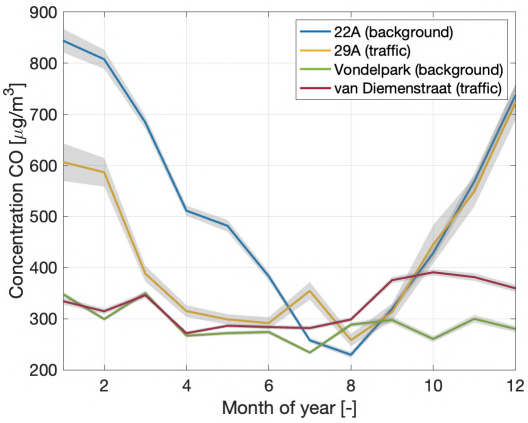

Figure 4.5: Average CO concentration per month of year. The 95% confidence interval has been annotated in grey.

Firstly, it is important to note the big confidence interval for the traffic station in Athens. There seems to be a lot of variance present in the results obtained at this station.

When we look at the CO concentration per hour of day, we find large differences between the results in Athens and the Netherlands. In Athens, a morning and night peak are present. These peaks are not present in the Netherlands, where the concentrations are fairly constant. This difference is caused by biomass burning and more polluting traffic in Athens. Due to the economic crisis in Greece, people started to burn cheap fuels for e.g. heating [29]. This has led to a steep increase in CO and particulate matter concentrations. This is in line with the obtained results, as the highest concentrations are obtained at the background station. Therefore, we conclude that traffic is not the only contributor to the CO concentration.

When looking at the day of the week, an increase in CO concentration is found for both stations in Athens during the weekend. This is likely caused by more activities such as cooking and heating occurring on these days. In the Netherlands, the CO concentration tends to be slightly higher during the weekdays. This could have to do with an increase in traffic, as biomass burning happens less in the Netherlands.

In the Netherlands, the CO concentrations are a bit higher towards the end of the year. This is especially found at the traffic station and could have to do with an increase in traffic. In Athens, way lower concentrations are found during the summer. All in all, we find that biomass burning and other environmental conditions greatly influence the CO concentration during the colder winter months.

4.1.2. NO_2 CONCENTRATION

Average NO_2 concentrations per hour of day, day of week and month of year can respectively be found in figure 4.6, figure 4.7 and figure 4.8. The 95% confidence intervals have been included in grey.

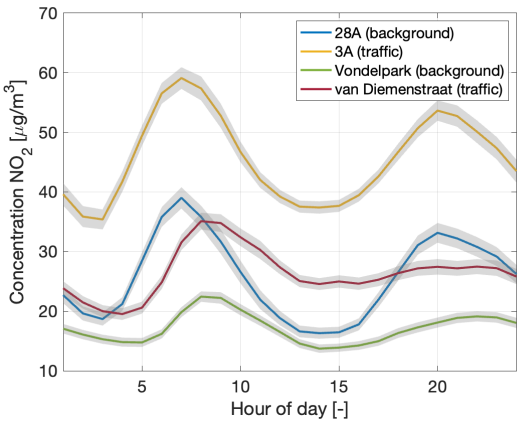

Figure 4.6: Average NO_2 concentration per hour of day. The 95% confidence interval has been annotated in grey.

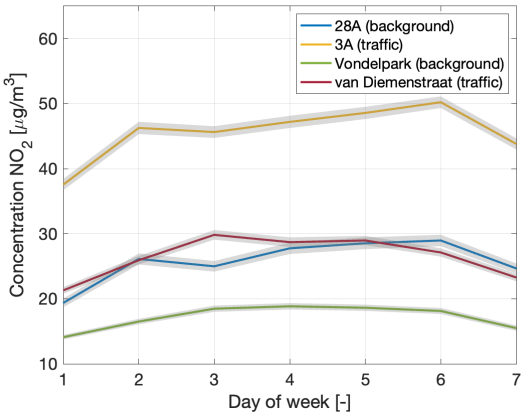

Figure 4.7: Average NO_2 concentration per day of week. The 95% confidence interval has been annotated in grey.

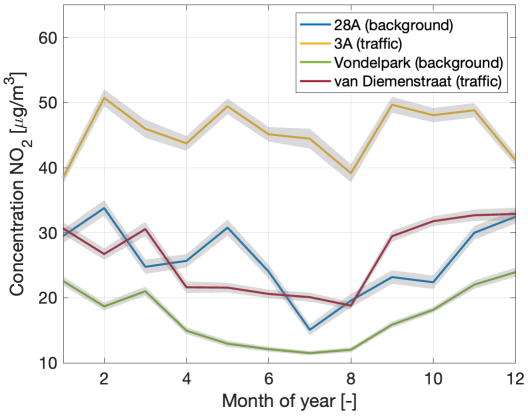

Figure 4.8: Average NO_2 concentration per month of year. The 95% confidence interval has been annotated in grey.

At all locations, increases in NO_2 concentration can be found in the morning and evening. These peaks are better visible in Athens than in the Netherlands. The NO_2 concentration at the traffic station in Athens is the highest, showing that traffic is the main contributor for NO_2. Moreover, these peaks are found during rush hour. Measured concentrations in the Netherlands are significantly lower than the ones in Athens.

At all locations, higher NO_2 concentrations are obtained during the weekdays. This is in line with earlier findings as less traffic is present during the weekend. The NO_2 concentration varies with month at all measurement stations. No trend can be found at the traffic station in Athens. Yet, for the other stations, a decrease is found during summer in NO_2 concentration.

Overall, the air quality in the Netherlands for NO_2 concentration is good. Especially at the traffic station in Athens, the air quality is moderate because of the relative high concentration of NO_2 in the air.

4.1.3. O_3 CONCENTRATION

The average O_3 concentrations per hour of day, day of week and month of year can be found in respectively figure 4.9, figure 4.10 and figure 4.11. The 95% confidence intervals have been included in grey.

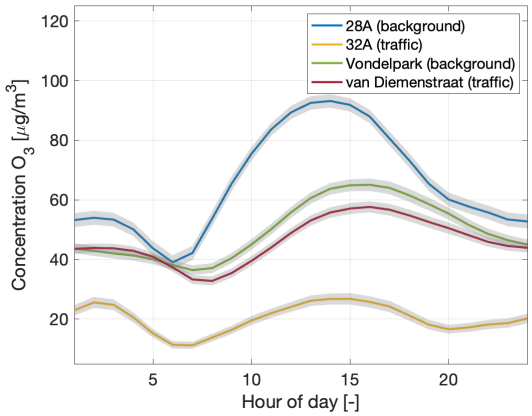

Figure 4.9: Average O_3 concentration per hour of day. The 95% confidence interval has been annotated in grey.

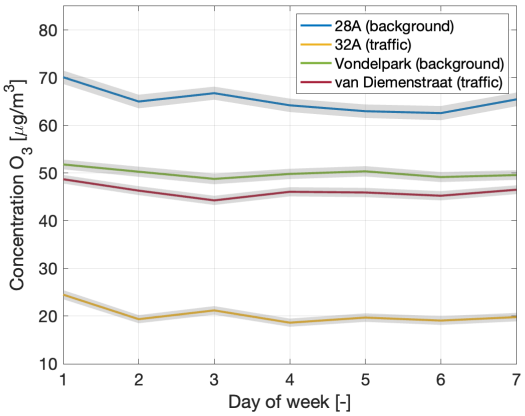

Figure 4.10: Average O_3 concentration per day of week. The 95% confidence interval has been annotated in grey.

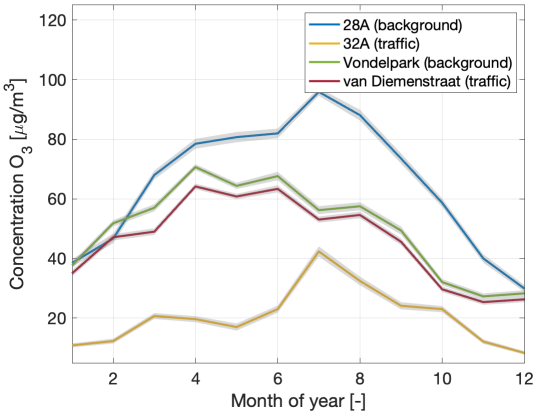

Figure 4.11: Average O_3 concentration per month of year. The 95% confidence interval has been annotated in grey.

At all stations, a peak in O_3 concentration is obtained during the afternoon because of its formation under sunlight. The highest O_3 concentration is obtained at the background station in Athens. Similar to NO_2, concentrations of O_3 are lower in the Netherlands than in Athens.

For the days of the week, a small increase is found during the weekend days. This demonstrates the non-linear effect on O_3 concentration when NO_2 concentration decreases. When looking at the variation of the O_3 concentration with the months of the year, it can clearly be seen these are higher during the summer months. This is in line with the previous conclusions. We find that the highest O_3 concentrations are obtained in a later month in Athens than in the Netherlands, which is explained by the fact that the highest number of sunshine hours occurs later in the year in Athens compared to the Netherlands.

Overall, the O_3 concentrations in Athens and the Netherlands are respectively moderate and fair. We should monitor these at both locations to ensure no dangerously high concentrations are present in the air.

4.1.4. SO_2 CONCENTRATION

The SO_2 concentrations per hour of day, day of week and month of year can be found found in figure 4.12, figure 4.13 and figure 4.14. Less data was available for the SO_2 concentration: the periods of the background and traffic data respectively resemble 2014-March 2015 and 2015. The 95% confidence intervals have been included in grey. The confidence interval is greater than for other measurements caused by the smaller number of data.

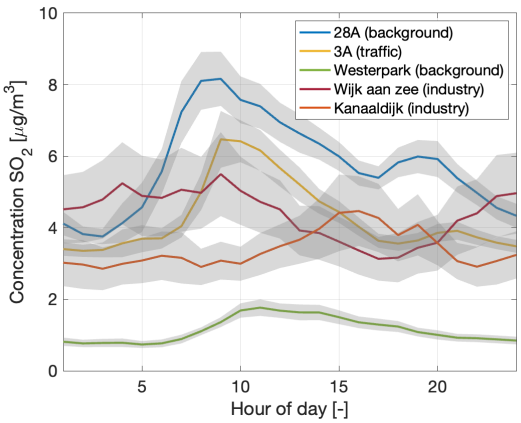

Figure 4.12: Average SO_2 concentration per hour of day. The 95% confidence interval has been annotated in grey.

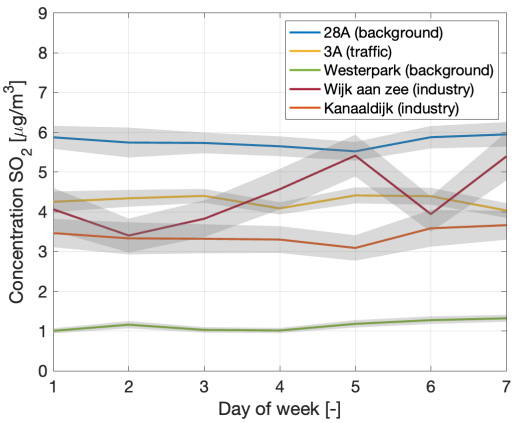

Figure 4.13: Average SO_2 concentration per day of week. The 95% confidence interval has been annotated in grey.

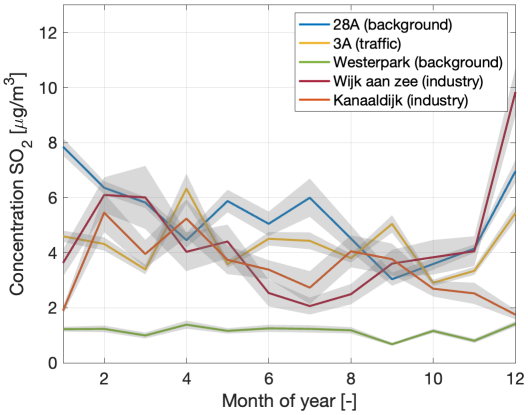

Figure 4.14: Average SO_2 concentration per month of year. The 95% confidence interval has been annotated in grey.

The highest SO_2 concentrations are obtained at the background station in Athens. This is spectacular, as measurements in the Netherlands were taken at very polluting industry location. In Athens, no trend can be found with the hour of day. In the Netherlands, SO_2 concentrations are significantly higher at the industry measurement stations than the background measurement station. Therefore, it can be concluded that industry greatly influences SO_2 concentration. For the measurement stations in Athens, an increase is found during the morning. It is expected that traffic has some influence on the SO_2 concentration.

At all locations except for Wijk aan Zee, the SO_2 concentration is almost constant with day of week. It is therefore hard to find conclusions here and this might again have to do with the low number of data which was available. Similarly, no conclusion can be found for the SO_2 concentration trend with month of year. Overall, we find that industry greatly impacts SO_2 concentration.

All in all, the SO_2 concentrations are at a good level for both Athens as well as for the Netherlands. The lack of data should be mentioned here as this might have had influence on the evaluation of the results.

4.1.5. $PM_{2.5}$ CONCENTRATION

The results per hour of day, day of week and month of year for a traffic and background measurement station of the $PM_{2.5}$ concentration can respectively be found in figure 4.15, figure 4.16 and figure 4.17. It should be noted that the background station is more remotely located than previously used background stations due to a lack of data. This will play a role as not only less traffic, but also less other polluting sources are present. The 95% confidence intervals have been included in grey.

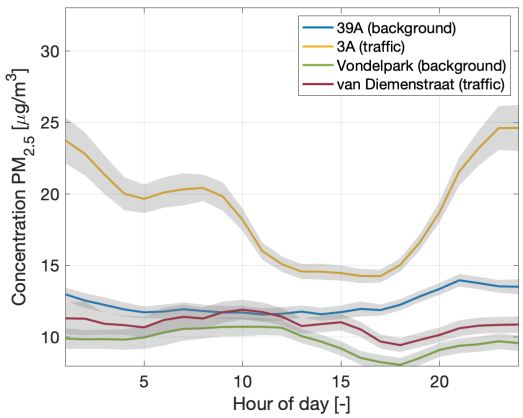

Figure 4.15: Average $PM_{2.5}$ concentration per hour of day. The 95% confidence interval has been annotated in grey.

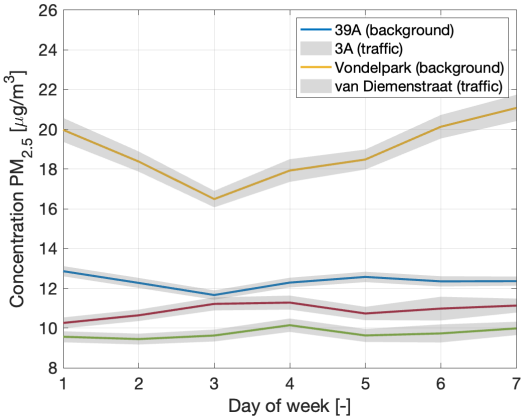

Figure 4.16: Average $PM_{2.5}$ concentration per day of week. The 95% confidence interval has been annotated in grey.

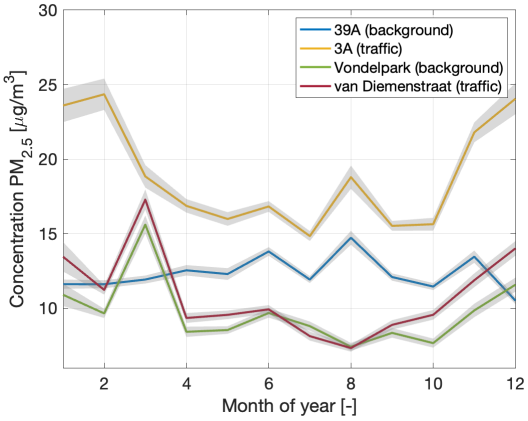

Figure 4.17: Average $PM_{2.5}$ concentration per month of year. The 95% confidence interval has been annotated in grey.

At the traffic measurement station in Athens, a clear increase in $PM_{2.5}$ concentration is found during the morning and evening. This is in line with the results obtained for the CO concentration. The $PM_{2.5}$ concentration at all other locations are significantly lower. At these stations, no similar trend is visible. All in all, it can be concluded that the $PM_{2.5}$ concentration is greatly determined by the presence of biomass burning and in lesser extent by the presence of traffic.

Looking into the data per day of week, it can be found that the $PM_{2.5}$ concentration is lower during the weekdays in Athens at the traffic station. At the other stations, no significant changes are found. This is in line with the results from the CO concentrations. The $PM_{2.5}$ concentration in Athens at the traffic station decreases during the summer months, as there will be less biomass burning in this period combined with a change in environmental conditions. A spectacular increase is found at both measurement stations in the Netherlands in March. It is unknown what the cause is of this event.

Overall, the air quality in Athens and the Netherlands can respectively be qualified as moderate and fair when only looking into the $PM_{2.5}$ concentration.

4.1.6. PM_{10} CONCENTRATION

The PM_{10} concentrations per hour of day, day of week and month of year can be found in respectively figure 4.18, figure 4.19 and figure 4.20. The 95% confidence intervals have been included in grey.

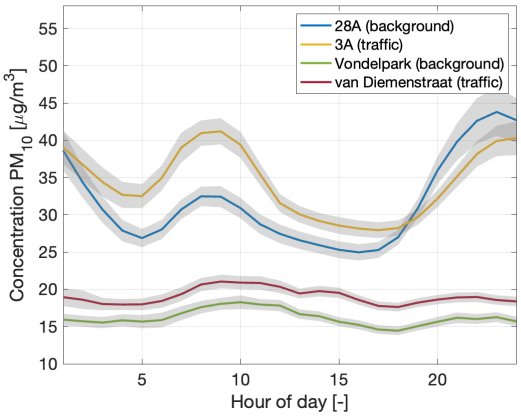

Figure 4.18: Average PM_{10} concentration per hour of day. The 95% confidence interval has been annotated in grey.

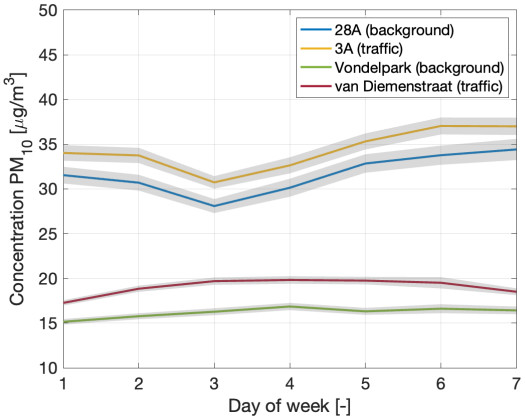

Figure 4.19: Average PM_{10} concentration per day of week. The 95% confidence interval has been annotated in grey.

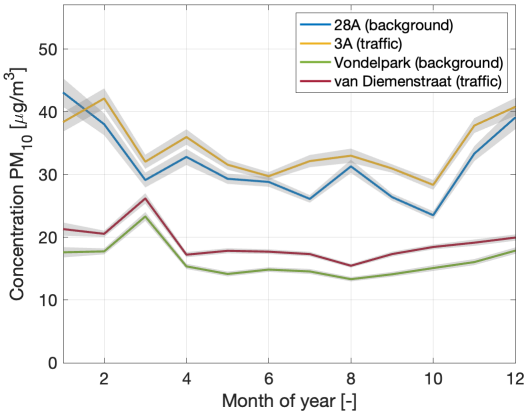

Figure 4.20: Average PM_{10} concentration per month of year. The 95% confidence interval has been annotated in grey.

The obtained PM_{10} concentration trends in Athens are quite similar to the results from the $PM_{2.5}$ concentration. Yet, the absolute concentrations are significantly higher. Here, the background station shows the same trend as the traffic station since this background station is located closer to urban activity. We observe that higher concentrations are recorded at the traffic station during the morning peak, whereas this is the case at the background station during the night. This has to do with traffic and biomass burning accounting for an increase in PM_{10} concentration. Moreover, the PM_{10} concentration tends to decrease faster than the $PM_{2.5}$ concentration, which has to do with the higher mass of the individual particles. At the measurement stations in the Netherlands, PM_{10} concentrations are quite constant.

The obtained PM_{10} concentrations are higher during the weekend in Athens, most likely due to the presence of urban activities such as cooking and heating during the weekend. In the Netherlands, PM_{10} concentrations are mainly determined by traffic, and therefore slightly decrease during the weekend days.

A decrease in PM_{10} concentration is found during the summer months for the measurement stations in Athens. This has to do with less heating during the summer months and therefore less biomass burning. For the measurement stations in the Netherlands, results are quite constant, apart from a peak found in March. This peak was also found for the $PM_{2.5}$ concentration. The exact cause remains unknown.

Overall, the PM_{10} concentration results in a moderate air quality level in Athens and a fair one in the Netherlands.

4.1.7. OVERVIEW

It can be concluded that the NO_2 concentration in Athens is mainly determined by traffic. This has an indirect effect on O_3, since NO_2 is a precursor of O_3. Yet, the amount of sunlight has the greatest effect on the

O_3 formation. The SO_2 concentration is mainly determined by industrial activities, although other factors such as traffic also have some effect on it. CO, $PM_{2.5}$ and PM_{10} concentrations are all greatly influenced by biomass burning and other urban sources. Traffic determines these concentrations in a lesser extent. Aside from these, other environmental factors should not be forgotten.

It should be noted that the conclusions above are found in Athens only. In the Netherlands for example, biomass burning happens less than in Athens and therefore $PM_{2.5}$ and PM_{10} are relatively more determined by traffic than biomass burning.

4.2. VALIDATION MEASUREMENTS

In March 2024, a number of validation measurements were carried out. The response time of the air quality sensors, the measured values from both the air quality sensors and the temperature sensor of the Sniffer4D Mini 2, and the wind algorithm developed by Airdata were investigated. We flew at different vertical speeds to find out if this had any effect on the accuracy of the measurements.

The following measurements were carried out between 12.00 and 14.00:

- 0.2 m/s vertical speed with stop every 20 m
- 0.2 m/s vertical speed without stop
- 0.8 m/s vertical speed without stop
- 0.4 m/s vertical speed without stop

Due to limited battery capacity, the last part of the measurements was sometimes flown at a slightly higher speed. The upward movement is therefore most reliable. Furthermore, the temperature was stabilised after the drone had taken off to account for external influences.

Firstly, we compare the concentrations found by the KMNI Cabauw measurement station with the measured concentrations of the Sniffer4D Mini 2. This KNMI Cabauw measurement station is a 213 m high tower which measures meteorological conditions (e.g. temperature and wind) at several altitudes. It can be seen in figure 4.21. Secondly, we investigate the response time of the sensors measured by starting a car engine. Hereafter, we look at the temperature profile of the Sniffer4D Mini 2 and its correlation with the KNMI Cabauw measurement station. We end with the wind speed and direction through comparison of the Airdata estimation and KNMI Cabauw measurement station data.

Figure 4.21: KNMI Cabauw measurement station. At the tower, meteorological conditions are measured from 0 to 213 m altitude [2].

4.2.1. ABSOLUTE CONCENTRATIONS

A comparison has been made between the air quality concentrations measured by the Sniffer4D Mini 2 and the KNMI Cabauw measurement station. For the Sniffer4D Mini 2, measurement data between 5 and 10 m altitude has been used. The KNMI measurement data is the average of 10 minutes of data and has been obtained at an altitude of 3 m. The comparison of NO_2, SO_2, O_3, $PM_{2.5}$ and PM_{10} concentrations can be found in respectively figure 4.22, figure 4.23, figure 4.24, figure 4.25 and figure 4.26. A 95% confidence interval has been included for the Sniffer4D Mini 2 data sets to show their variability. The CO concentration has been excluded here because of its zero readings.

We observe that the measured NO_2 and SO_2 concentrations, which traffic can be the source of, are about 4 times as high for the Sniffer4D Mini 2 in comparison to the KNMI measurement station. The Sniffer4D Mini

2 measured closer to a road with traffic than the KNMI measurement station; this could explain explain why higher concentrations were measured with the Sniffer4D Mini 2.

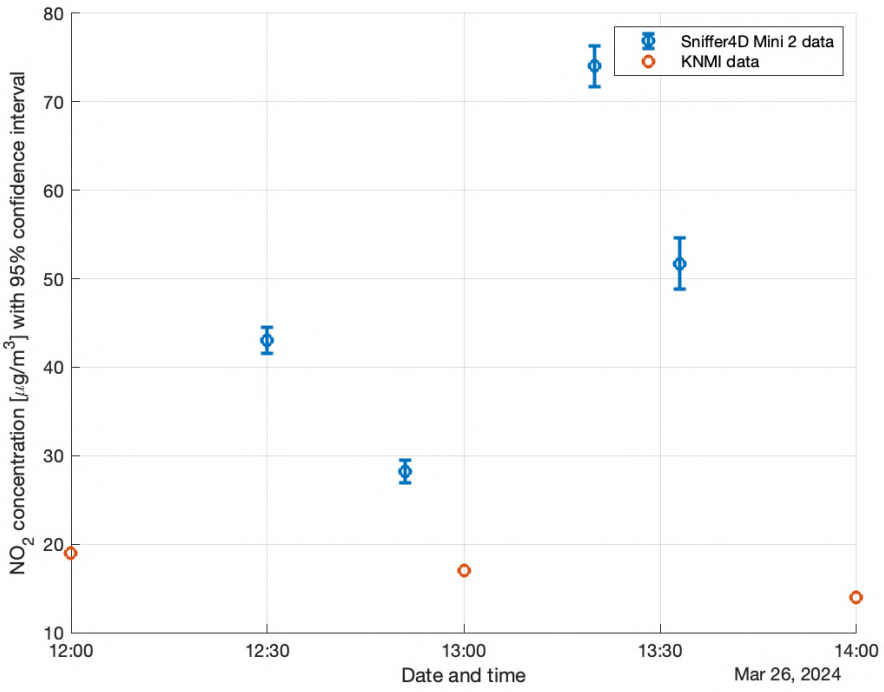

Figure 4.22: NO_2 concentration comparison. The 95% confidence interval has been included for the Sniffer4D Mini 2 data.

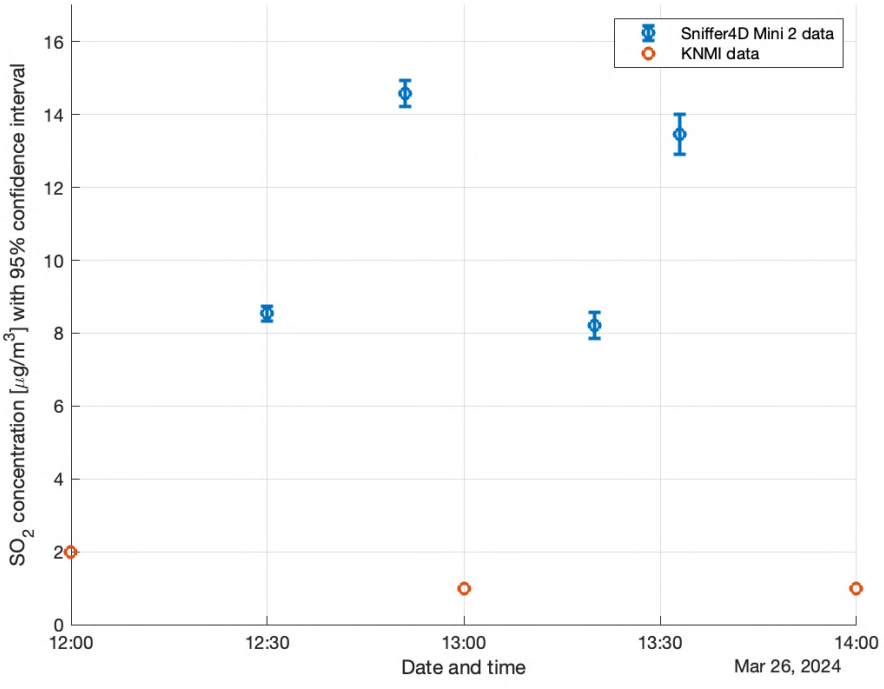

Figure 4.23: SO_2 concentration comparison. The 95% confidence interval has been included for the Sniffer4D Mini 2 data.

The other air quality concentrations, O_3, $PM_{2.5}$ and PM_{10}, are somewhat higher for the Sniffer4D Mini 2 than the KNMI measurement station; a factor of 1.5 to 2 is typically found. Overall, we thus find that the Sniffer4D

Mini 2 measures higher concentrations than the KNMI measurement station. An explanation could be that the KNMI measurement station is an average over 10 minutes, whereas the Sniffer4D Mini 2 is the average of less than 1 minute. Another conclusion found here is that the measured concentrations vary greatly with the exact location measured at. The Sniffer4D Mini 2 is calibrated at 20 °C, significantly higher than the temperature on the day of the validation measurements. Although it makes use of temperature algorithms, there will still be an impact on the recordings. Most likely, a combination of these environmental factors can be seen as an explanation why the measured concentrations differ.

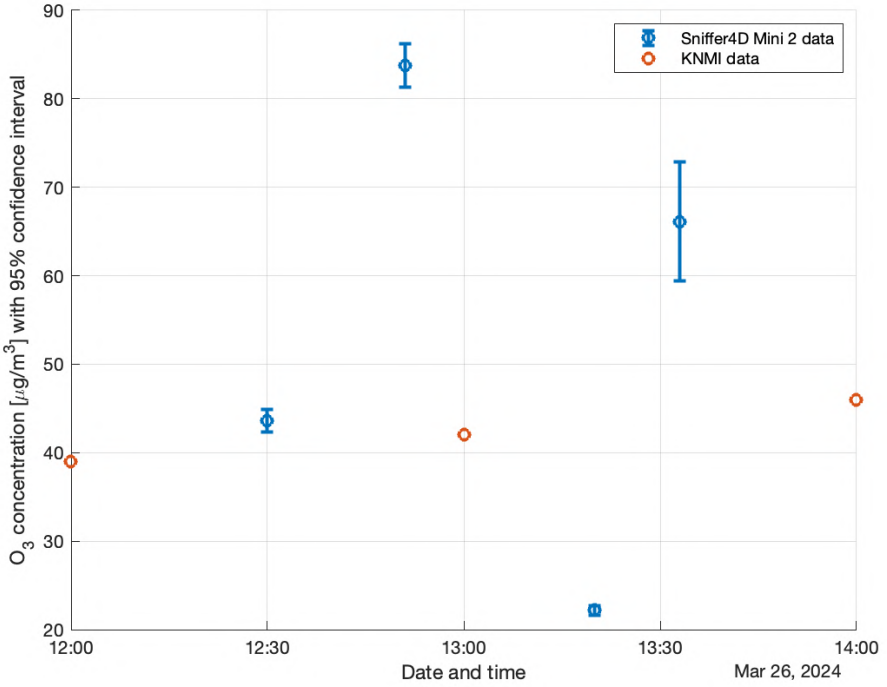

Figure 4.24: O_3 concentration comparison. The 95% confidence interval has been included for the Sniffer4D Mini 2 data.

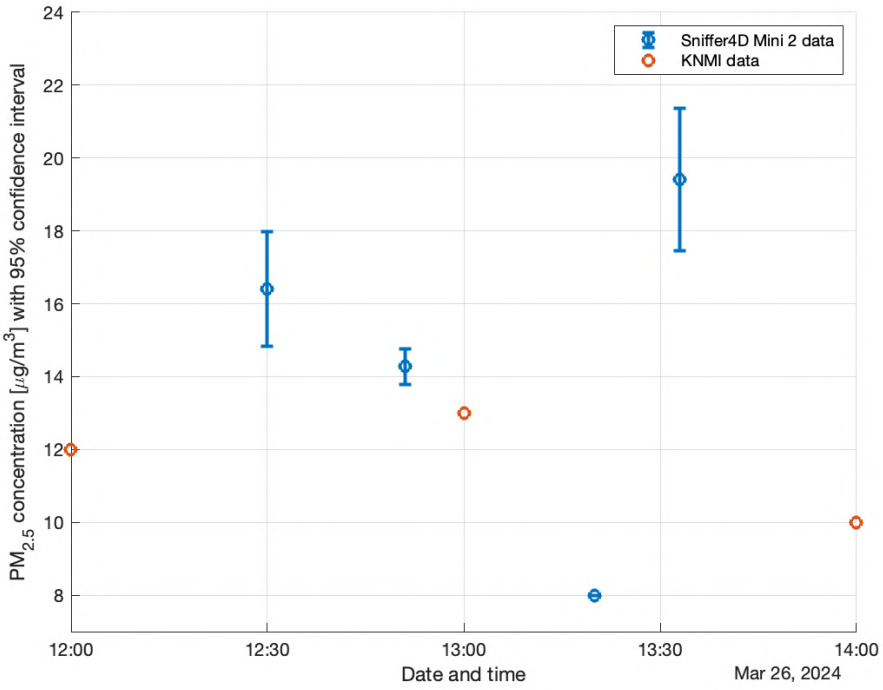

Figure 4.25: $PM_{2.5}$ concentration comparison. The 95% confidence interval has been included for the Sniffer4D Mini 2 data.

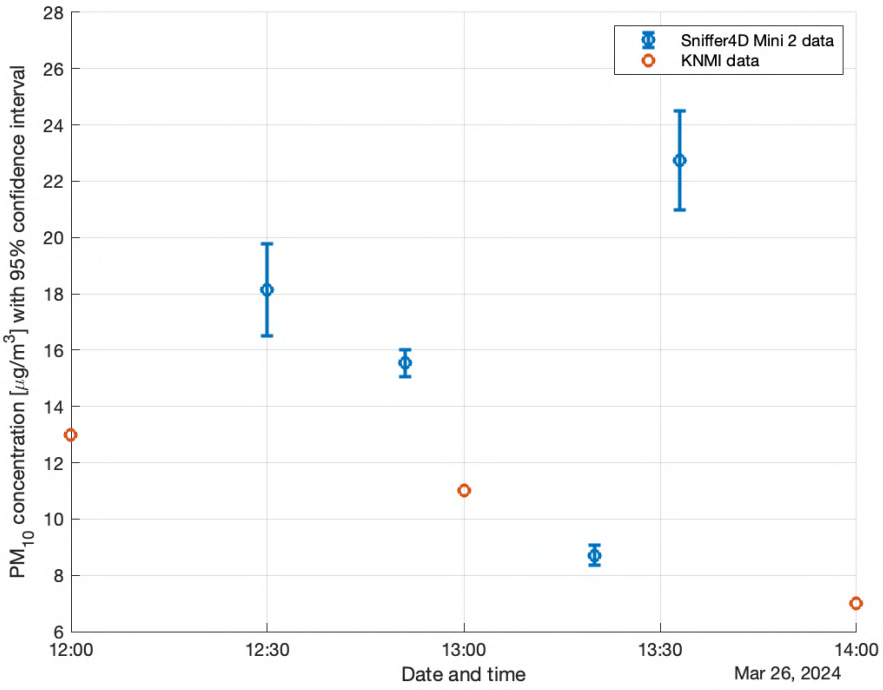

Figure 4.26: PM_{10} concentration comparison. The 95% confidence interval has been included for the Sniffer4D Mini 2 data.

4.2.2. RESPONSE TIME SENSORS

The response time of the different sensors in the Sniffer4D Mini 2 can be found in table 4.2. The $PM_{2.5}$ and PM_{10} concentrations are measured using the same sensor. Moreover, the O_3 concentration is found by subtracting the concentration of the NO_2 sensor from the NO2 + O_3 sensor. The response times are listed for a relative high change in concentration; the measured changes in concentration during the measurements are

much smaller than the listed values. Therefore, the response time of the sensors to a diesel car starting has been measured. The Sniffer4D Mini 2 was placed about 30 cm from its exhaust.

Sensor	Response time [s]
NO_2	<60s to 2ppm
NO	<60s to 10ppm
$NO_2 + O_3$	<45s to 1ppm
SO_2	<40s to 2ppm
CO	<20s to 10ppm
Particulate matter	<10s

Table 4.2: Response time of sensors.

In figure 4.27, the response of the NO_2 sensor to a diesel car starting can be seen. Although the NO_2 concentration increases, we cannot conclude whether this comes from the emission of the car or a shift in temperature (which was still stabilising at the time).

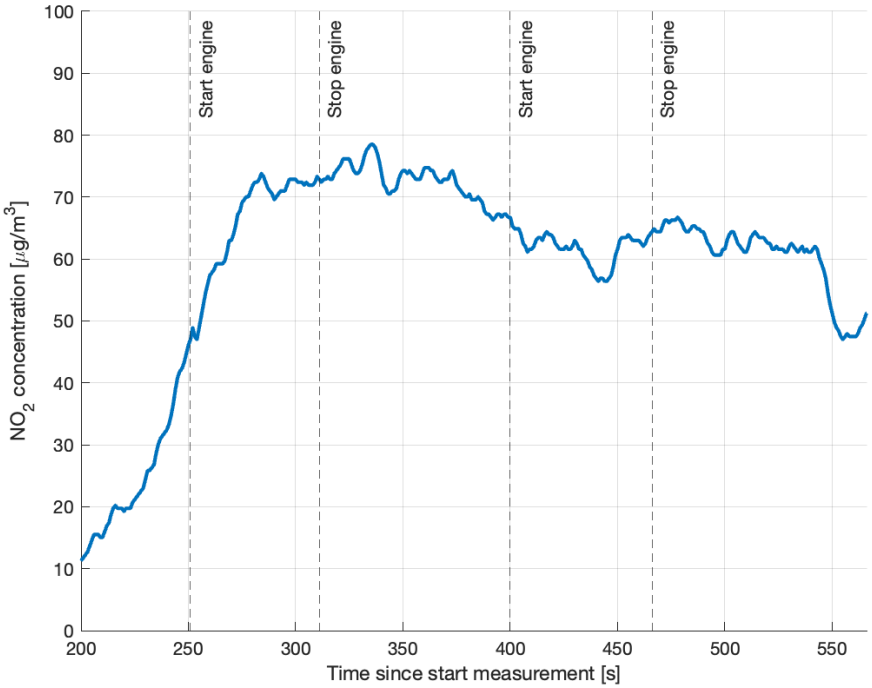

Figure 4.27: NO_2 concentration response to engine. Moments engine started & stopped have been indicated.

The NO sensor was contaminated, resulting in very high measured concentrations. As can be seen in figure 4.28, it is still stabilising. However, an immediate response can be seen when the car starts.

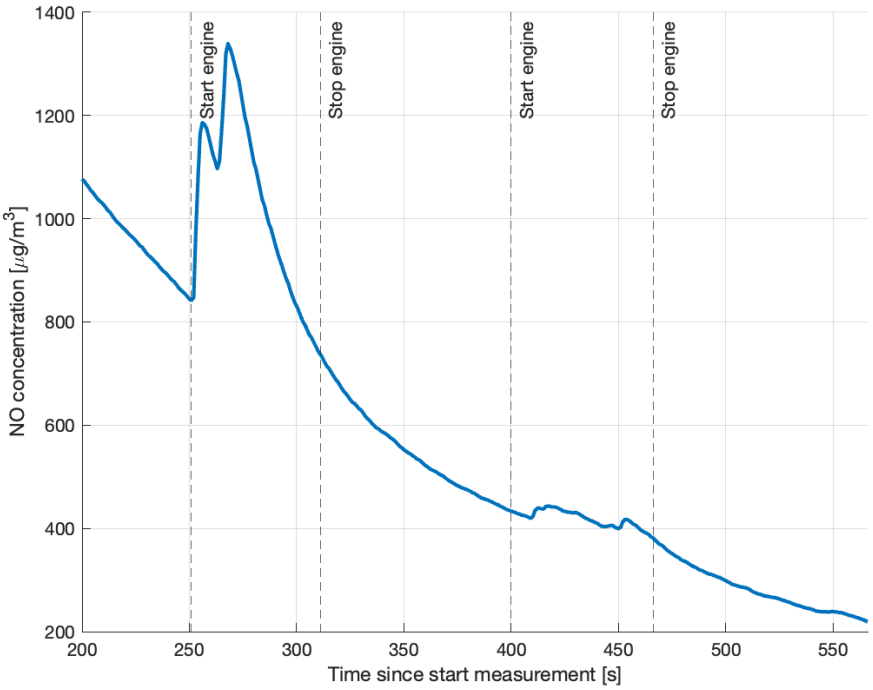

Figure 4.28: NO concentration response to engine. Moments engine started & stopped have been indicated.

Although the measured CO concentration is often zero, due to the threshold of the sensor, a peak can be found immediately after the car has been turned on as seen in figure 4.29. It returns to zero once the engine of the car is stopped.

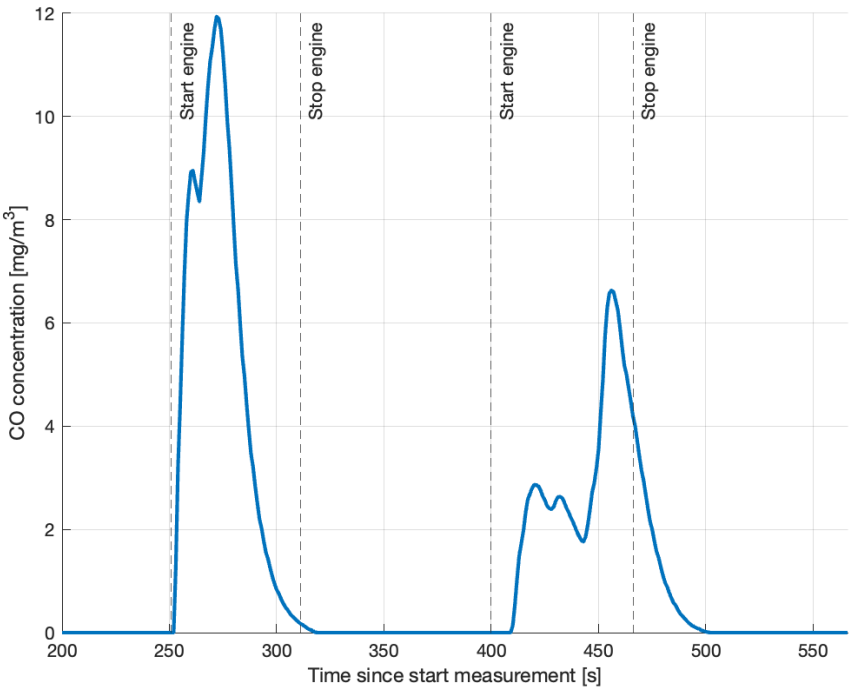

Figure 4.29: CO concentration response to engine. Moments engine started & stopped have been indicated.

The response of the SO_2 sensor to a starting engine can be seen in figure 4.30. The measured SO_2 strongly increases immediately after the engine of the car has been started. Once the engine has been turned off, the measured SO_2 strongly decreases again.

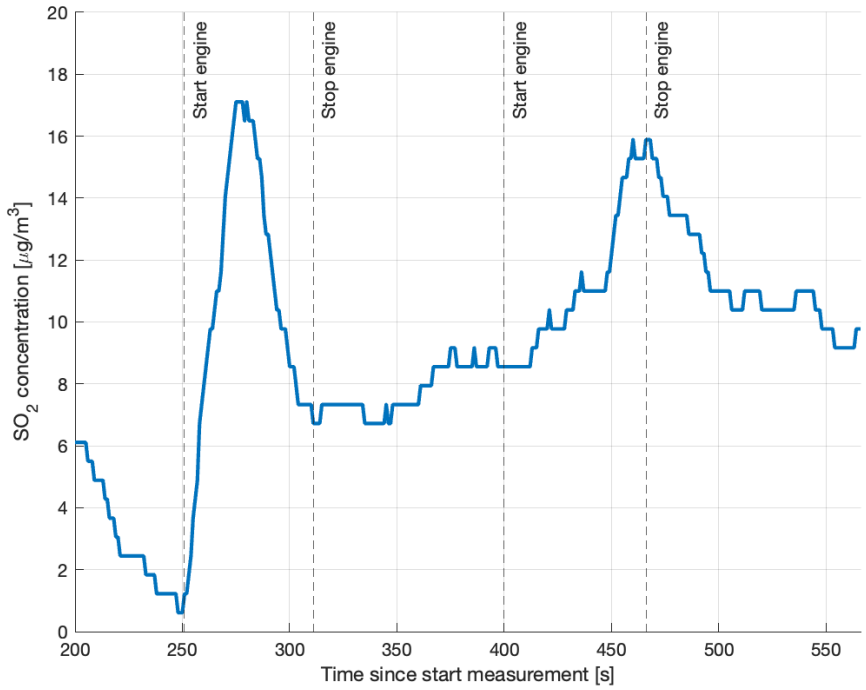

Figure 4.30: SO_2 concentration response to engine. Moments engine started & stopped have been indicated.

No clear increase of the $PM_{2.5}$ concentration as a result of the starting engine can be found in figure 4.31. It is assumed that the diesel car does not emit enough $PM_{2.5}$ to show an increase in the readings of the sensor. Therefore, we have decided to not include the reaction of the PM_{10} sensor here, as this is similar to the $PM_{2.5}$ sensor.

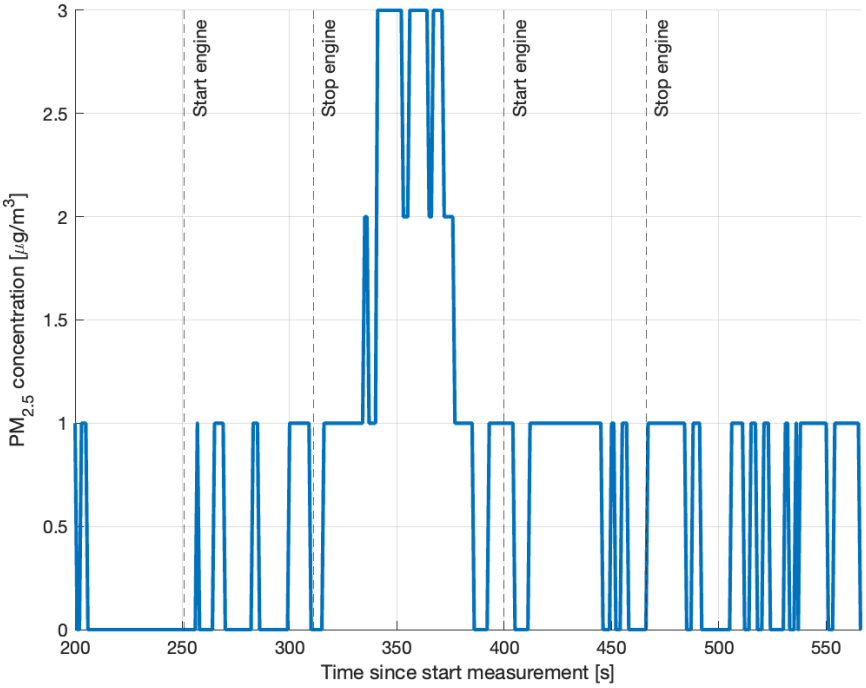

Figure 4.31: $PM_{2.5}$ concentration response to engine. Moments engine started & stopped have been indicated.

We have seen that most sensors response quickly (less than 5 seconds) to changes in the air composition caused by a starting diesel car. The other sensors do not show an increase because the pollutants they detect

are not present in the exhaust gases. All in all, stopping at certain altitudes is not necessary as the sensors are capable of measuring the changes in concentration when flying up- or downwards at a reasonable speed (less than 0.8 m/s).

4.2.3. TEMPERATURE ACCURACY SNIFFER4D MINI 2

Comparisons have been made of the temperature profile measured with the Sniffer4D Mini 2 and the KNMI measurement station. Different flying speeds have been evaluated in order to find out if this has an effect on the accuracy.

An overview with the Pearson correlation coefficients (R) obtained during both upward as well as downward flight can be found in table 4.3. The comparison of the temperature profile for a vertical flying speed of 0.8 m/s can be found in figure 4.32.

Flying speed [m/s]	R temperature upwards [-]	R temperature downwards [-]
Hover at every 20 m altitude	0.95	0.96
0.2	0.90	0.77
0.4	0.88	0.91
0.8	0.98	0.63

Table 4.3: Pearson correlation coefficients of temperature for different flying speeds. Results from both the upward as well as downward part of the flights have been included.

High Pearson correlation coefficients are obtained during the upwards flight phase for all flight speed. During the downward flight phase, some of the found Pearson correlation coefficients are lower. This is caused by an increase in flying speed towards the end of the flight as the battery was almost dead.

Overall, the flying speed does not have a impact on the correlation coefficient as long as it is kept below 0.8 m/s.

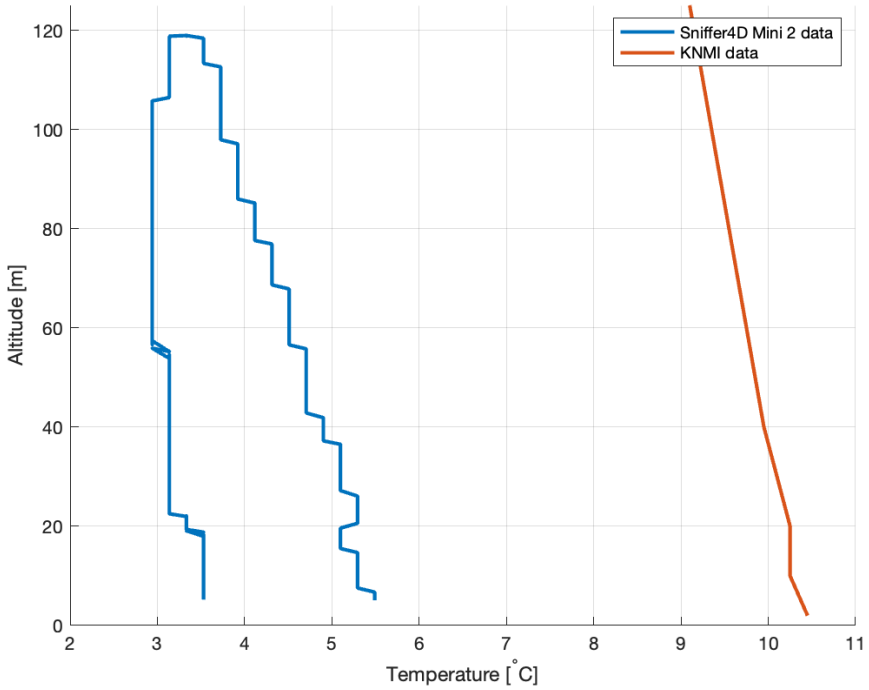

Figure 4.32: Temperature profile comparison for vertical flight at 0.8 m/s. Both the upward as well as downward part of the flight have been included.

4.2.4. WIND SPEED & DIRECTION ACCURACY AIRDATA

The estimated wind speed by the Airdata algorithm has been compared to the KNMI measurement data for the same flight speeds as earlier discussed. We look at the upward phase of the flight, since the battery was

sometimes empty at the end of the flight resulting in higher flight speeds. Again, the Pearson correlation coefficients can be found in table 4.4. Moreover, a comparison of the wind speeds from Airdata and the KNMI data has been visualised and is shown in figure 4.33 for a flying speed of 0.8 m/s. For better readability, a moving average filter with a window size of 5 has been used for the results of Airdata.

Flying speed [m/s]	**R wind speed [-]**
Hover at every 20 m altitude	0.86
0.2	0.61
0.4	0.62
0.8	0.80

Table 4.4: Pearson correlation coefficients for wind speed at different flying speeds. Only results from the upward part of the flights have been included.

No relation is found between the flying speed and the accuracy of the wind speed estimation. All flight speeds obtain good Pearson correlation coefficients, which are enough to resemble the effect of the wind speed. The Airdata wind speeds are typically higher than the ones from the KNMI data. Yet, the KNMI data is an average taken over 10 minutes, which explains this overestimation. The wind speeds from Airdata have a relative high variability compared to the KNMI data. Moreover, higher wind speeds are measured at higher altitudes.

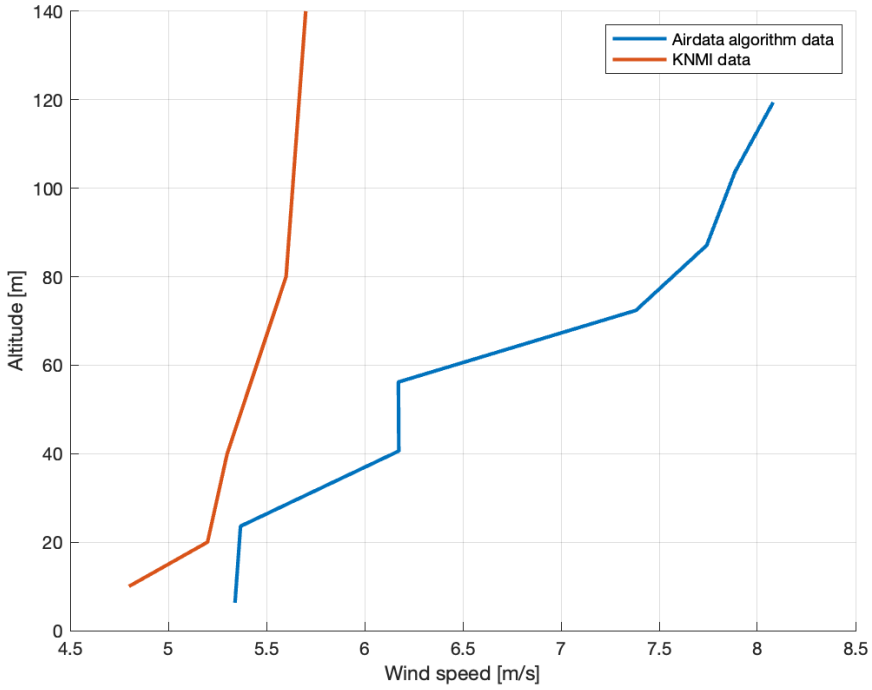

Figure 4.33: Wind speed comparison with a vertical flying speed of 0.8 m/s. Only the upward phase of the flight has been included.

The estimated wind direction has been compared as well, as can be found in table 4.5. Again, the accuracy of the results from Airdata is not dependent on the flying speed. Overall, Airdata is well capable of estimating the wind direction.

Flying speed [m/s]	**Average wind direction Airdata [°]**	**Average wind direction KNMI [°]**	**Difference [°]**
Hover at every 20 m altitude	141	152	11
0.2	146	139	7
0.4	155	156	1
0.8	146	149	3

Table 4.5: Average and difference between wind direction from Airdata and KNMI measurement station at different flying speeds. Only results from the upward part of the flights have been included.

A comparison of the wind direction from Airdata and the KNMI data has been visualised and is shown in figure 4.34 for a flying speed of 0.8 m/s. A moving average filter with a window size of five has been used for the results of Airdata. Both results show the same trend with increasing altitude.

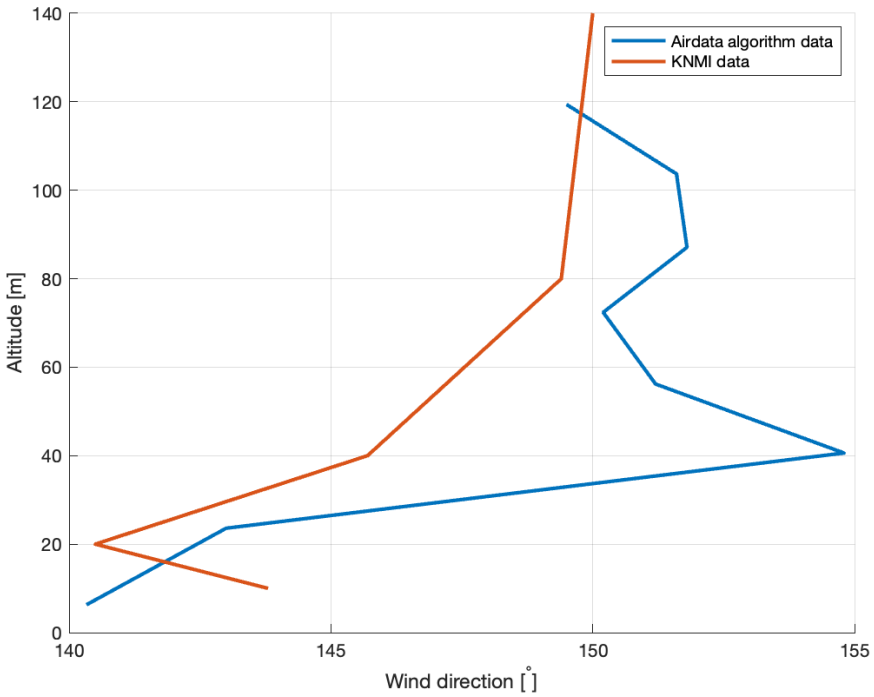

Figure 4.34: Wind direction comparison with a vertical flying speed of 0.8 m/s. Only the upward phase of the flight has been included.

4.3. MEASUREMENTS ATHENS

This section discusses all the point and continuous measurements carried out during the measurement campaign in Aigaleo (Athens) in February 2024. During another measurement campaign on drone noise in May 2024, some extra measurements were obtained. These will be shortly touched upon as well.

4.3.1. POINT MEASUREMENTS

An overview of all point measurements can be found in table 4.6. All flights were carried out at a speed of 0.8 m/s, except for B* and B**; these were respectively carried out at respectively a vertical speed of 0.4 m/s and while hovering for 30 seconds at every 10 m altitude.

Day	Time	Location
19/02/2024	10:52	A
19/02/2024	14:29	A
19/02/2024	16:32	A
20/02/2024	13:01	A
20/02/2024	14:46	A
20/02/2024	17:05	A
19/02/2024	11:05	B
19/02/2024	14:46	B
19/02/2024	16:48	B
20/02/2024	10:27	B*
20/02/2024	10:59	B**
20/02/2024	12:52	B
20/02/2024	16:02	B
19/02/2024	11:13	C
19/02/2024	15:06	C
19/02/2024	17:00	C
20/02/2024	12:31	C
20/02/2024	15:47	C
19/02/2024	11:34	D
19/02/2024	15:26	D
19/02/2024	17:12	D
20/02/2024	12:16	D
20/02/2024	15:30	D
19/02/2024	11:46	E
19/02/2024	15:38	E
19/02/2024	17:21	E
20/02/2024	11:59	E
20/02/2024	15:08	E

Table 4.6: Overview of all point measurements with their respective time, day and location.

The downward movement of the drone is included in the results for the point measurements, as the temperature was still stabilising during the upward movement of the drone. Only the results between 5 and 119 m altitude are included since the temperature is more stable here. The results for the gaseous pollutants and particulate matter are filtered with a moving average filter of the five nearest neighbours on both sides. These are plotted per five points to improve readability of the graphs. Below, the results will only be shown and not further discussed, as often the temperature is not stable enough to find conclusions. In the research article, however, results with a stable enough temperature profile have been included to make sure we could find conclusions.

TEMPERATURE

The temperature variations with altitude of all measurements at locations A, B, C, D and E, can respectively be seen in figure 4.35, figure 4.36, figure 4.37, figure 4.38 and figure 4.39. Since the temperature affects the sensor readings, the temperature should be kept as constant as possible. Therefore, in the research article, only measurements have been included which have a temperature variation of less than 0.5 °C.

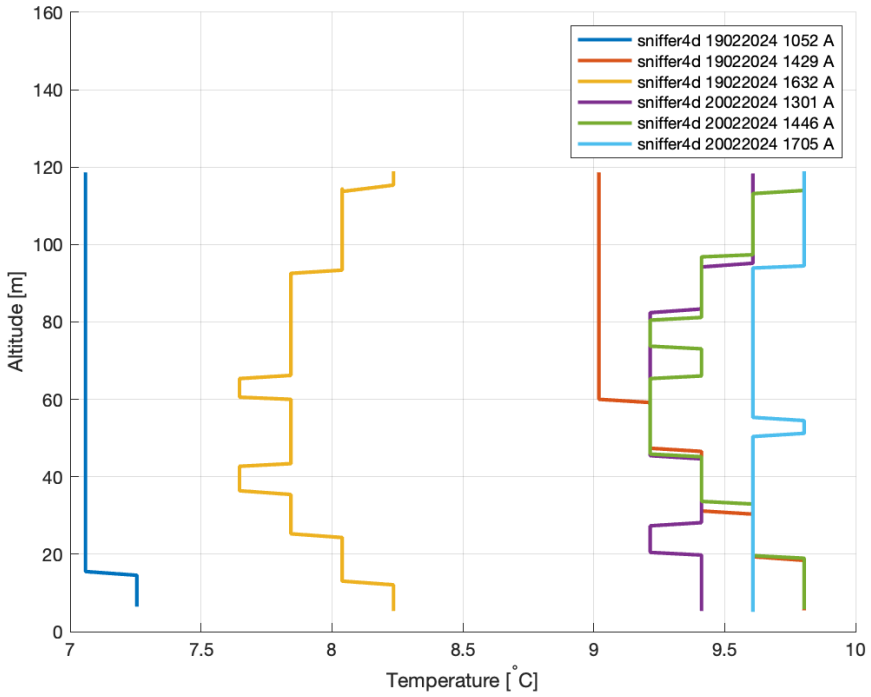

Figure 4.35: Temperature variation with altitude of all measurements at location A.

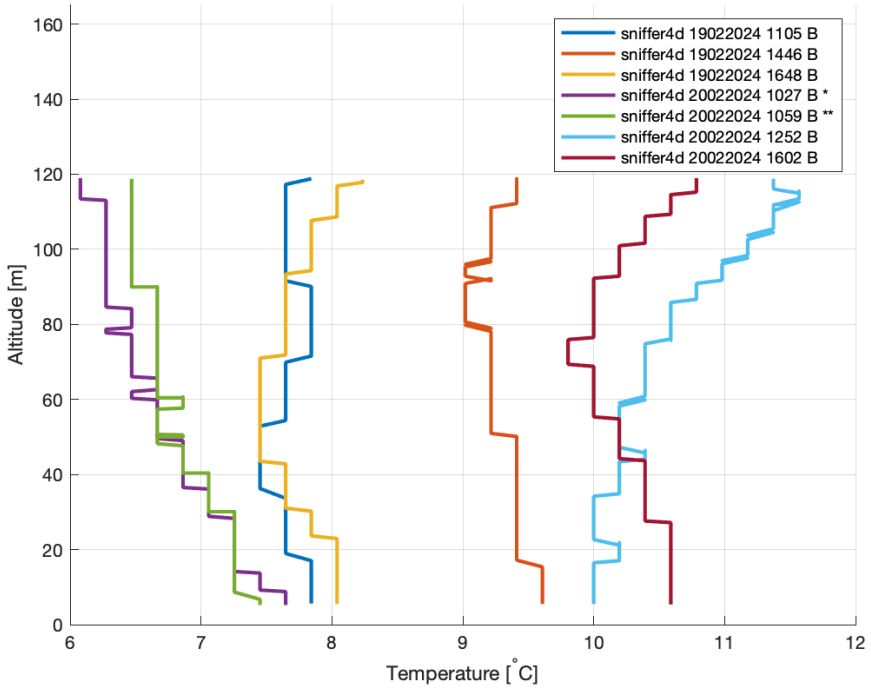

Figure 4.36: Temperature variation with altitude of all measurements at location B.

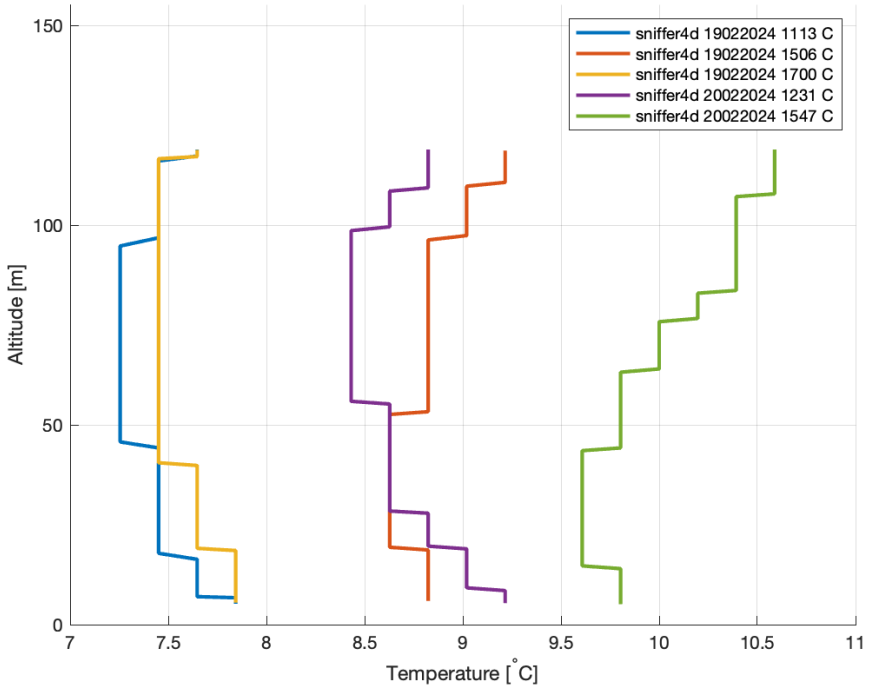

Figure 4.37: Temperature variation with altitude of all measurements at location C.

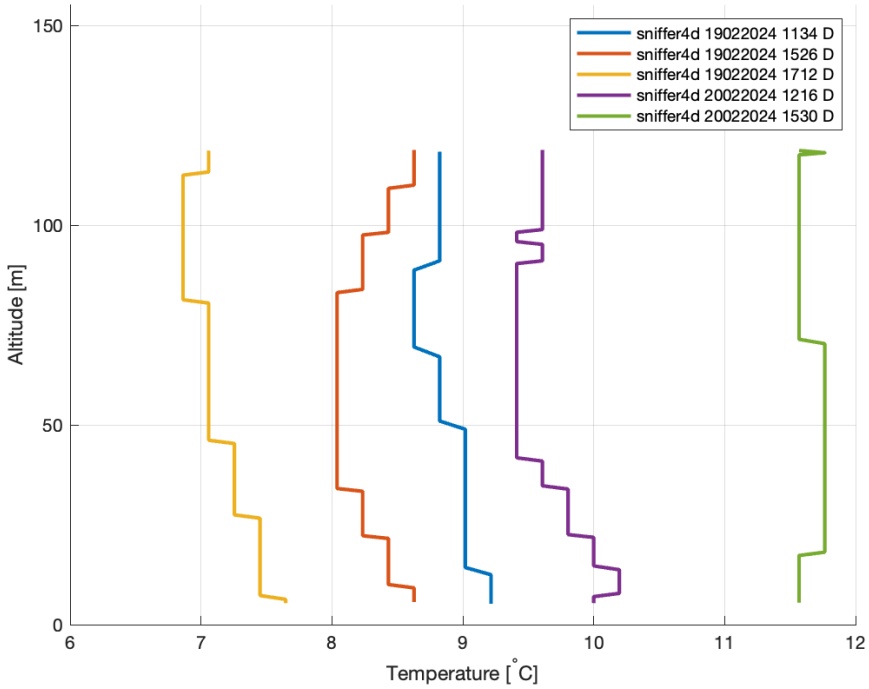

Figure 4.38: Temperature variation with altitude of all measurements at location D.

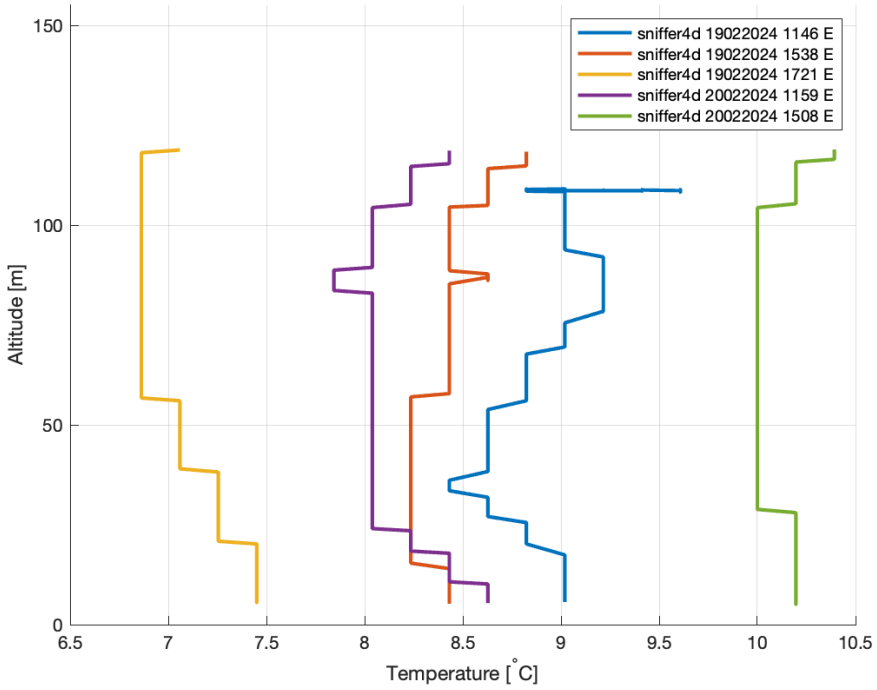

Figure 4.39: Temperature variation with altitude of all measurements at location E.

CO CONCENTRATION

The CO concentration variations with altitude of all measurements at locations A, B, C, D and E, can respectively be seen in figure 4.40, figure 4.41, figure 4.42, figure 4.43 and figure 4.44. Since the measured value is often zero, it is harder to find conclusions for this air pollutant.

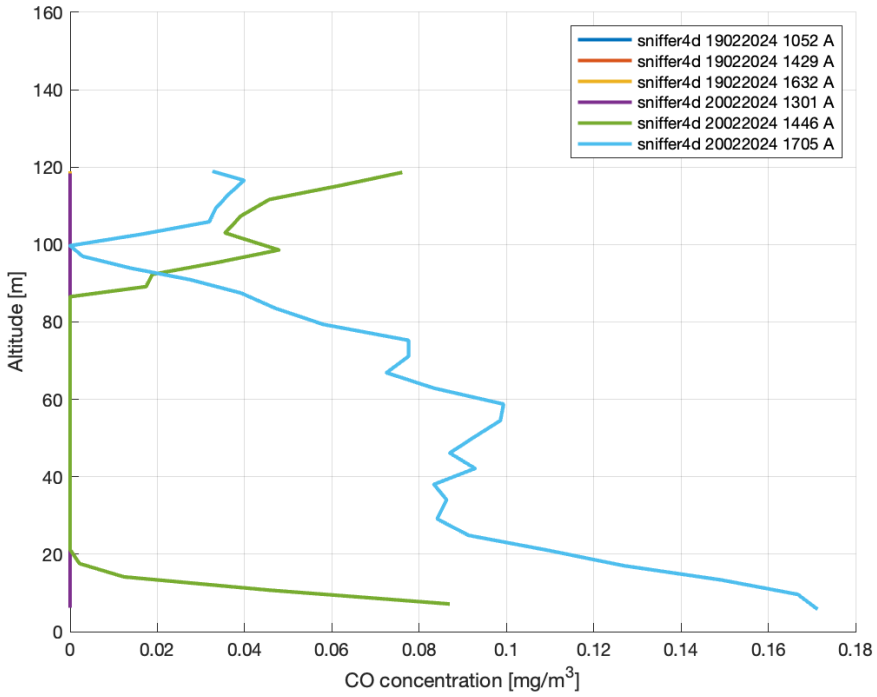

Figure 4.40: CO concentration variation with altitude of all measurements at location A.

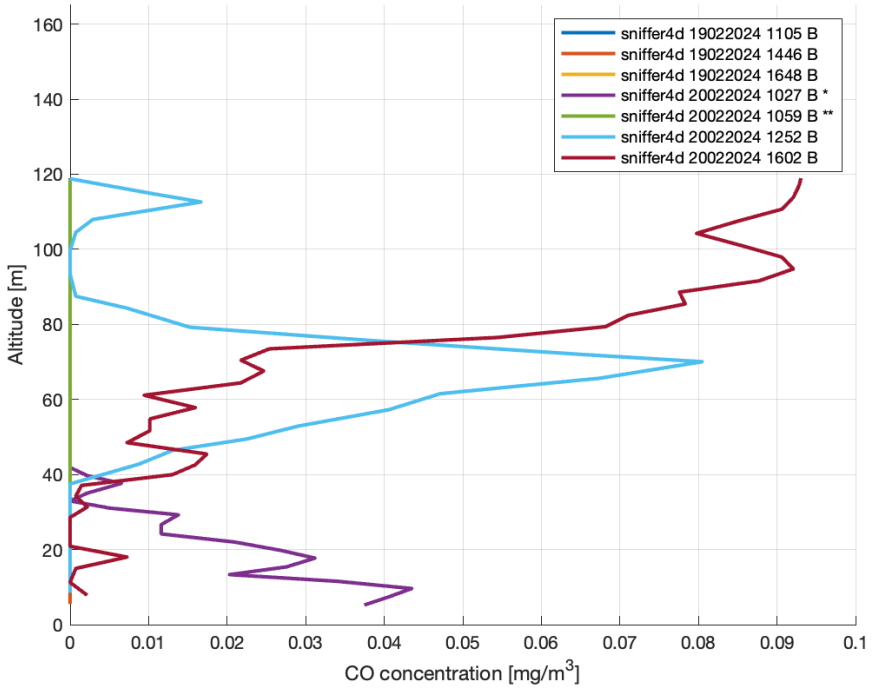

Figure 4.41: CO concentration variation with altitude of all measurements at location B.

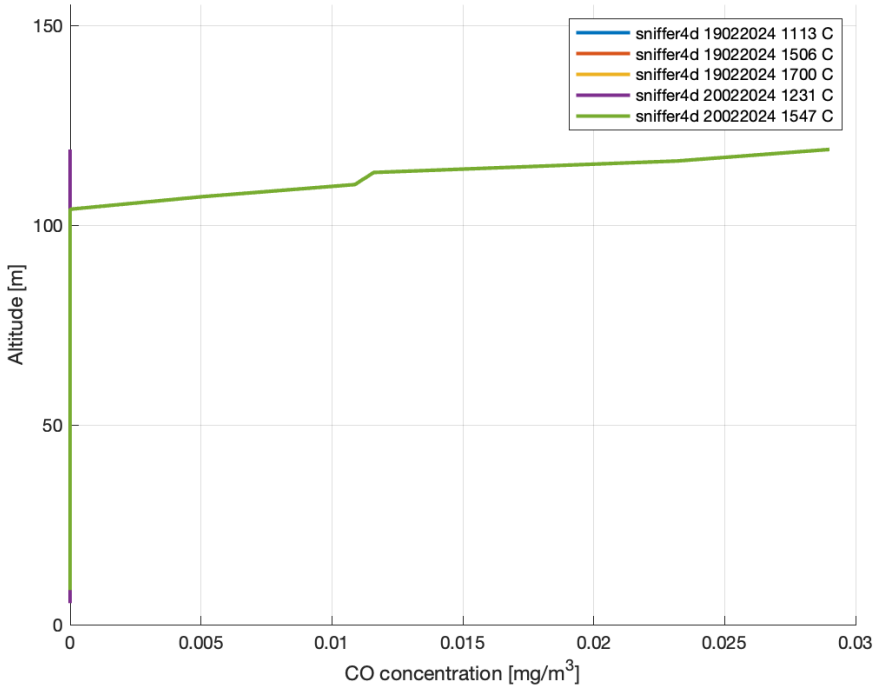

Figure 4.42: CO concentration variation with altitude of all measurements at location C.

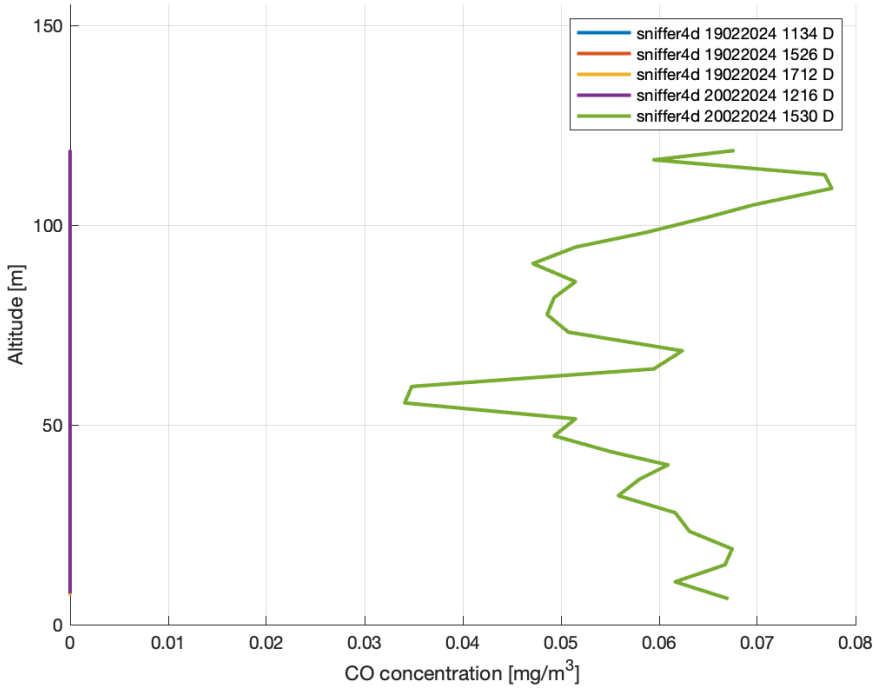

Figure 4.43: CO concentration variation with altitude of all measurements at location D.

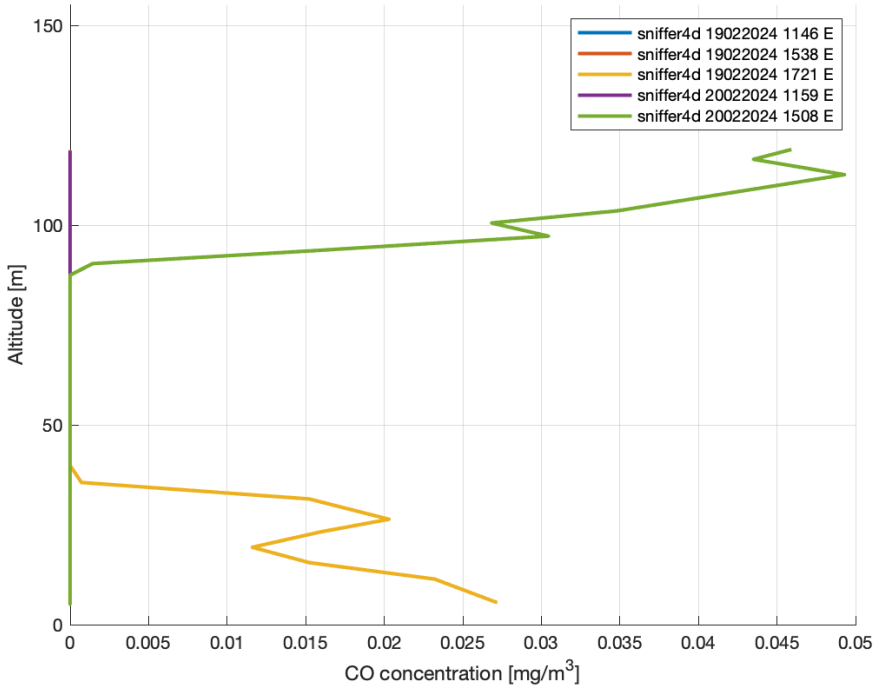

Figure 4.44: CO concentration variation with altitude of all measurements at location E.

NO_2 CONCENTRATION

The NO_2 concentration variations with altitude of all measurements at locations A, B, C, D and E, can respectively be seen in figure 4.45, figure 4.46, figure 4.47, figure 4.48 and figure 4.49.

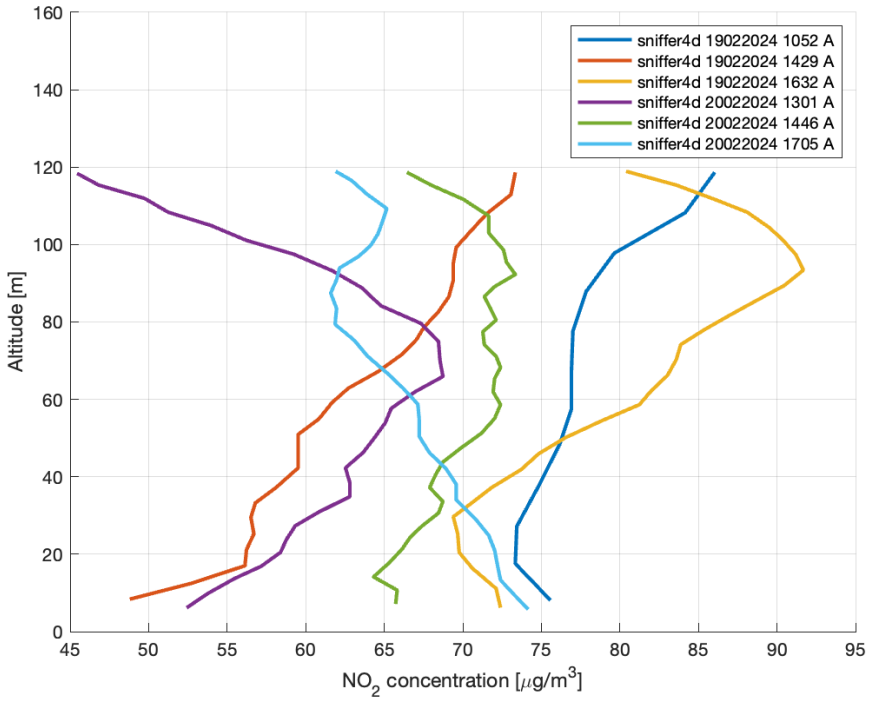

Figure 4.45: NO_2 concentration variation with altitude of all measurements at location A.

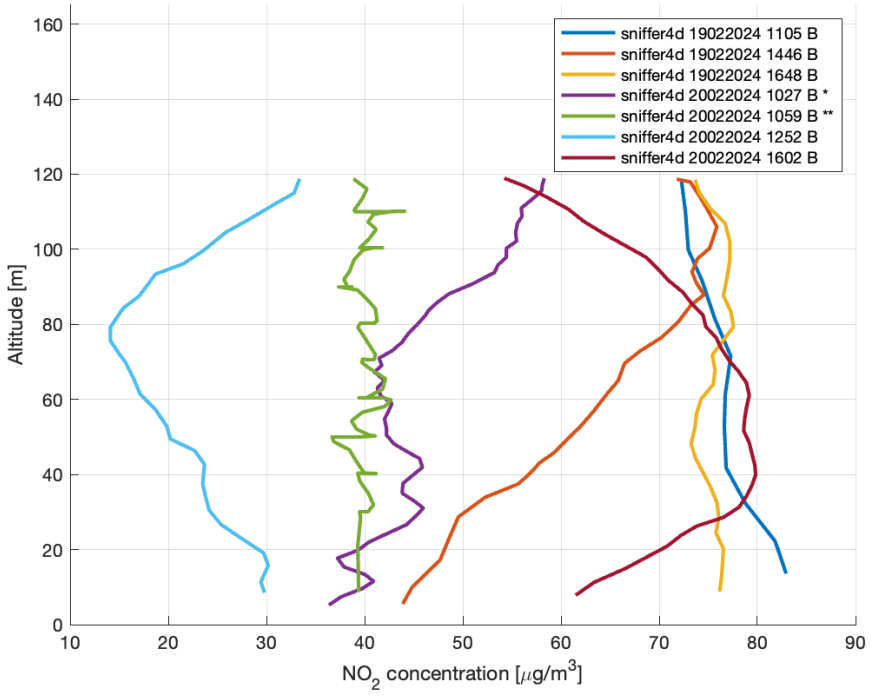

Figure 4.46: NO_2 concentration variation with altitude of all measurements at location B.

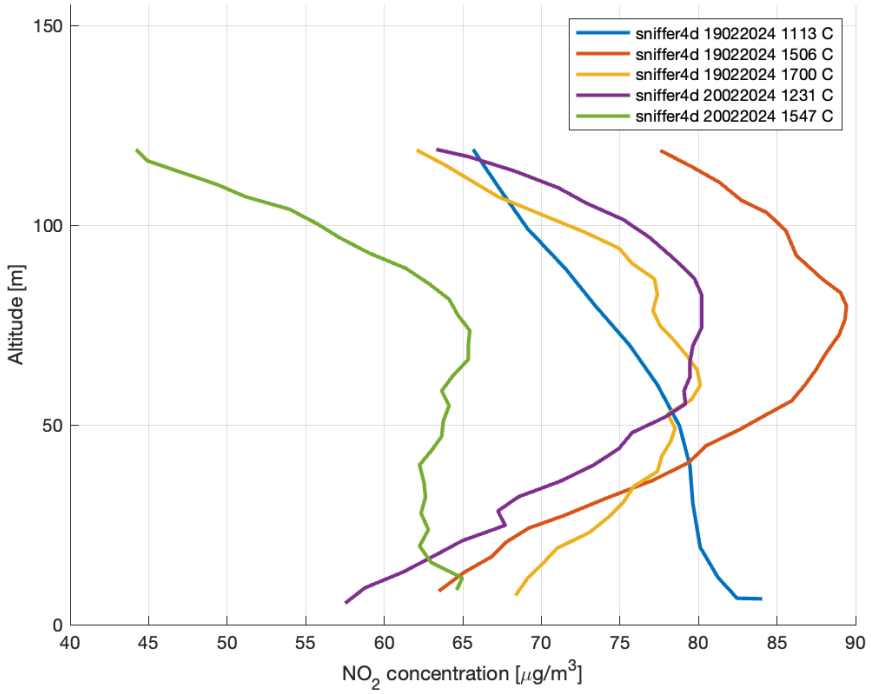

Figure 4.47: NO_2 concentration variation with altitude of all measurements at location C.

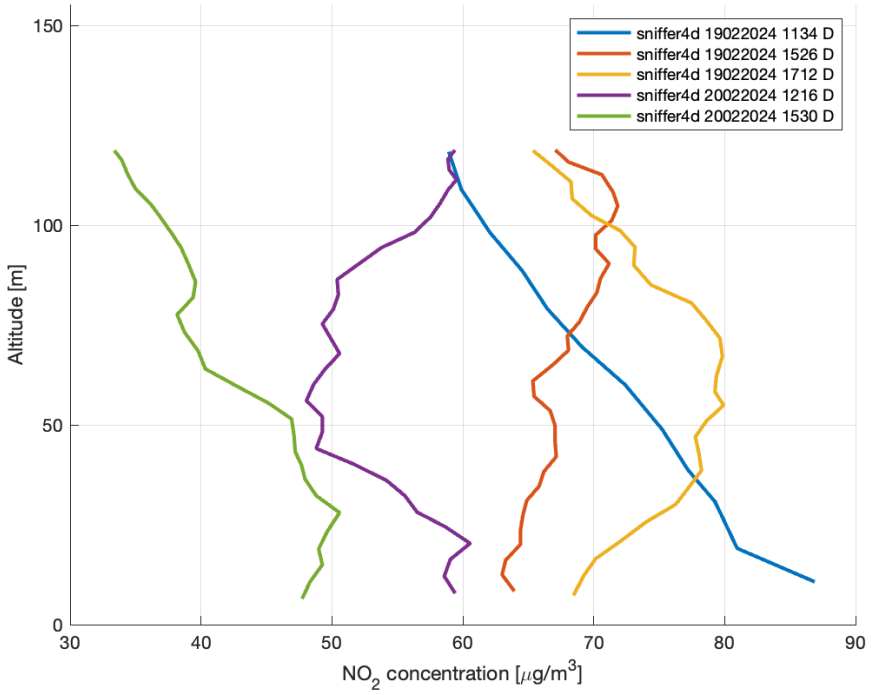

Figure 4.48: NO_2 concentration variation with altitude of all measurements at location D.

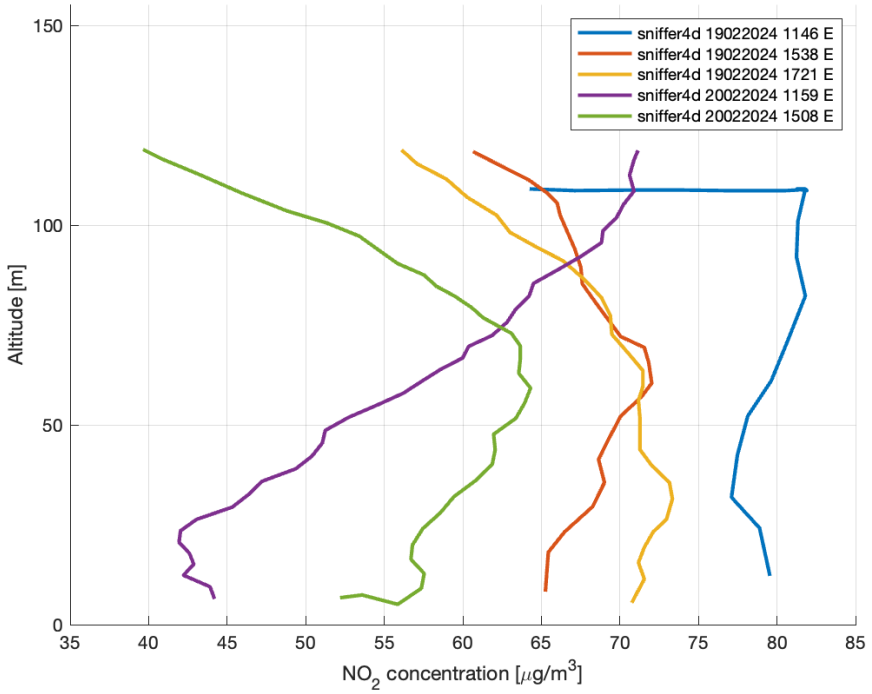

Figure 4.49: NO_2 concentration variation with altitude of all measurements at location E.

O_3 CONCENTRATION

The O_3 concentration variations with altitude of all measurements at locations A, B, C, D and E, can respectively be seen in figure 4.50, figure 4.51, figure 4.52, figure 4.53 and figure 4.54.

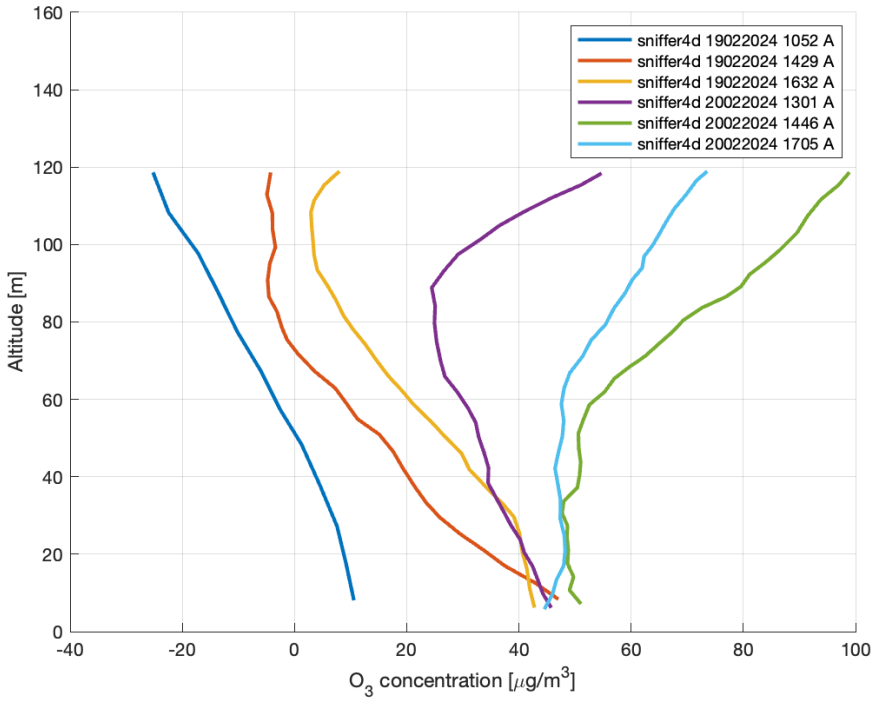

Figure 4.50: O_3 concentration variation with altitude of all measurements at location A.

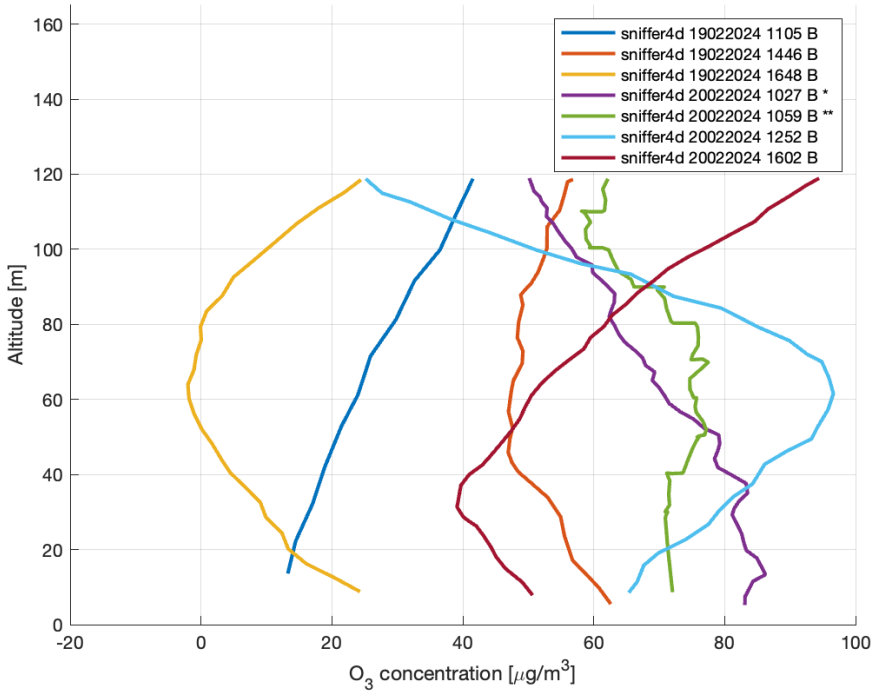

Figure 4.51: O_3 concentration variation with altitude of all measurements at location B.

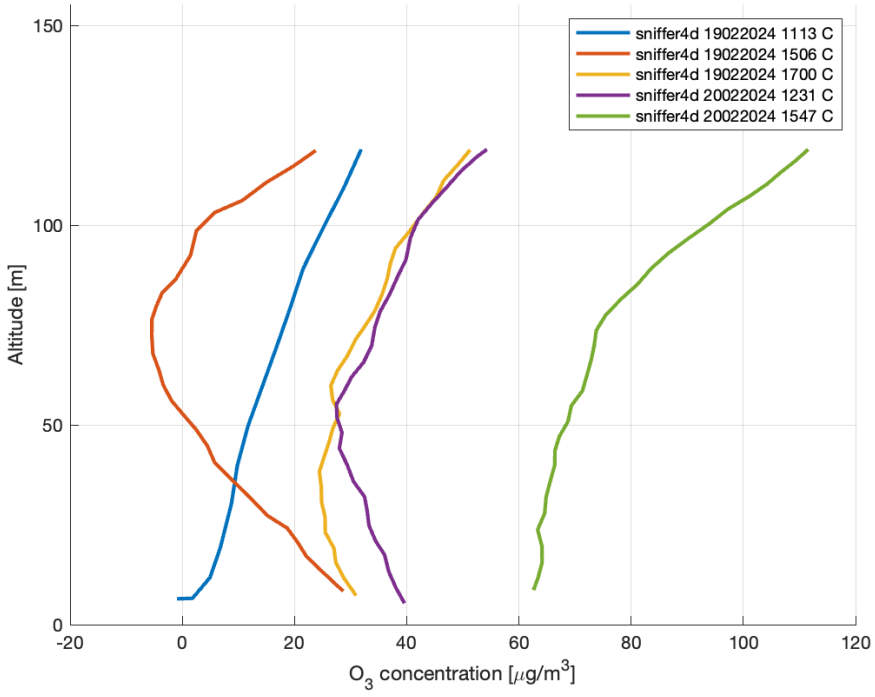

Figure 4.52: O_3 concentration variation with altitude of all measurements at location C.

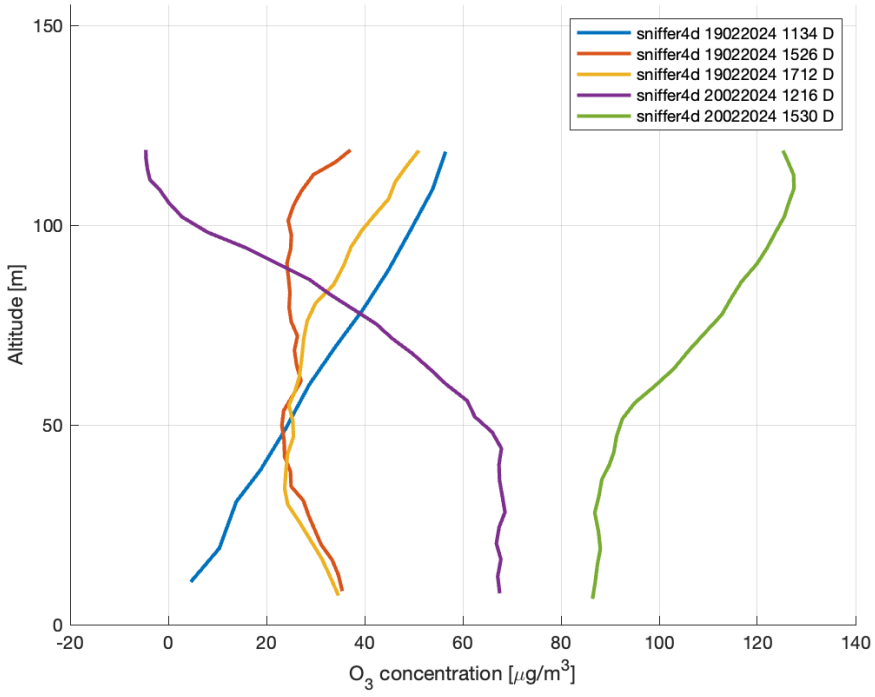

Figure 4.53: O_3 concentration variation with altitude of all measurements at location D.

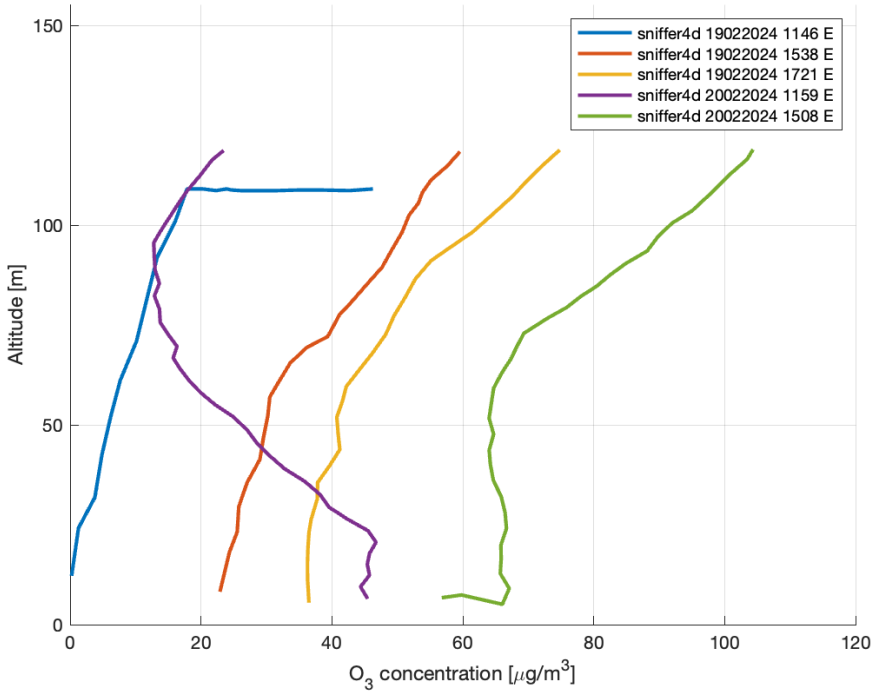

Figure 4.54: O_3 concentration variation with altitude of all measurements at location E.

SO_2 CONCENTRATION

The SO_2 concentration variations with altitude of all measurements at locations A, B, C, D and E, can respectively be seen in figure 4.55, figure 4.56, figure 4.57, figure 4.58 and figure 4.59.

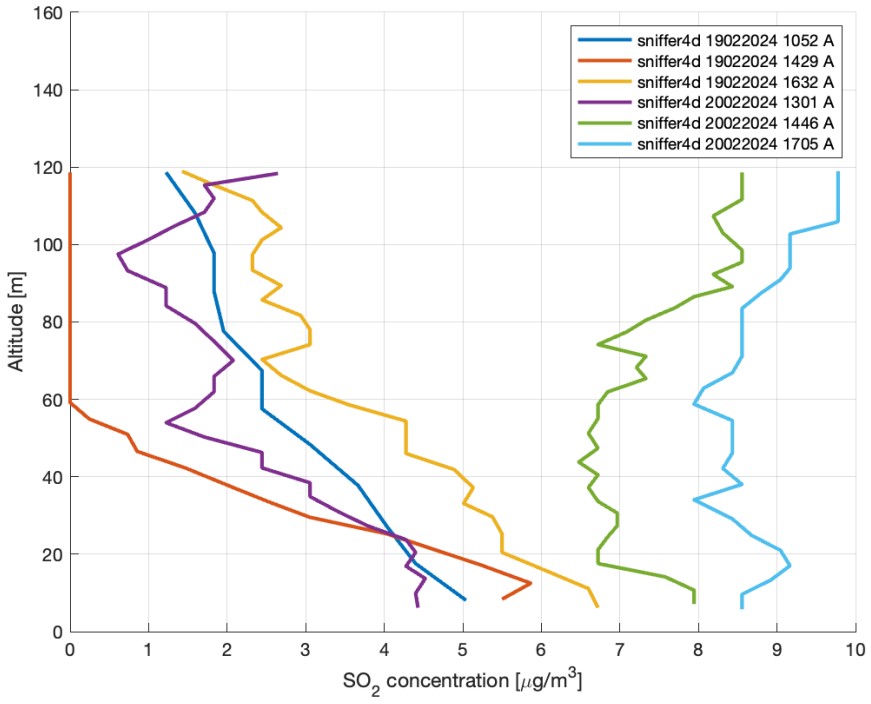

Figure 4.55: SO_2 concentration variation with altitude of all measurements at location A.

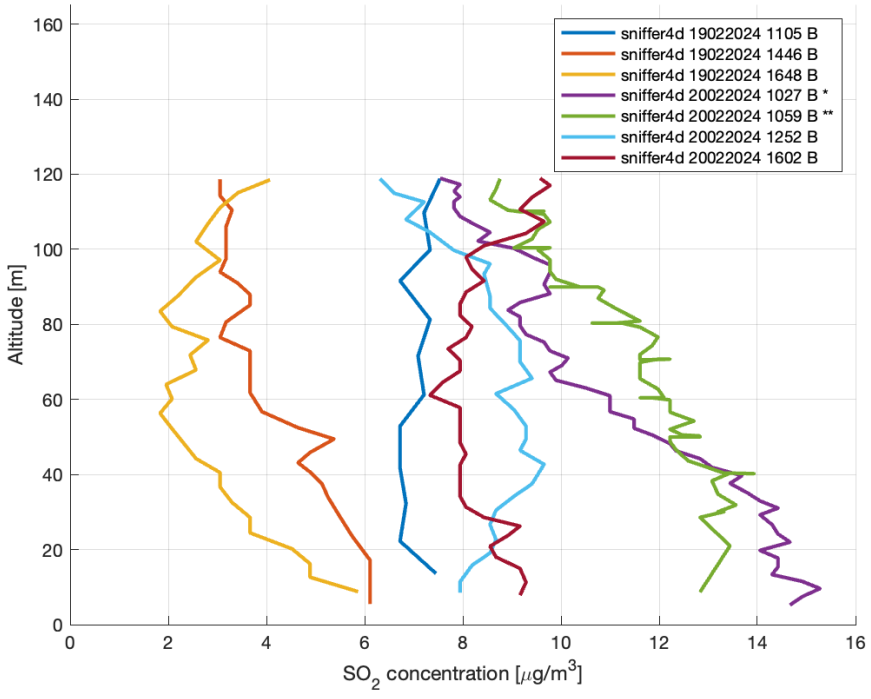

Figure 4.56: SO_2 concentration variation with altitude of all measurements at location B.

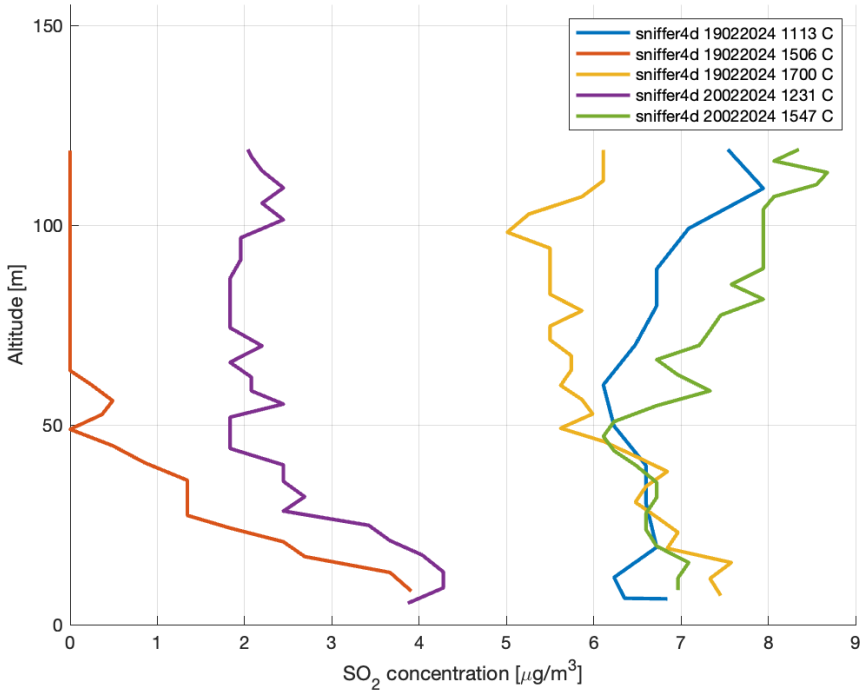

Figure 4.57: SO_2 concentration variation with altitude of all measurements at location C.

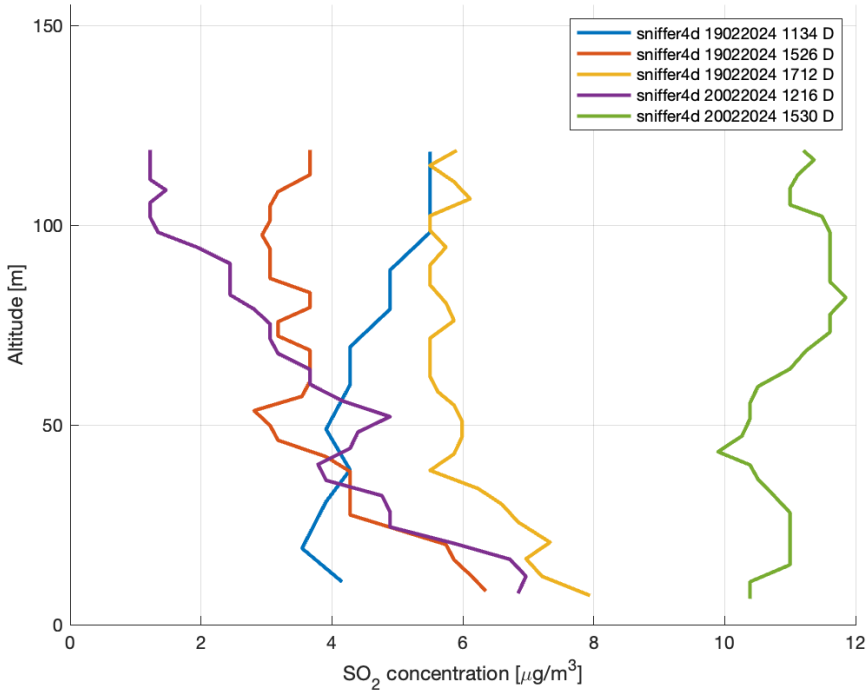

Figure 4.58: SO_2 concentration variation with altitude of all measurements at location D.

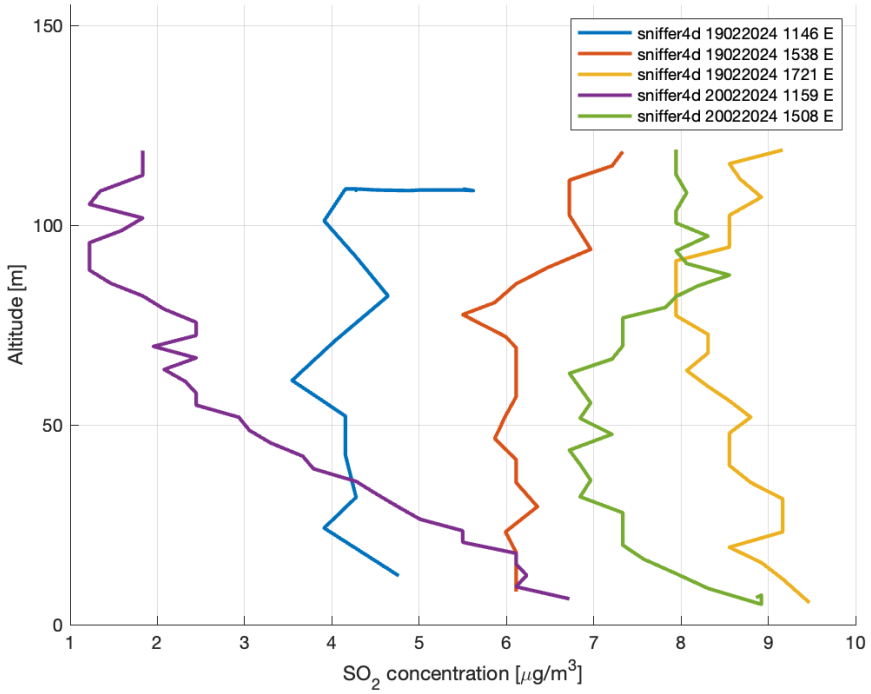

Figure 4.59: SO_2 concentration variation with altitude of all measurements at location E.

$PM_{2.5}$ CONCENTRATION

The $PM_{2.5}$ concentration variations with altitude of all measurements at locations A, B, C, D and E, can respectively be seen in figure 4.60, figure 4.61, figure 4.62, figure 4.63 and figure 4.64.

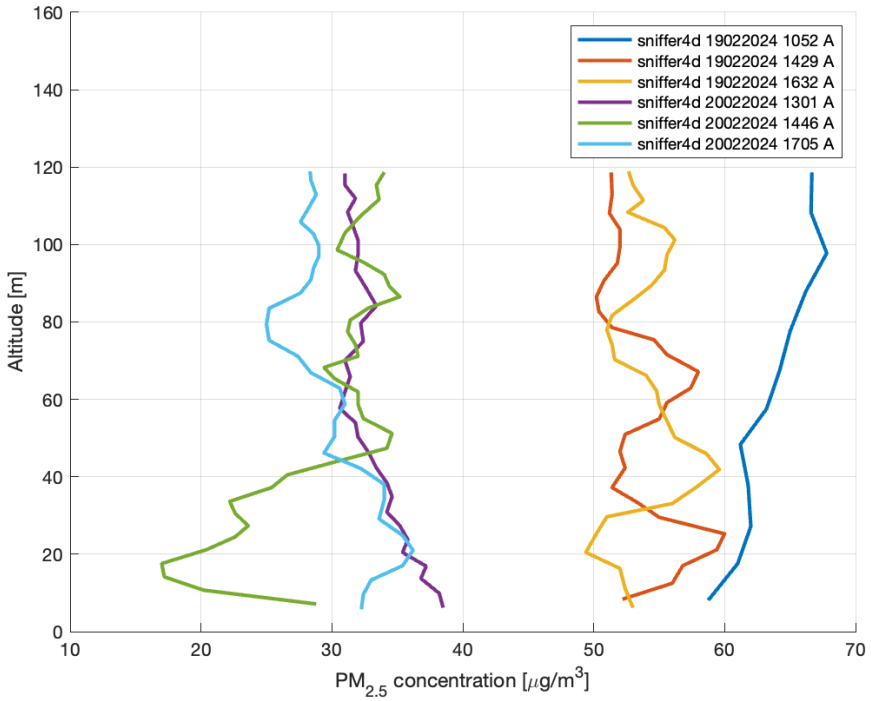

Figure 4.60: $PM_{2.5}$ concentration variation with altitude of all measurements at location A.

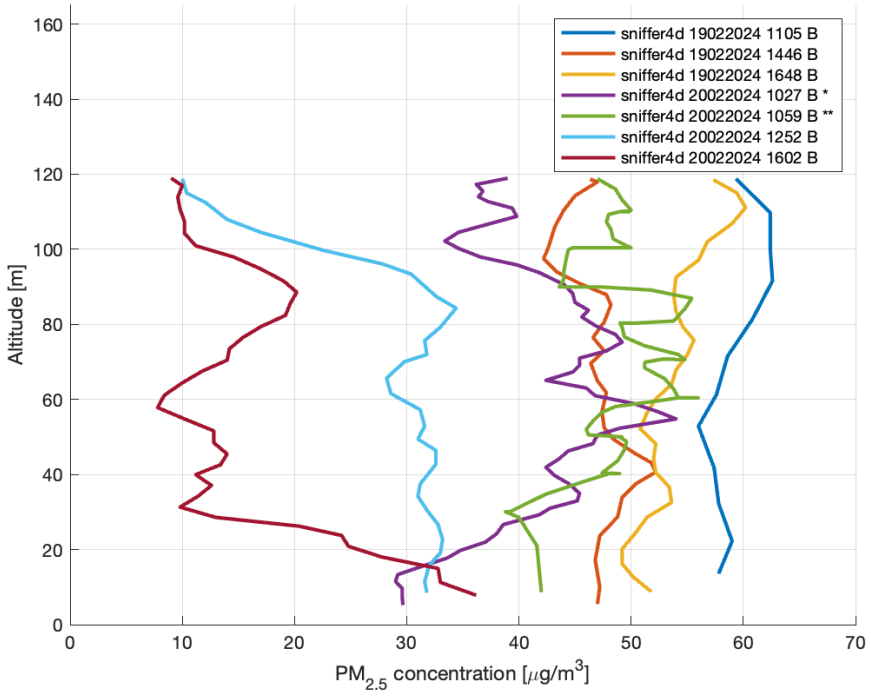

Figure 4.61: $PM_{2.5}$ concentration variation with altitude of all measurements at location B.

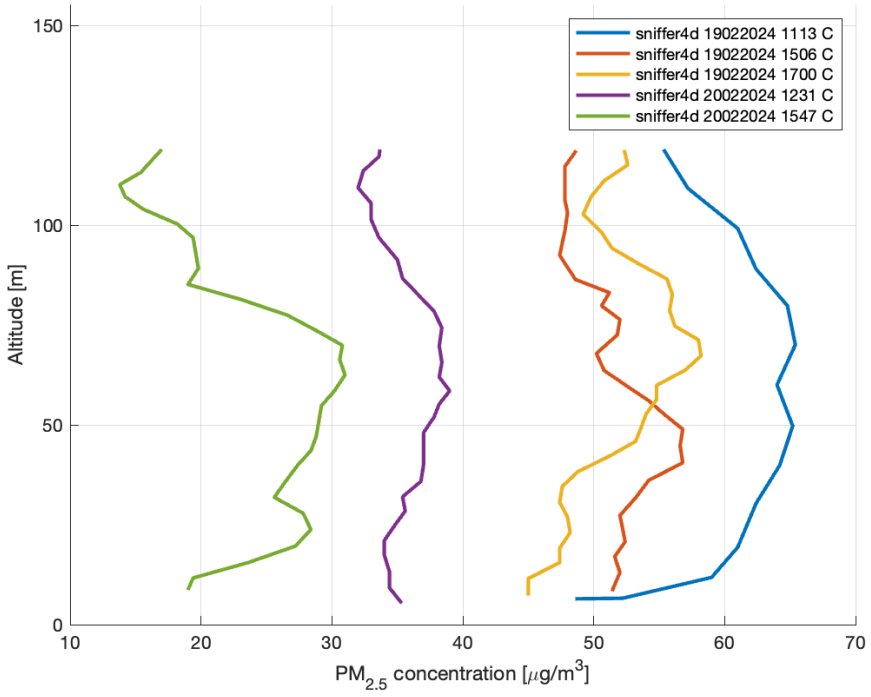

Figure 4.62: $PM_{2.5}$ concentration variation with altitude of all measurements at location C.

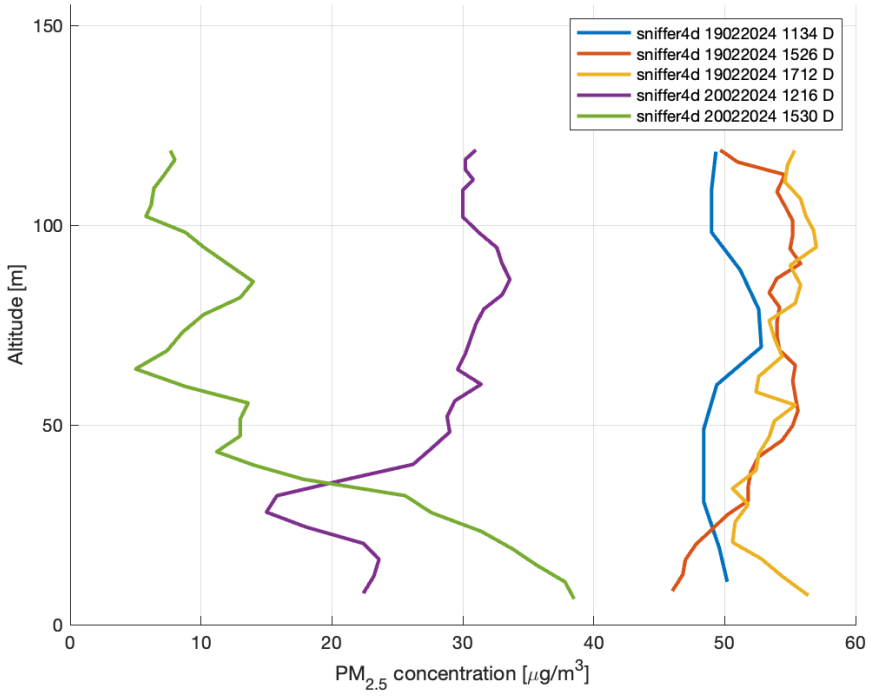

Figure 4.63: $PM_{2.5}$ concentration variation with altitude of all measurements at location D.

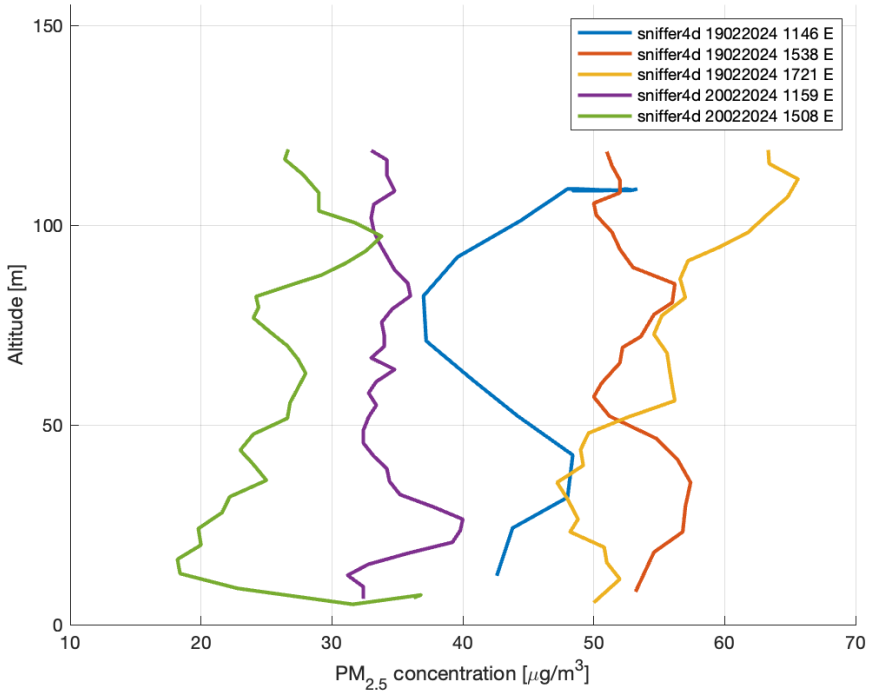

Figure 4.64: $PM_{2.5}$ concentration variation with altitude of all measurements at location E.

PM_{10} CONCENTRATION

The PM_{10} concentration variations with altitude of all measurements at locations A, B, C, D and E, can respectively be seen in figure 4.65, figure 4.66, figure 4.67, figure 4.68 and figure 4.69.

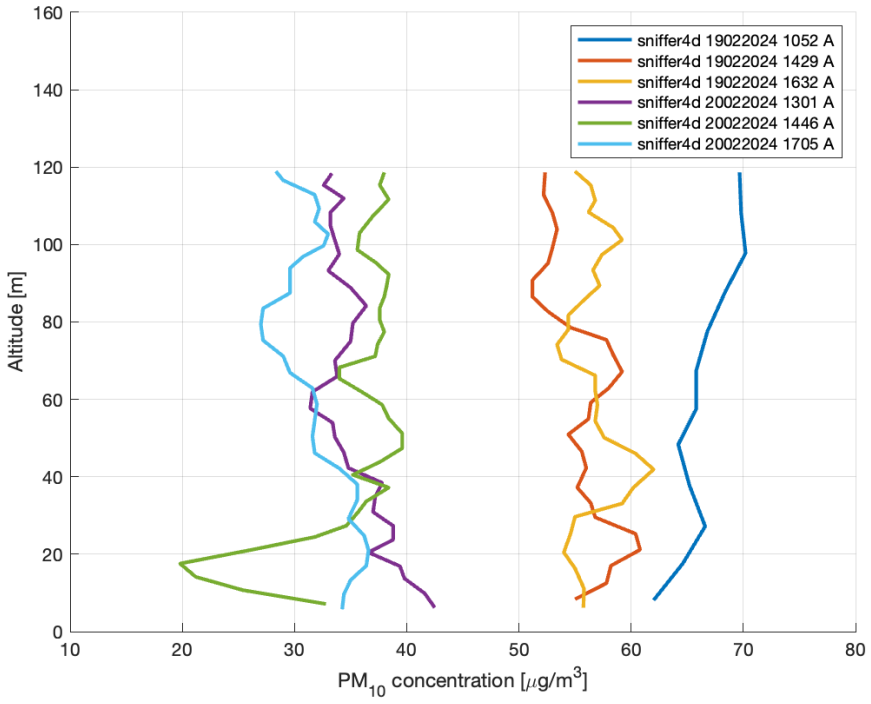

Figure 4.65: PM_{10} concentration variation with altitude of all measurements at location A.

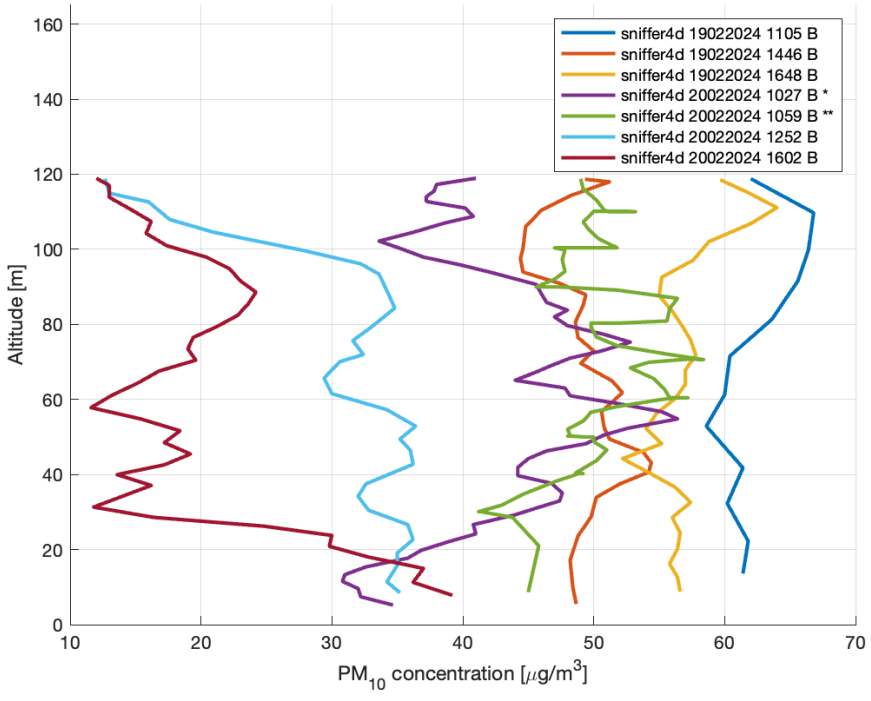

Figure 4.66: PM_{10} concentration variation with altitude of all measurements at location B.

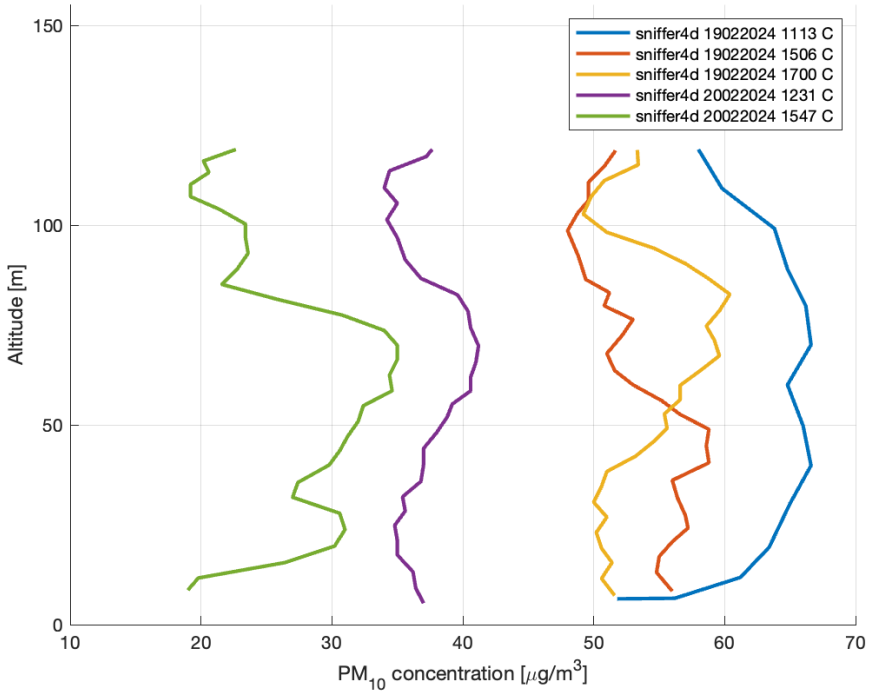

Figure 4.67: PM_{10} concentration variation with altitude of all measurements at location C.

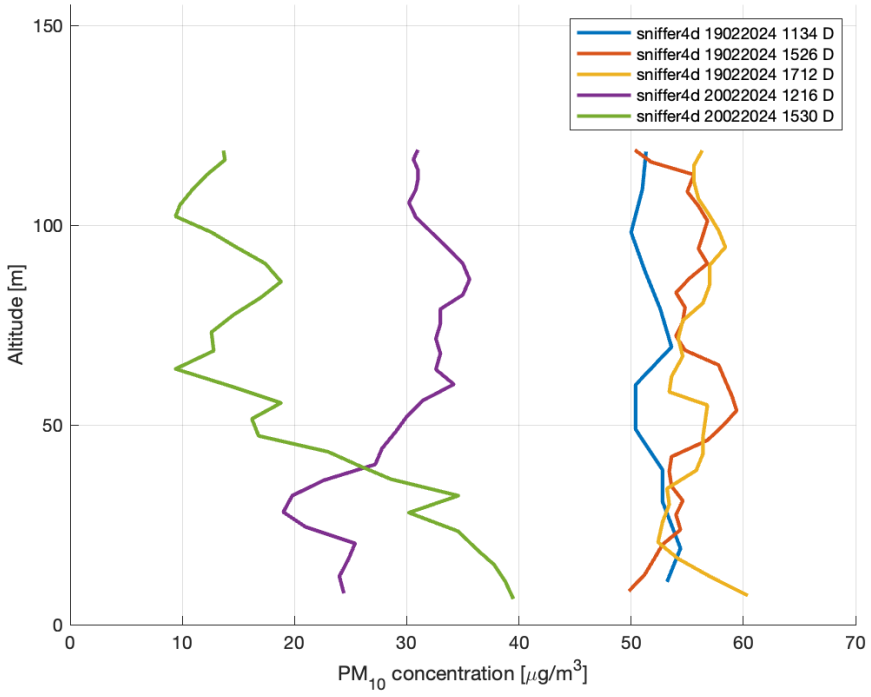

Figure 4.68: PM_{10} concentration variation with altitude of all measurements at location D.

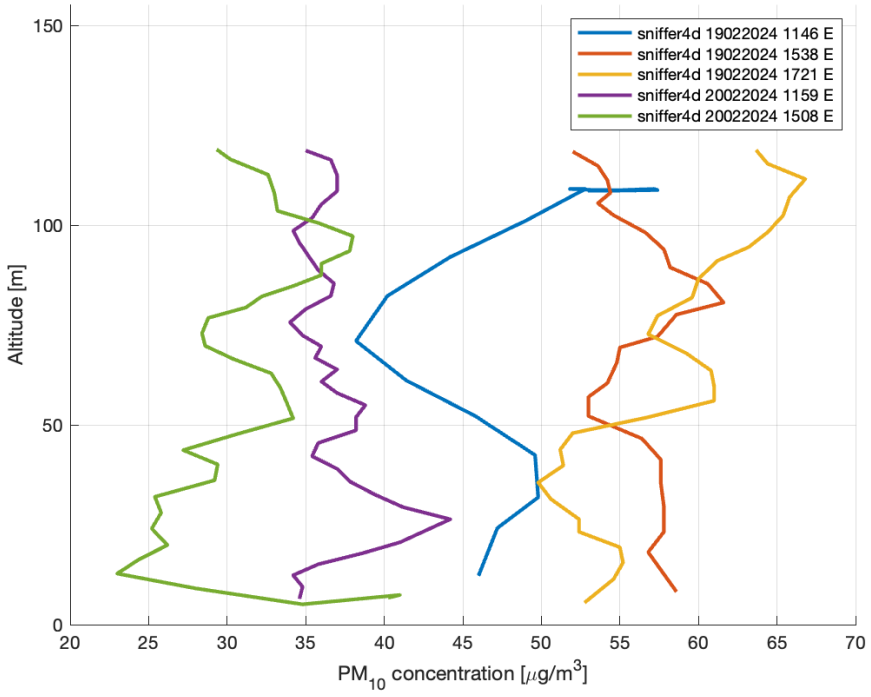

Figure 4.69: PM_{10} concentration variation with altitude of all measurements at location E.

4.3.2. CONTINUOUS MEASUREMENTS

An overview of all continuous measurements can be found in table 4.7.

Day	Start time	Location	Temperature range [°C]
20/02/2024	13:20	F-G-H-I-J-K	8.0-12.2
20/02/2024	16:22	F-G-H-I-J-K	10.2-11.2
20/02/2024	16:43	F-G-H-I-J-K	9.2-11.4

Table 4.7: Overview of all continuous measurements with their respective time, day and location.

An example of the data points which are used for the interpolation can be found in figure 4.70. In this figure, it is also shown how the interpolation is built around the data points. The motivation to exclude the diagonal phase of the flights (to e.g. move from location F to G) is included in figure 4.3.2.

Figure 4.70: Interpolation based on data from the continuous measurements.

INTERPOLATION ACCURACY

A cross validation has been carried out for each of the 3D interpolations. One of the points from the data set is excluded and the rest of the interpolation is used to estimate the value at that missing point. This is done for each of the data points, resulting in a set of statistics showing how good the interpolation is.

The interpolation has been carried out with only the vertical data, only the diagonal data and both combined. Moreover, the interpolation has been executed with respectively the lower and upper half of the vertical data points. An overview of the different data referred to can be found in figure 4.71. The flight speeds during the vertical and diagonal phases of the flights were respectively 0.8 and 3.0 m/s, since the vertical phase was of interest. Because the flight speed should not be higher than 0.8 m/s to obtain accurate data [35], it is expected that using only the data from the vertical phase of the flight will result in the best interpolation accuracy.

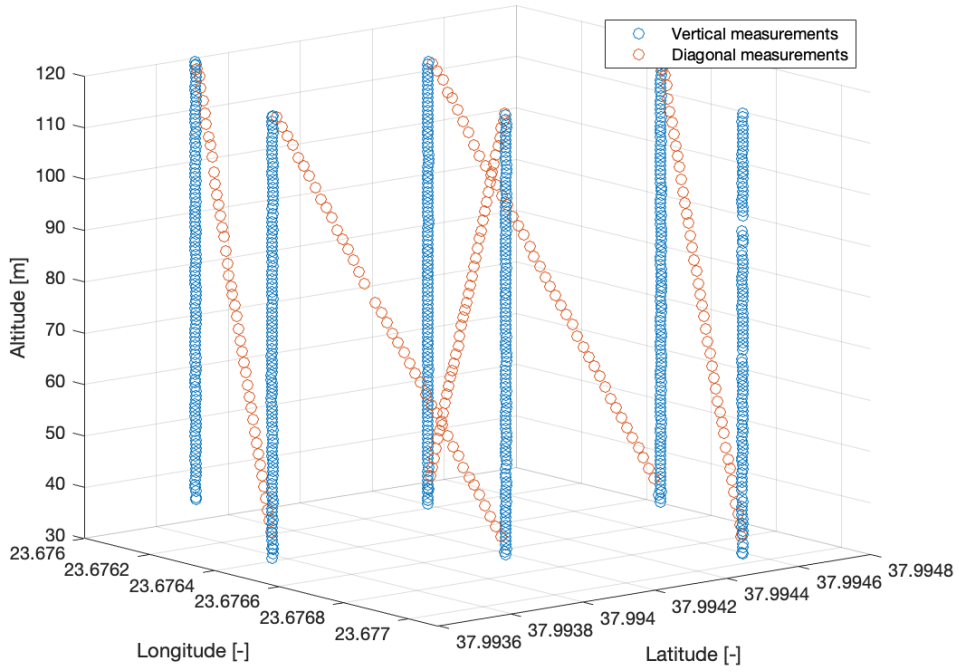

Figure 4.71: Data points grouped into vertical and diagonal flights.

In table 4.8, the statistics from the cross validation of the previously discussed data sets can be found. The Continuous Ranked Probability Score (CRPS) measures the deviation from the predictive cumulative distribution function to each observed data value [47]. Making use of simulations, it compares data to a full distribution instead of single-point predictions. It should be as low as possible; using all vertical data, the lowest CRPS is obtained. The mean, Root-Mean-Square average and Standard Error are calculated for the set of deviations between the predicted value and the actual data point.

The best results are obtained with the vertical data set. It has the lowest average CRPS, Root-Mean-Square Average and Standard error; therefore, we carry out all interpolations with the data points from only the vertical phase of the flights.

	Vertical data	**Lower half vertical data**	**Upper half vertical data**	**Diagonal & vertical data**	**Diagonal data**
Average CRPS [-]	0.140	0.148	0.147	0.147	0.151
Mean error [$\mu g/m^3$]	-0.002	0.002	0.001	0.003	0.001
Root-Mean-Square Error [$\mu g/m^3$]	0.245	0.260	0.260	0.253	0.269
Average Standard Error [$\mu g/m^3$]	0.284	0.381	0.316	0.346	0.297

Table 4.8: Cross validation outcomes for different interpolations of NO_2 data. Data used from second day at 16.22.

TEMPERATURE

The interpolation of the temperature for the three measurements of continuous data can be found in figure 4.72, figure 4.73 and figure 4.74. Since the total temperature variation is the smallest for the second measurement (second day at 16.22), we have included this measurement in the research article. The other measurements have been included here for completeness; yet, due to greater temperature variability, one should interpret these with caution.

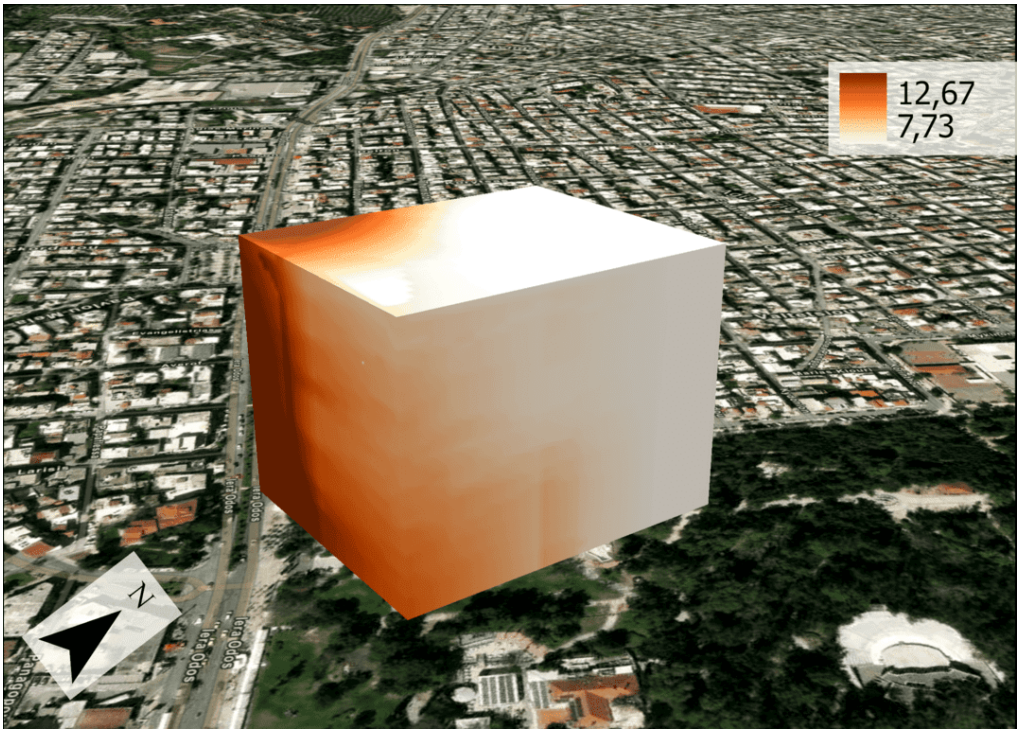

Figure 4.72: Empirical Bayesian Kriging 3D interpolation of temperature [°C]. Data used from second day at 13.20.

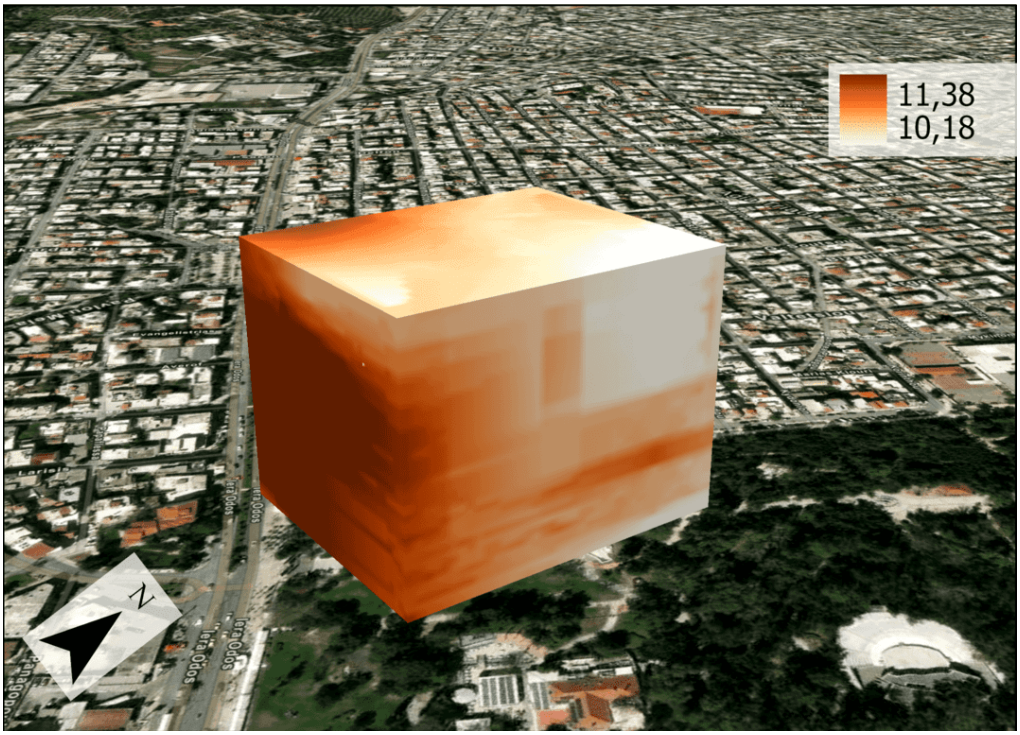

Figure 4.73: Empirical Bayesian Kriging 3D interpolation of temperature [°C]. Data used from second day at 16.22.

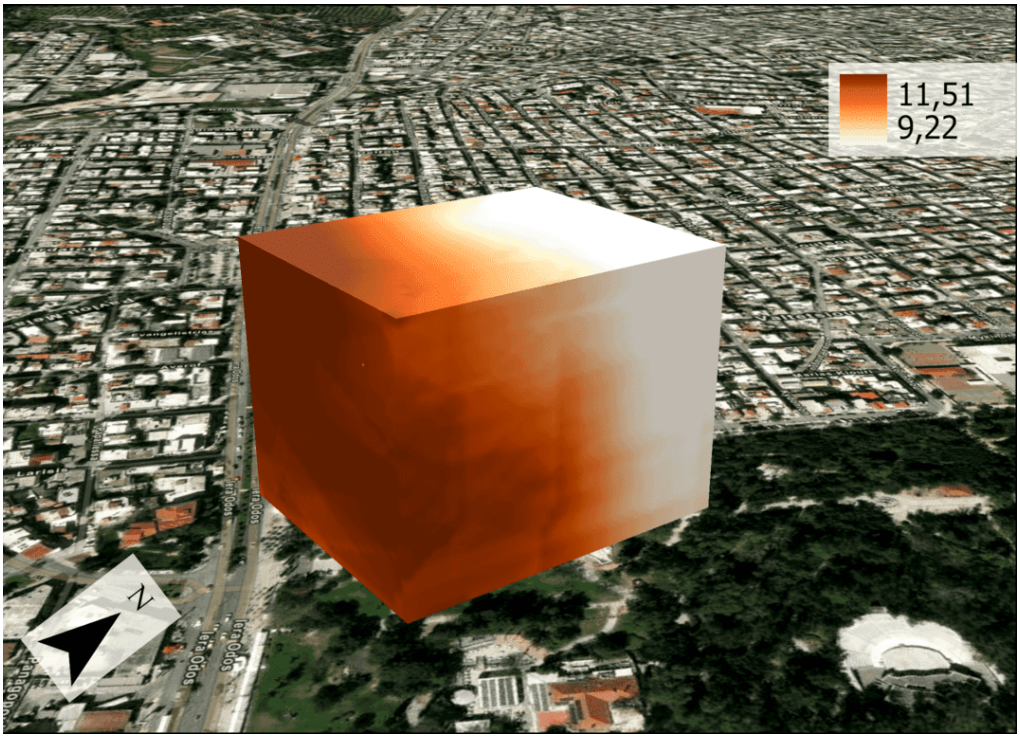

Figure 4.74: Empirical Bayesian Kriging 3D interpolation of temperature [°C]. Data used from second day at 16.43.

CO CONCENTRATION

The interpolation of the CO concentrations for the second and third measurements of continuous data can be found in figure 4.75 and figure 4.76. The interpolation of the first measurement is missing, as this one could not be created due to zero readings of the CO sensor. The obtained results are very different, which has to do with the large temperature variability at the first and third measurement. For that reason, only the second measurement is included and discussed in the paper.

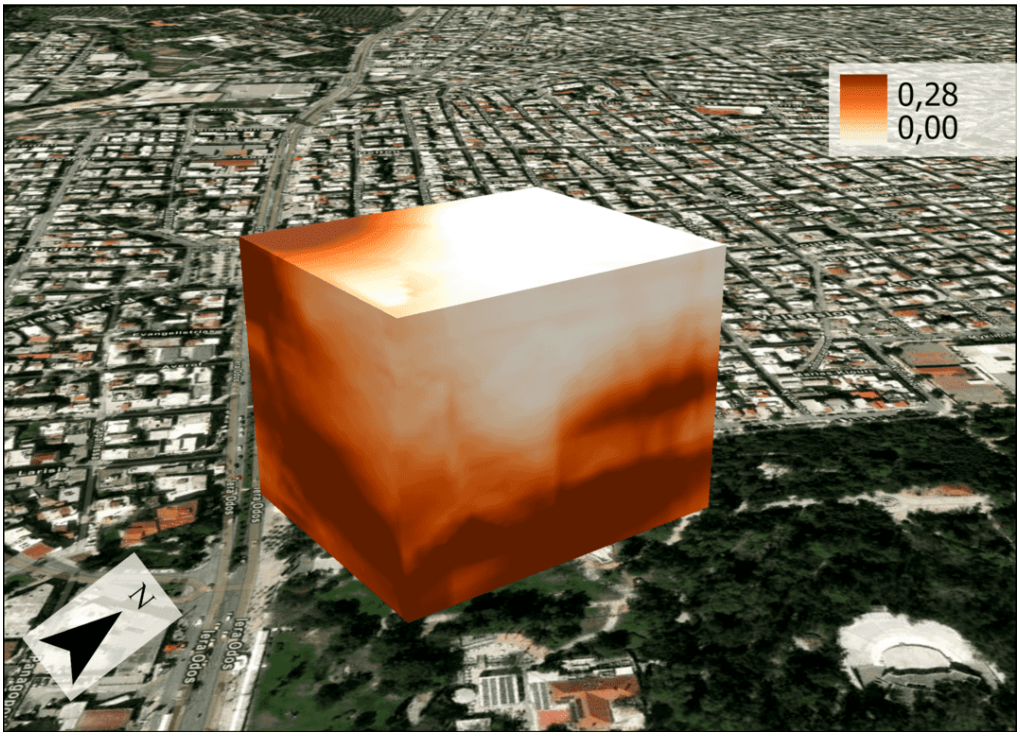

Figure 4.75: Empirical Bayesian Kriging 3D interpolation of CO concentration [mg/m^3]. Data used from second day at 16.22.

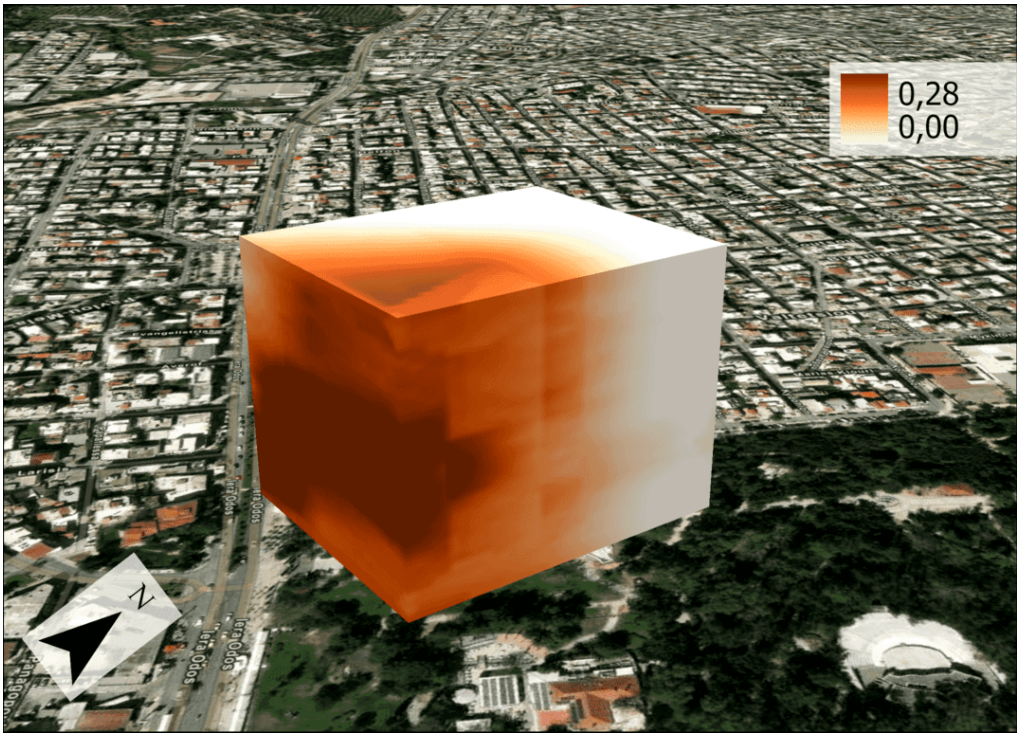

Figure 4.76: Empirical Bayesian Kriging 3D interpolation of CO concentration [mg/m^3]. Data used from second day at 16.43.

NO_2 CONCENTRATION

The interpolation of the NO_2 concentrations for the three measurements of continuous data can be found in figure 4.77, figure 4.78 and figure 4.79. The obtained results are very different, which has to do with the large temperature variability at the first and third measurement. For that reason, only the second measurement is included and discussed in the paper.

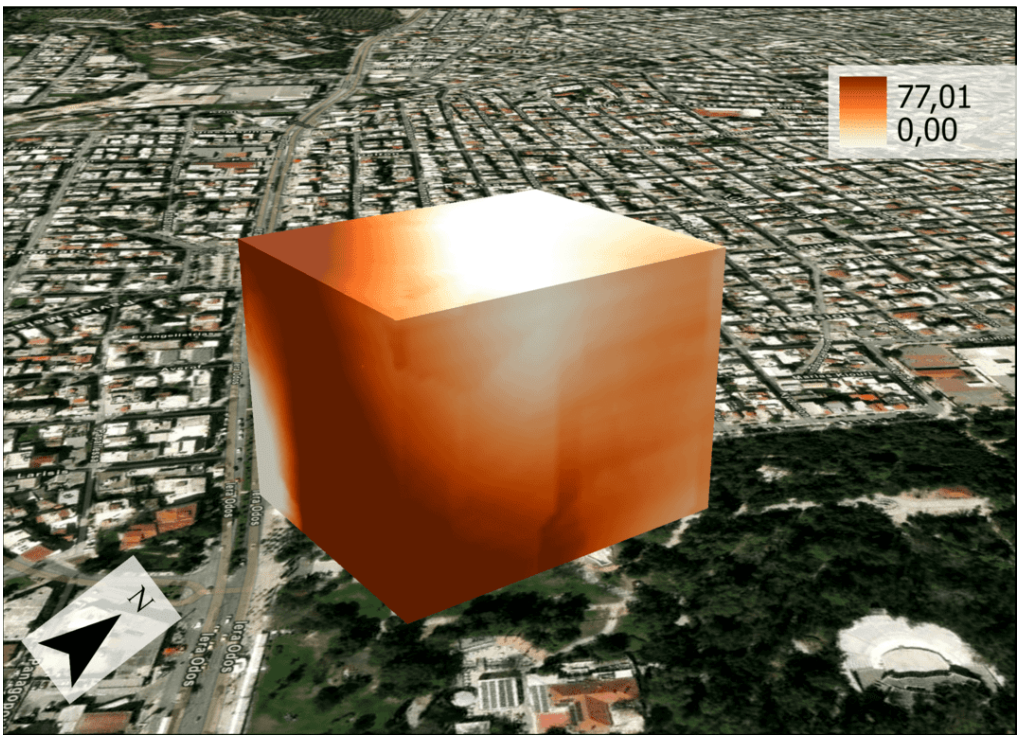

Figure 4.77: Empirical Bayesian Kriging 3D interpolation of NO_2 concentration [µg/m^3]. Data used from second day at 13.20.

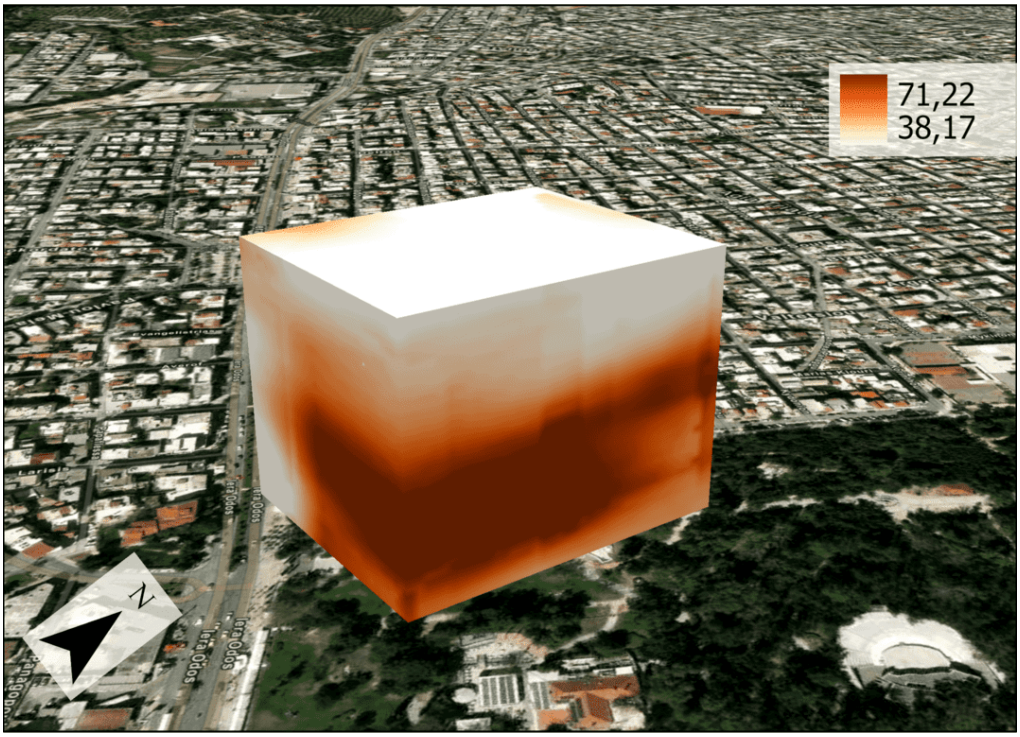

Figure 4.78: Empirical Bayesian Kriging 3D interpolation of NO_2 concentration [$\mu g/m^3$]. Data used from second day at 16.22.

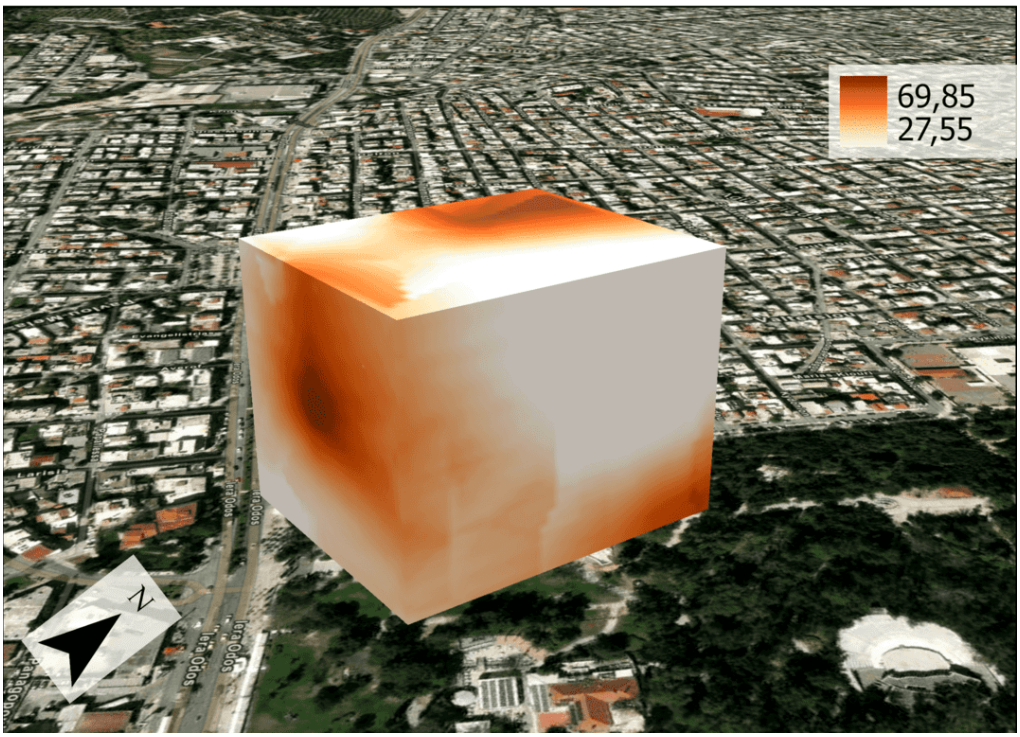

Figure 4.79: Empirical Bayesian Kriging 3D interpolation of NO_2 concentration [$\mu g/m^3$]. Data used from second day at 16.43.

O_3 CONCENTRATION

The interpolation of the O_3 concentrations for the three measurements of continuous data can be found in figure 4.80, figure 4.81 and figure 4.82. The obtained results are very different, which has to do with the large temperature variability at the first and third measurement. For that reason, only the second measurement is included and discussed in the paper.

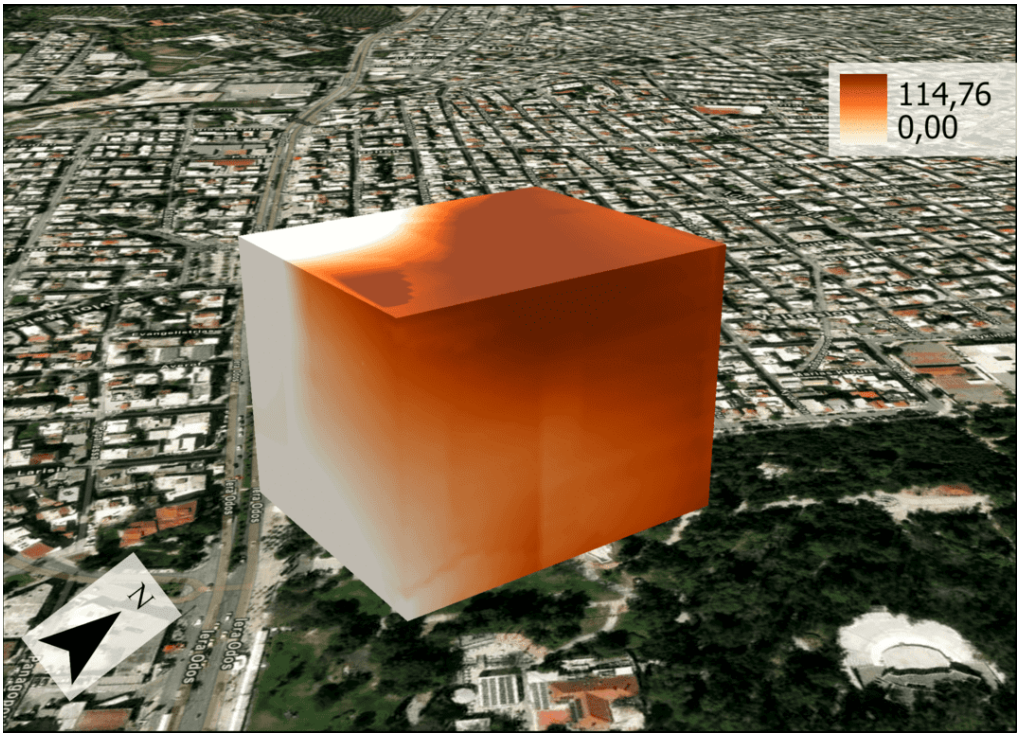

Figure 4.80: Empirical Bayesian Kriging 3D interpolation of O_3 concentration [$\mu g/m^3$]. Data used from second day at 13.20.

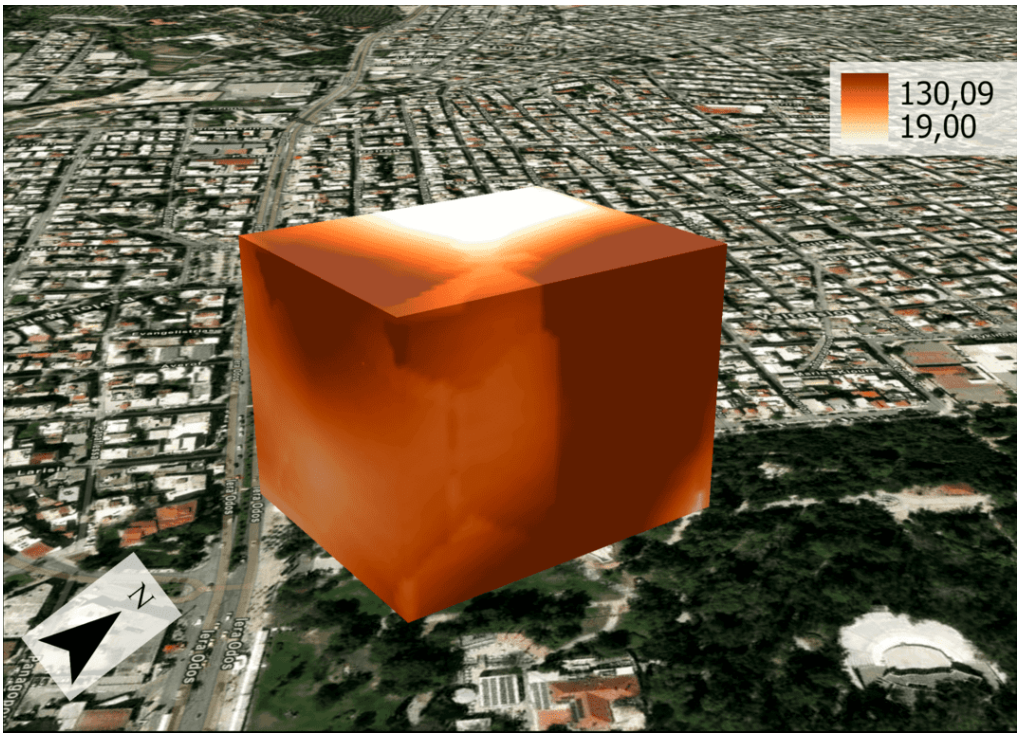

Figure 4.81: Empirical Bayesian Kriging 3D interpolation of O_3 concentration [$\mu g/m^3$]. Data used from second day at 16.22.

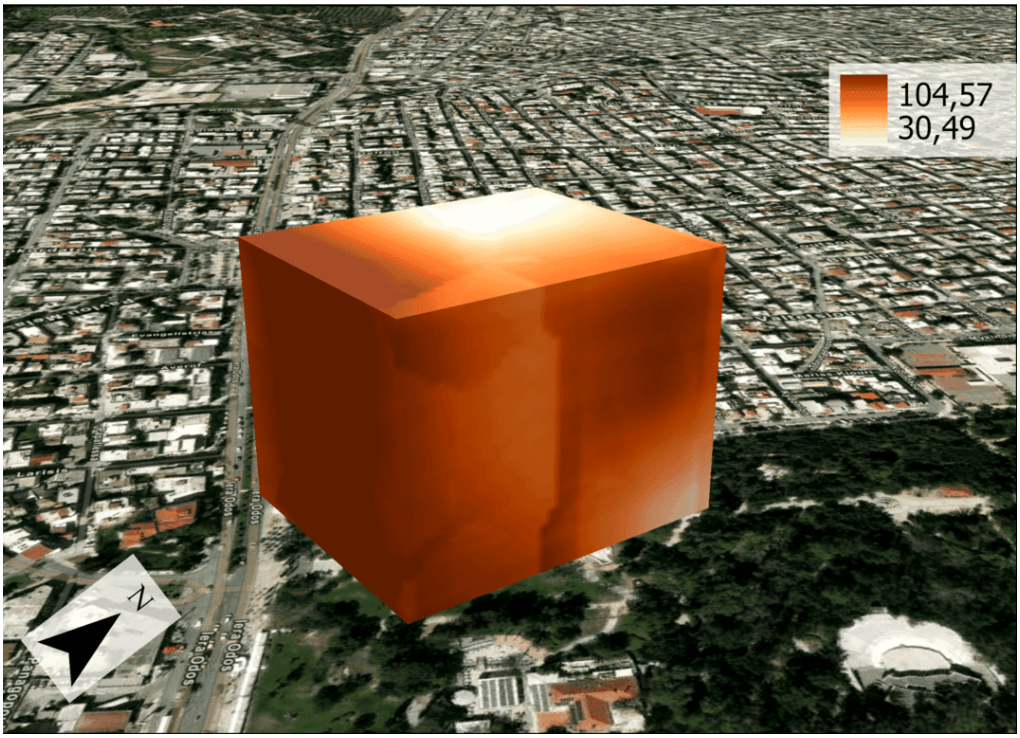

Figure 4.82: Empirical Bayesian Kriging 3D interpolation of O_3 concentration [$\mu g/m^3$]. Data used from second day at 16.43.

SO_2 CONCENTRATION

The interpolation of the SO_2 concentrations for the three measurements of continuous data can be found in figure 4.83, figure 4.84 and figure 4.85. The obtained results are very different, which has to do with the large temperature variability at the first and third measurement. For that reason, only the second measurement is included and discussed in the paper.

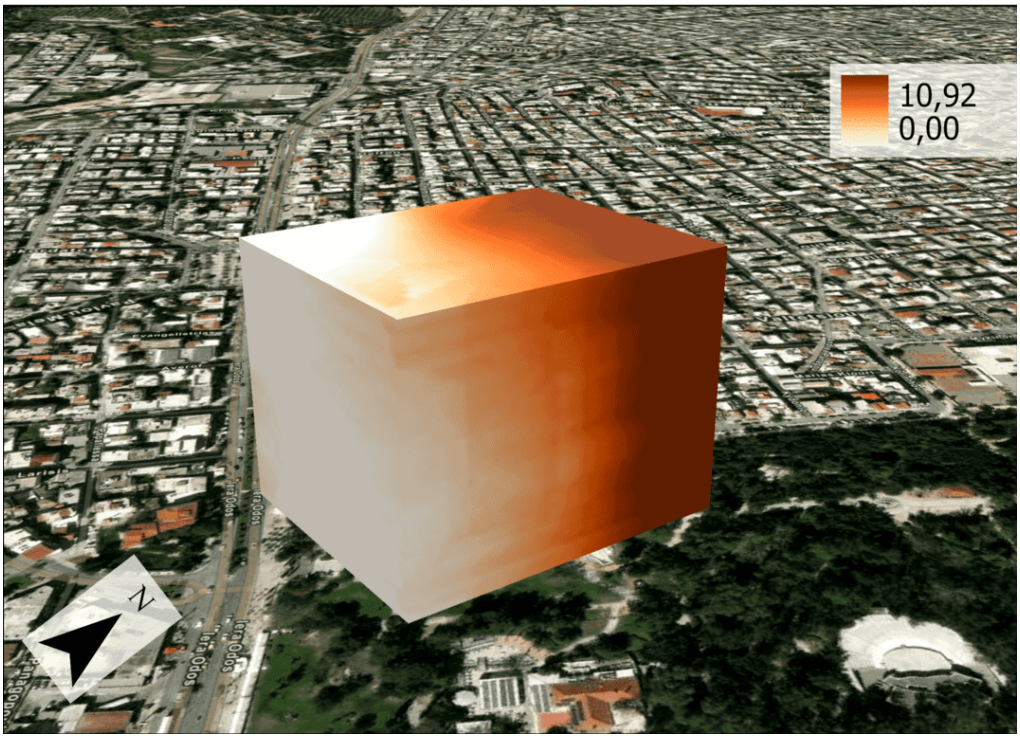

Figure 4.83: Empirical Bayesian Kriging 3D interpolation of SO_2 concentration [$\mu g/m^3$]. Data used from second day at 13.20.

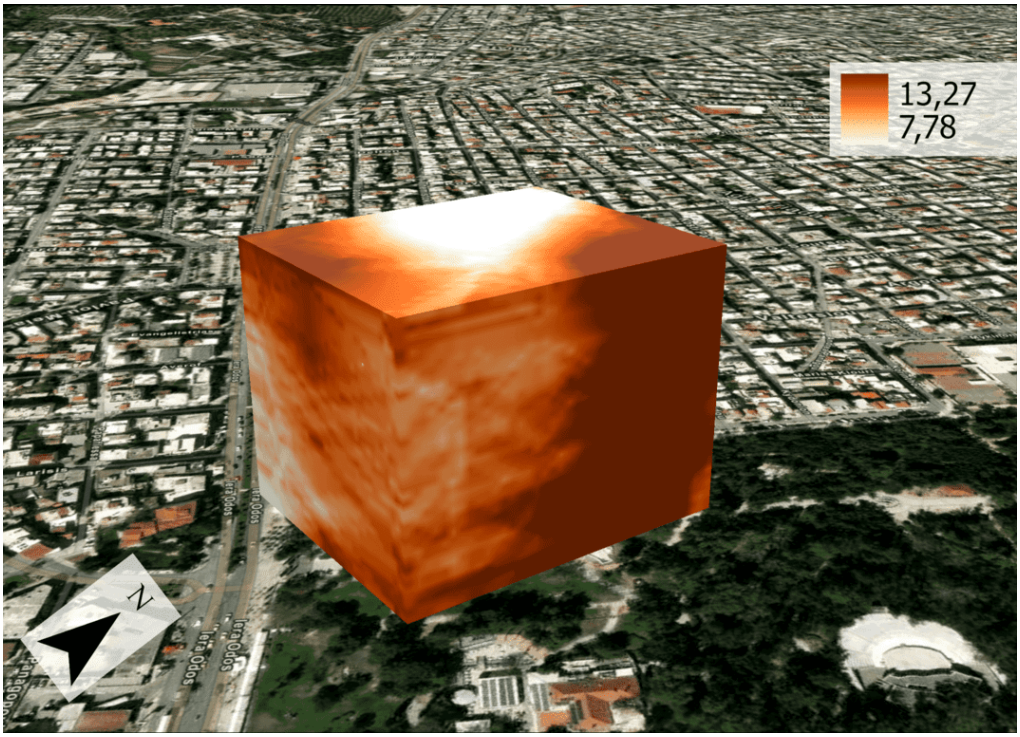

Figure 4.84: Empirical Bayesian Kriging 3D interpolation of SO_2 concentration [$\mu g/m^3$]. Data used from second day at 16.22.

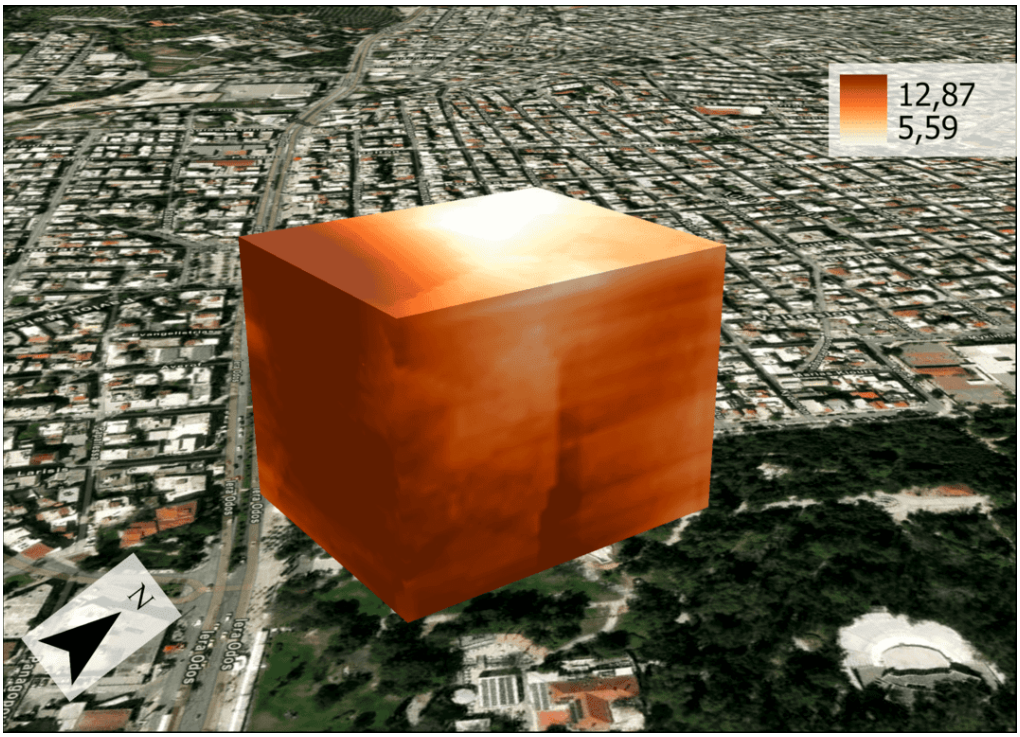

Figure 4.85: Empirical Bayesian Kriging 3D interpolation of SO_2 concentration [$\mu g/m^3$]. Data used from second day at 16.43.

$PM_{2.5}$ CONCENTRATION

The interpolation of the $PM_{2.5}$ concentrations for the three measurements of continuous data can be found in figure 4.86, figure 4.87 and figure 4.88. The obtained results are very different, which has to do with the large temperature variability at the first and third measurement. For that reason, only the second measurement is included and discussed in the paper.

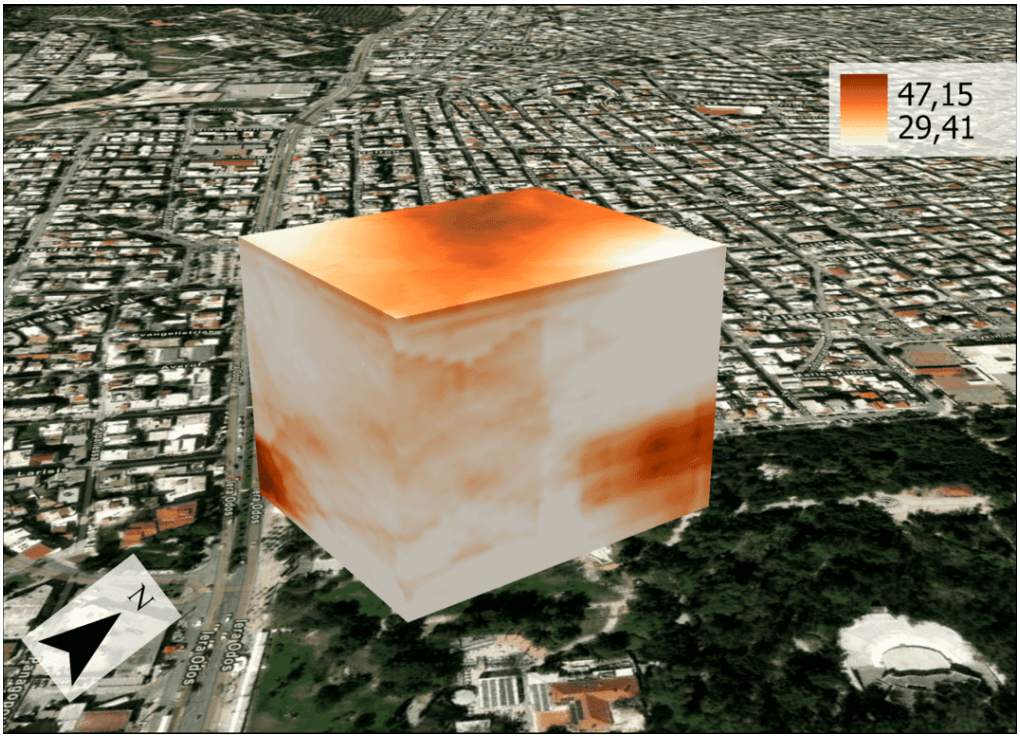

Figure 4.86: Empirical Bayesian Kriging 3D interpolation of $PM_{2.5}$ concentration [mg/m^3]. Data used from second day at 13.20.

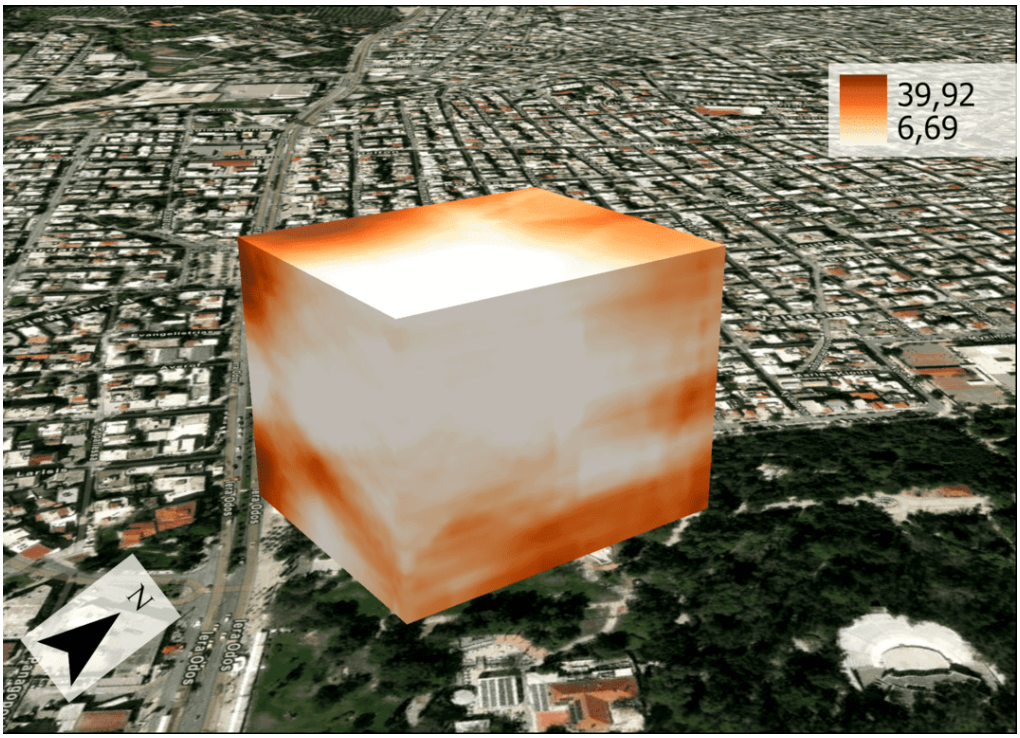

Figure 4.87: Empirical Bayesian Kriging 3D interpolation of $PM_{2.5}$ concentration [$\mu g/m^3$]. Data used from second day at 16.22.

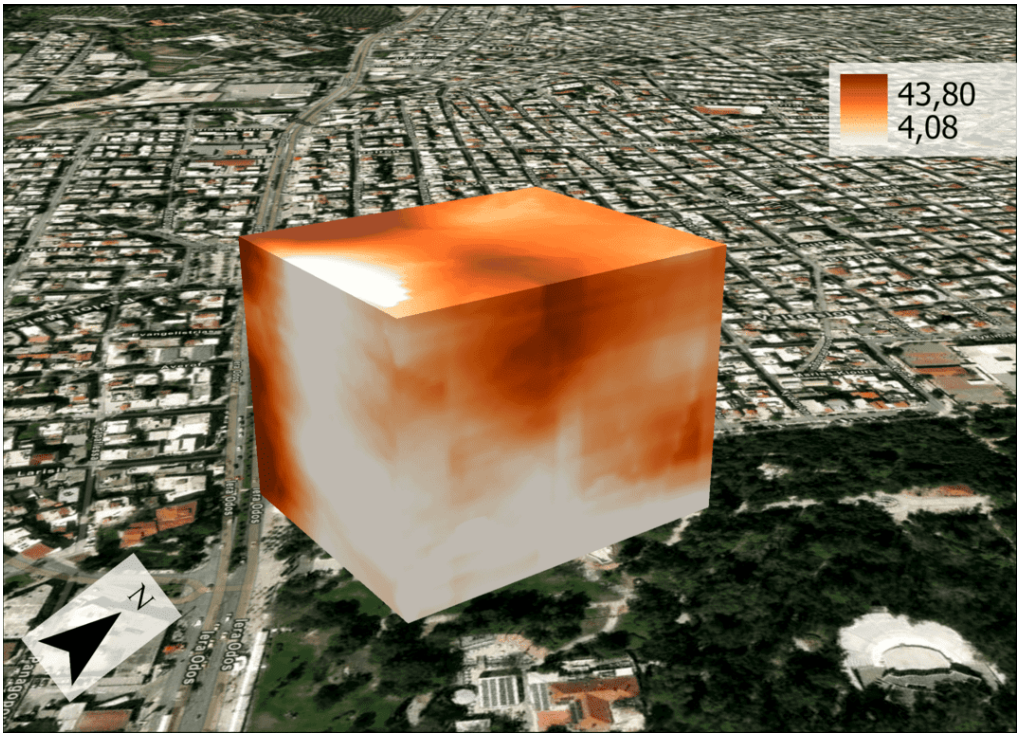

Figure 4.88: Empirical Bayesian Kriging 3D interpolation of $PM_{2.5}$ concentration [$\mu g/m^3$]. Data used from second day at 16.43.

PM_{10} CONCENTRATION

The interpolation of the PM_{10} concentrations for the three measurements of continuous data can be found in figure 4.89, figure 4.90 and figure 4.91. The obtained results are very different, which has to do with the large temperature variability at the first and third measurement. For that reason, only the second measurement is included and discussed in the paper. The results are, however, very similar to $PM_{2.5}$ as it makes use of the same sensor.

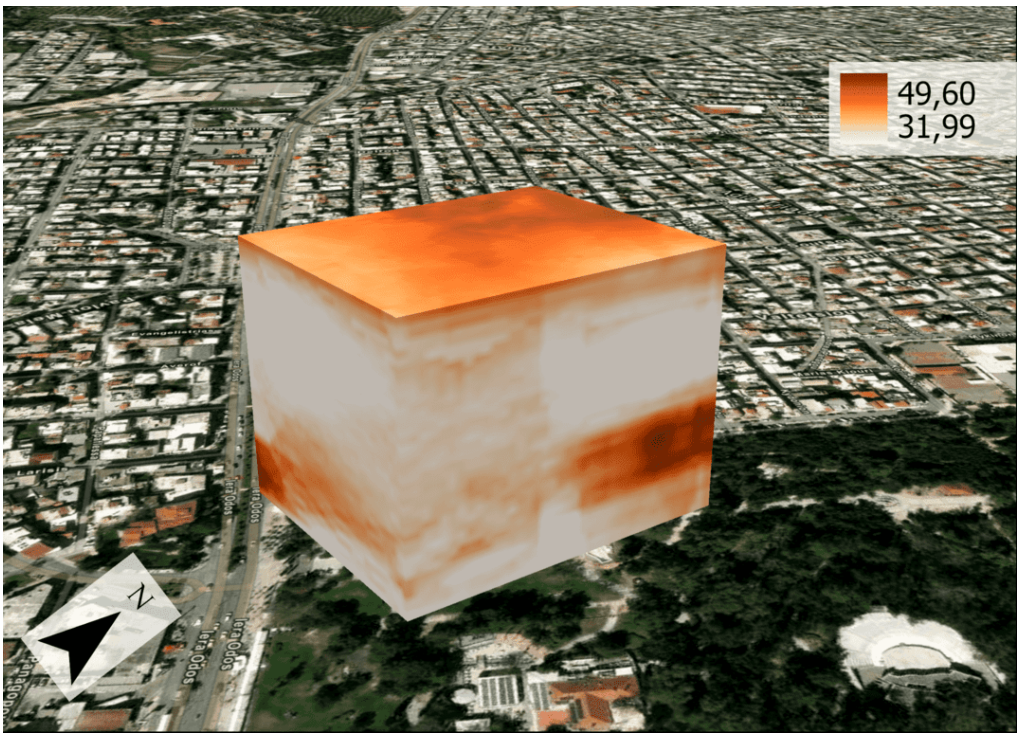

Figure 4.89: Empirical Bayesian Kriging 3D interpolation of PM_{10} concentration [$\mu g/m^3$]. Data used from second day at 13.20.

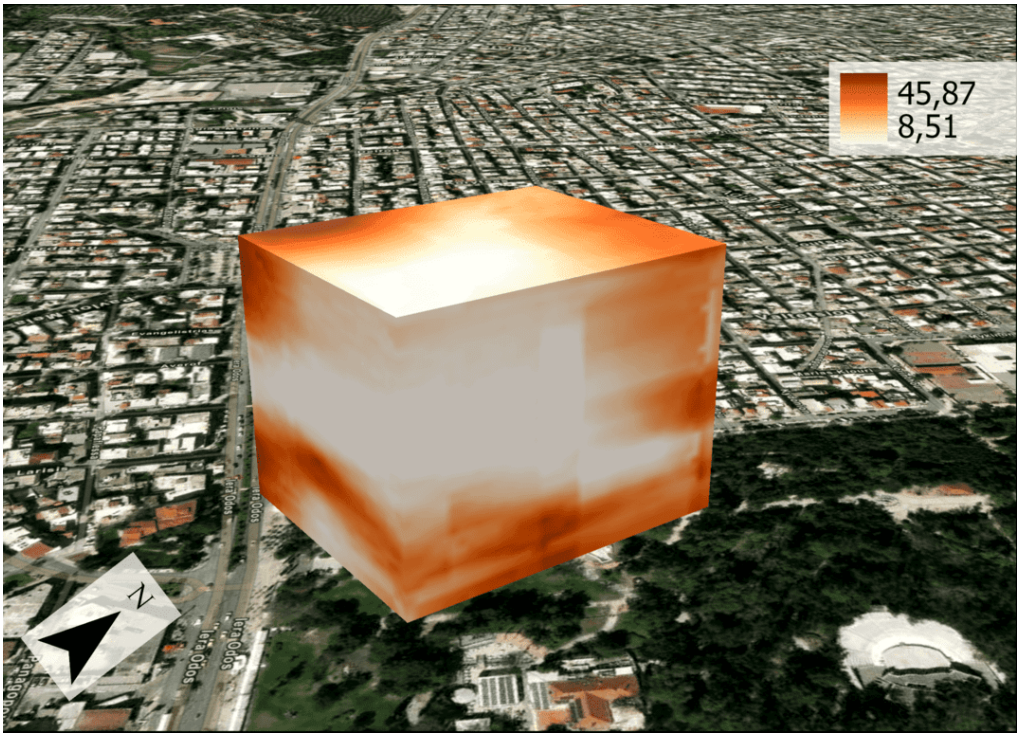

Figure 4.90: Empirical Bayesian Kriging 3D interpolation of PM_{10} concentration [$\mu g/m^3$]. Data used from second day at 16.22.

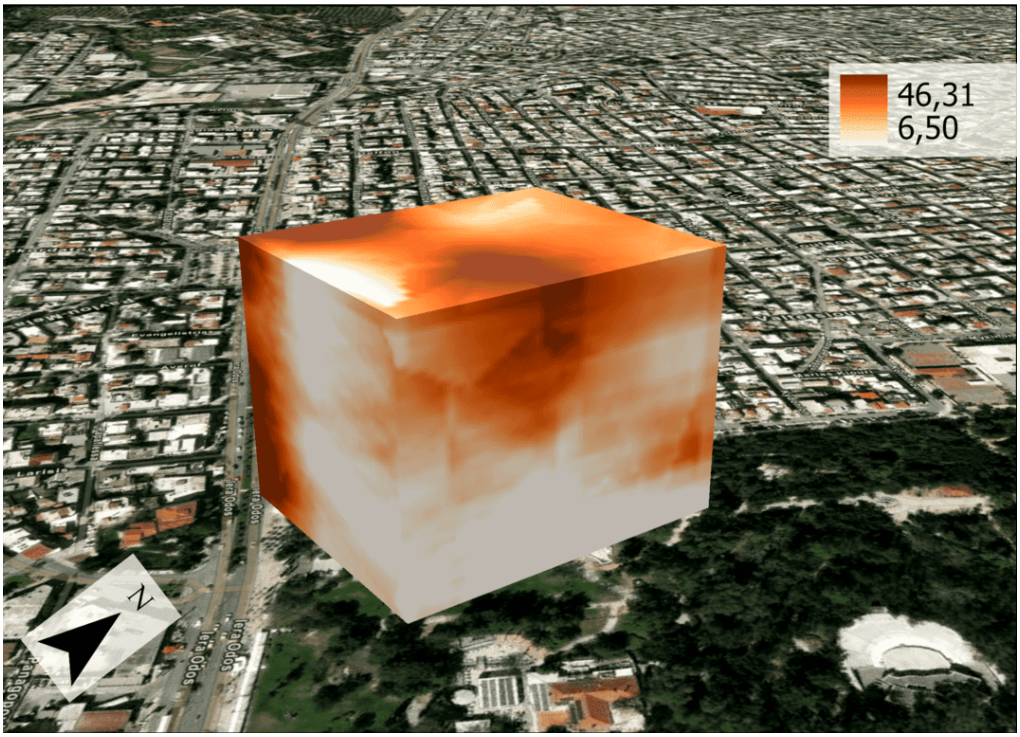

Figure 4.91: Empirical Bayesian Kriging 3D interpolation of PM_{10} concentration [$\mu g/m^3$]. Data used from second day at 16.43.

4.3.3. COMPARISON POINT AND CONTINUOUS MEASUREMENTS

In figure 4.92, the locations of the data compared from the point and continuous measurements can be found. In the remaining part of this section, the locations will be indicated according to the point measurements; locations A, B and C. We compare the second (16.22) and third (16.43) measurement of the point with continuous measurements during rush hour and non rush hour. We focus on the 16.22 continuous measurement (which has the lowest temperature variability) and a rush hour point measurement (around 17.00).

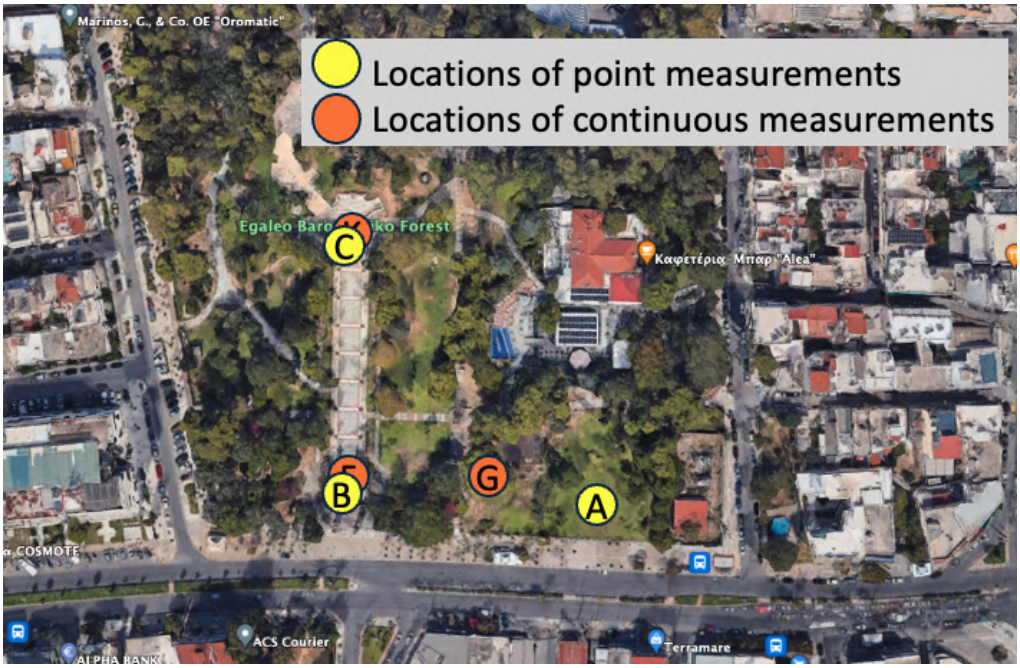

Figure 4.92: Locations of measurement comparisons point and continuous measurements.

TEMPERATURE

The different temperature profiles can be found in figure 4.93, figure 4.94 and figure 4.95. Note that a lot of temperature variation is present in the point data from location B. Therefore, the focus during the analysis is on locations A and C.

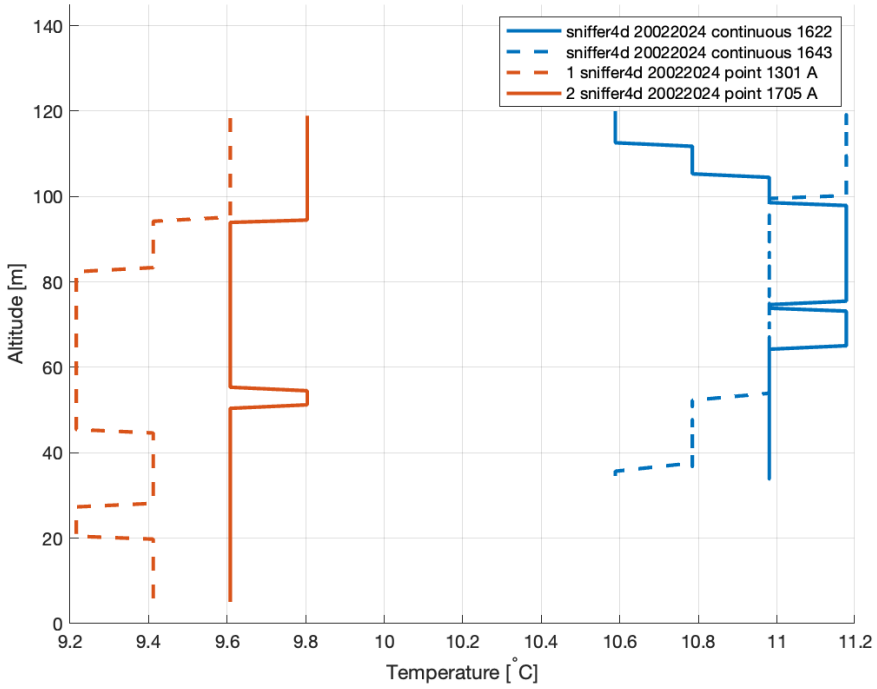

Figure 4.93: Comparison of temperature profile with altitude from point and continuous measurements at location A.

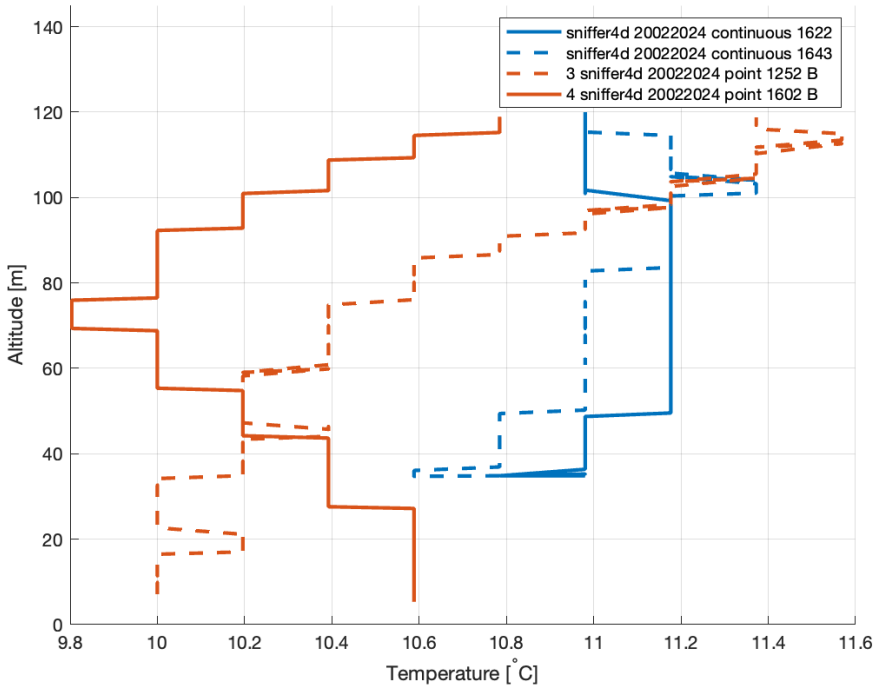

Figure 4.94: Comparison of temperature profile with altitude from point and continuous measurements at location B.

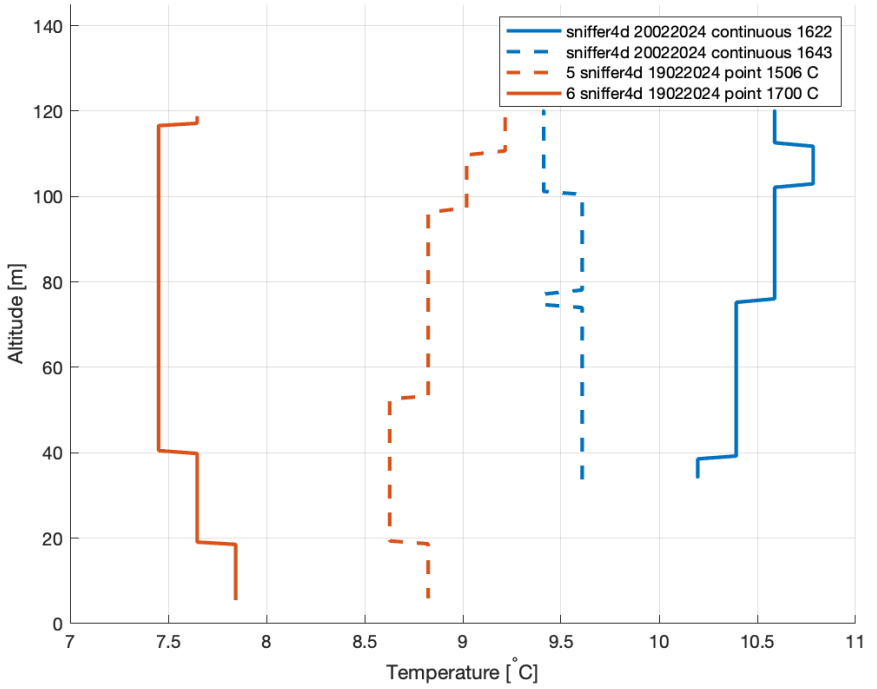

Figure 4.95: Comparison of temperature profile with altitude from point and continuous measurements at location C.

CO CONCENTRATION

The measured CO concentrations against altitude at locations A, B and C can respectively be found in figure 4.96, figure 4.97 and figure 4.98.

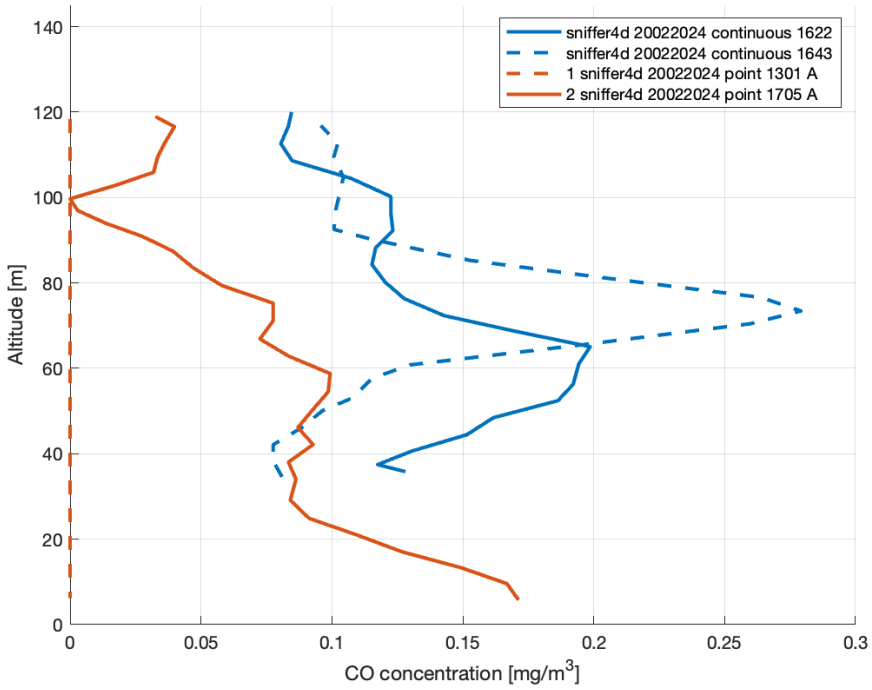

Figure 4.96: Comparison of CO profile with altitude from point and continuous measurements at location A.

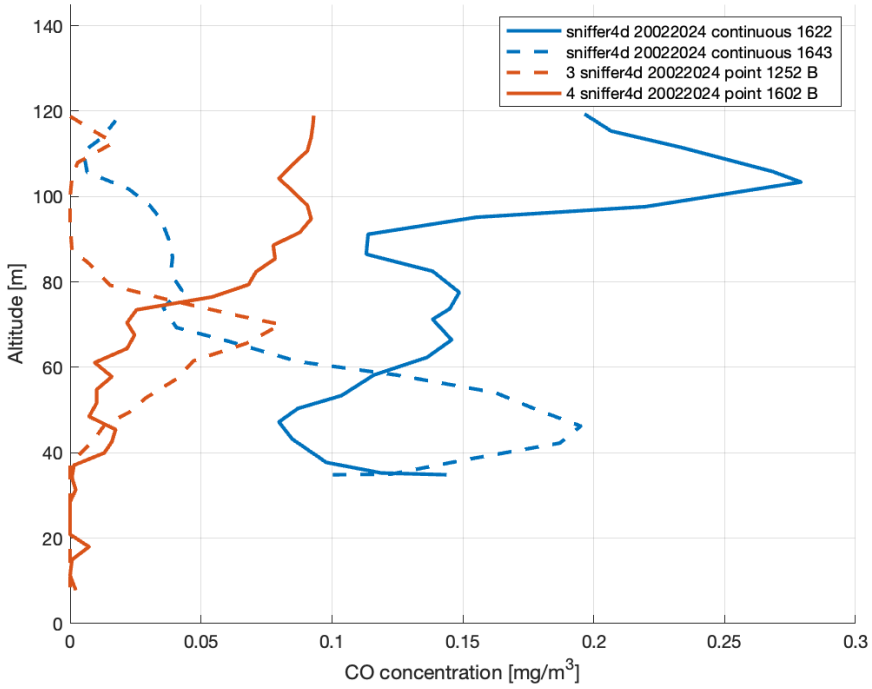

Figure 4.97: Comparison of CO profile with altitude from point and continuous measurements at location B.

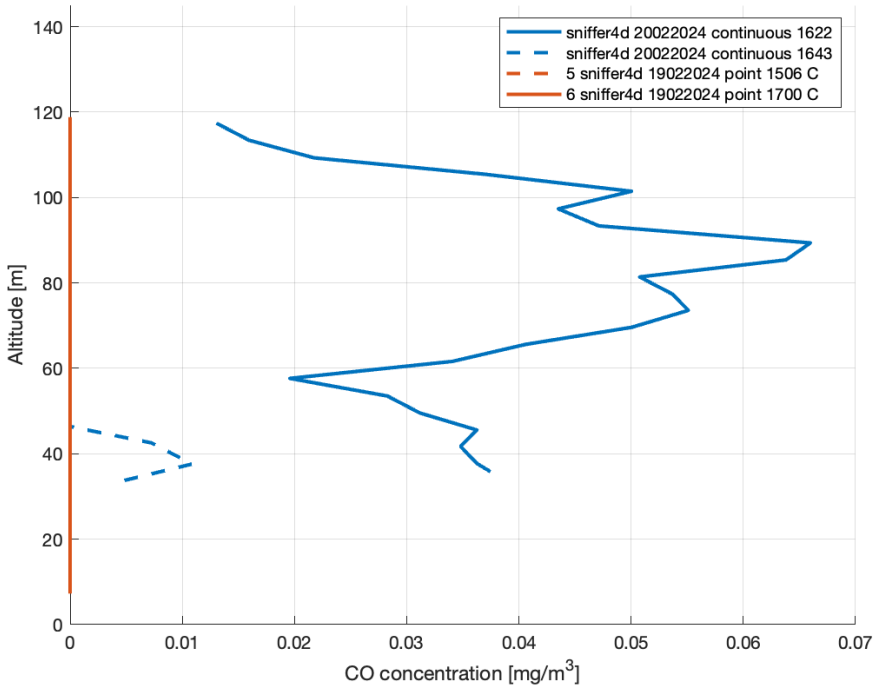

Figure 4.98: Comparison of CO profile with altitude from point and continuous measurements at location C.

At location A, we clearly see how the CO concentration decreases with altitude for the continuous data; this is similar to what was found for the point data. This trend is not found at location B; yet, because of the unstable temperature, no conclusion can be found. The data at location C is incomplete and can therefore not be compared.

NO_2 CONCENTRATION

The measured NO_2 concentrations against altitude at locations A, B and C can respectively be found in figure 4.99, figure 4.100 and figure 4.101.

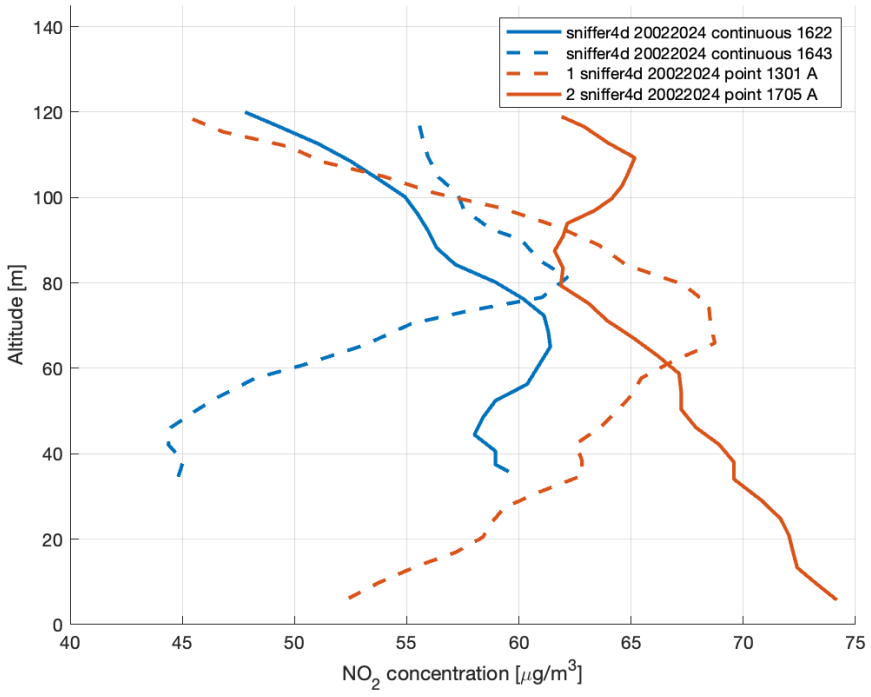

Figure 4.99: Comparison of NO_2 profile with altitude from point and continuous measurements at location A.

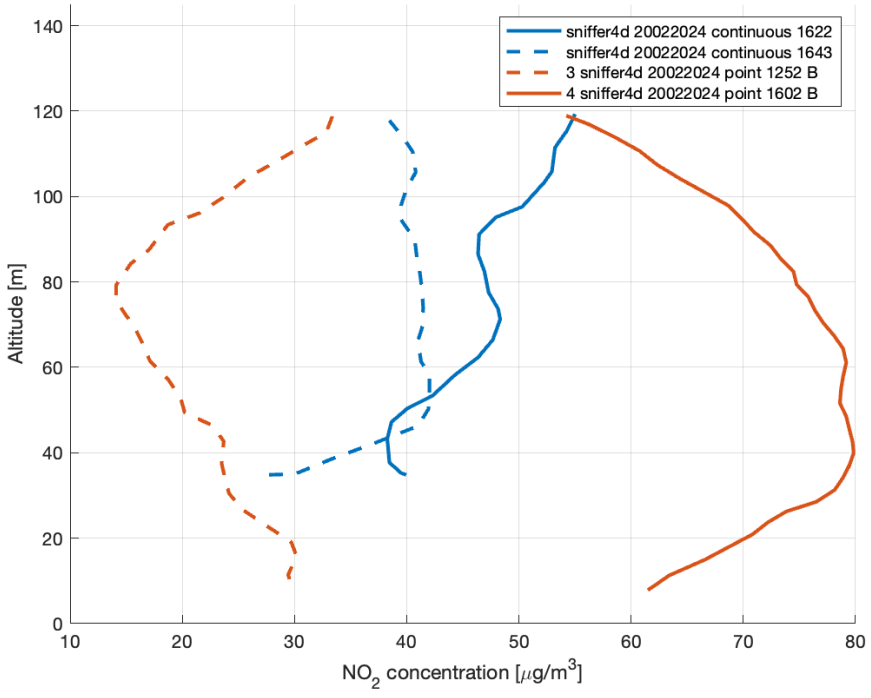

Figure 4.100: Comparison of NO_2 profile with altitude from point and continuous measurements at location B.

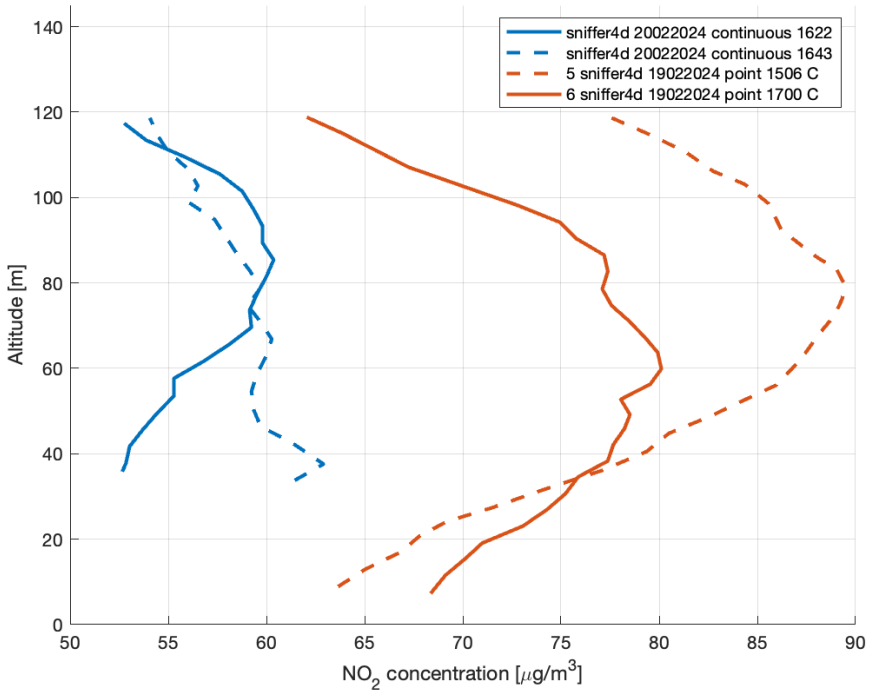

Figure 4.101: Comparison of NO_2 profile with altitude from point and continuous measurements at location C.

At location A, we find a decrease of NO_2 concentration with altitude, as this location is relatively close to the busy road. At location B, we see somewhat of an increase with altitude; however, as the continuous measurements start at this location, it could be that the temperature was not yet stabilised. At location C, we clearly see the non-linear trend with altitude which was also found in the point data. Note that location C is further away from the busy road, which indicates that the highest NO_2 concentration is not found near the ground.

O_3 CONCENTRATION

The measured O_3 concentrations against altitude at locations A, B and C can respectively be found in figure 4.102, figure 4.103 and figure 4.104.

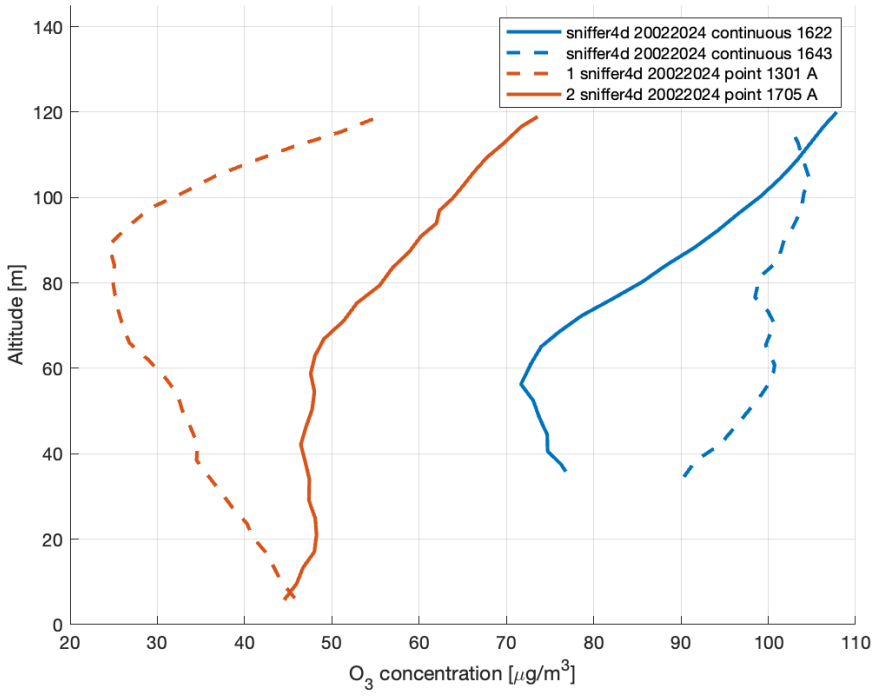

Figure 4.102: Comparison of O_3 profile with altitude from point and continuous measurements at location A.

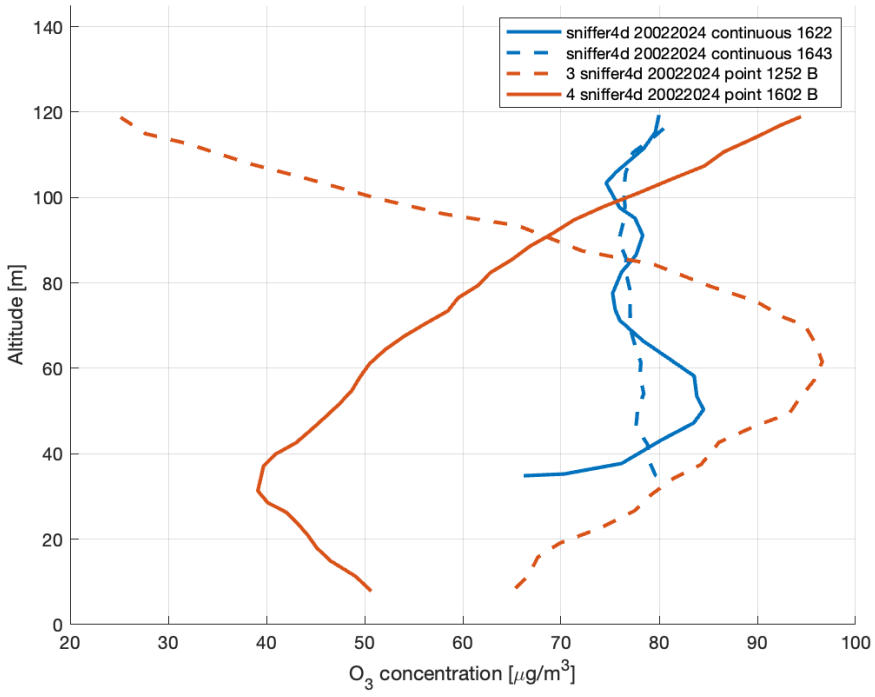

Figure 4.103: Comparison of O_3 profile with altitude from point and continuous measurements at location B.

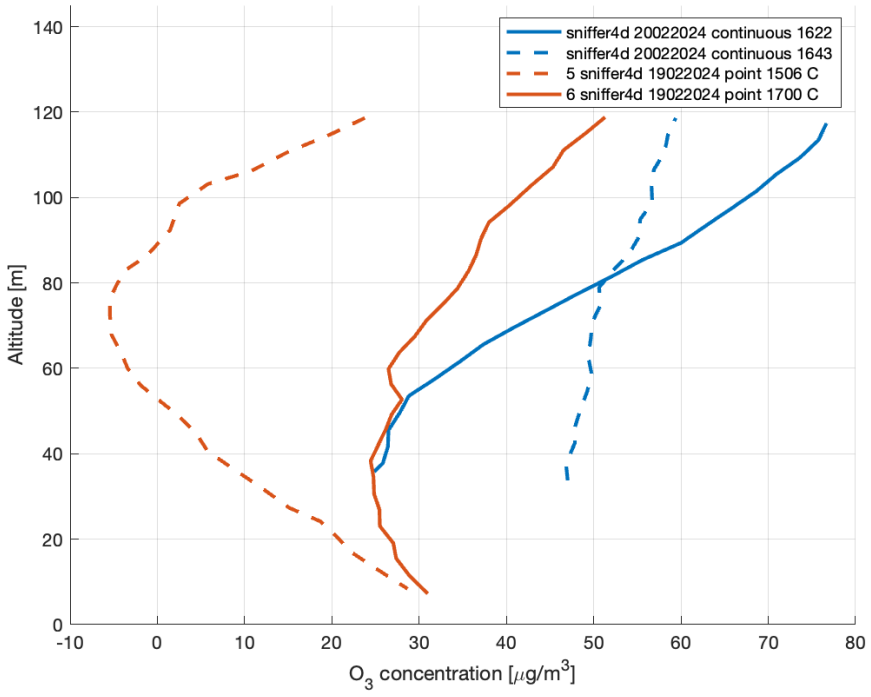

Figure 4.104: Comparison of O_3 profile with altitude from point and continuous measurements at location C.

At location A, the O_3 concentration of the point as well as continuous data shows an increase with altitude. at location B, the O_3 concentration from the continuous data is relatively constant with increasing altitude. This could again originate from the unstable temperature. At location C, we clearly see the increase of O_3 concentration with altitude for the point as well as continuous data.

SO_2 CONCENTRATION

The measured SO_2 concentrations against altitude at locations A, B and C can respectively be found in figure 4.105, figure 4.106 and figure 4.107.

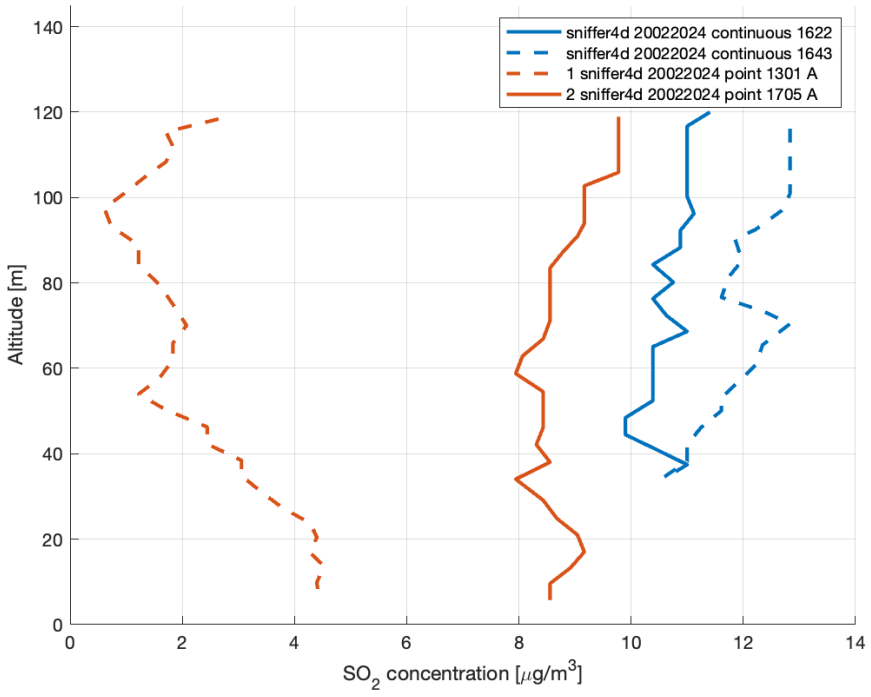

Figure 4.105: Comparison of SO_2 profile with altitude from point and continuous measurements at location A.

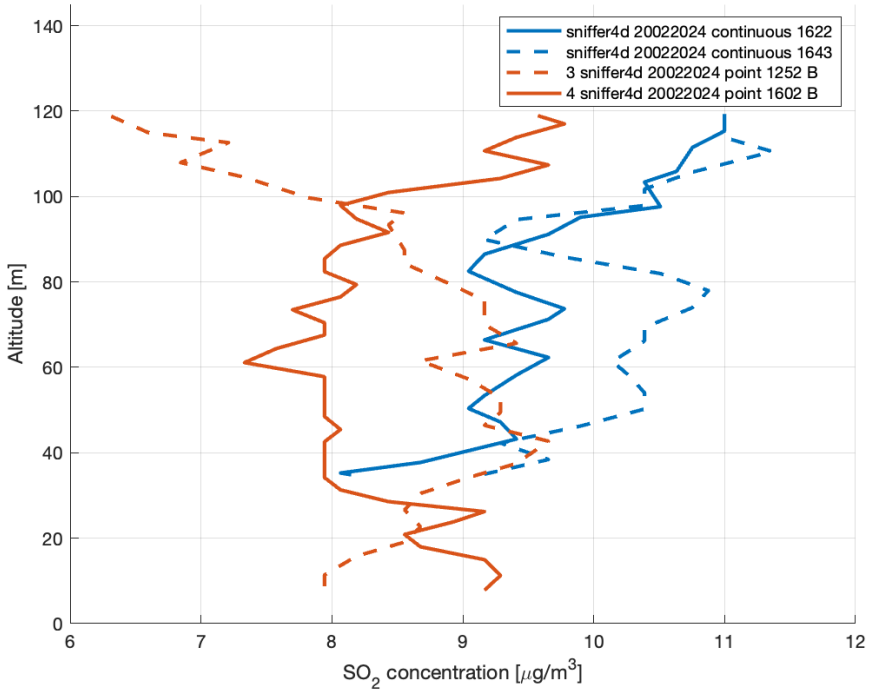

Figure 4.106: Comparison of SO_2 profile with altitude from point and continuous measurements at location B.

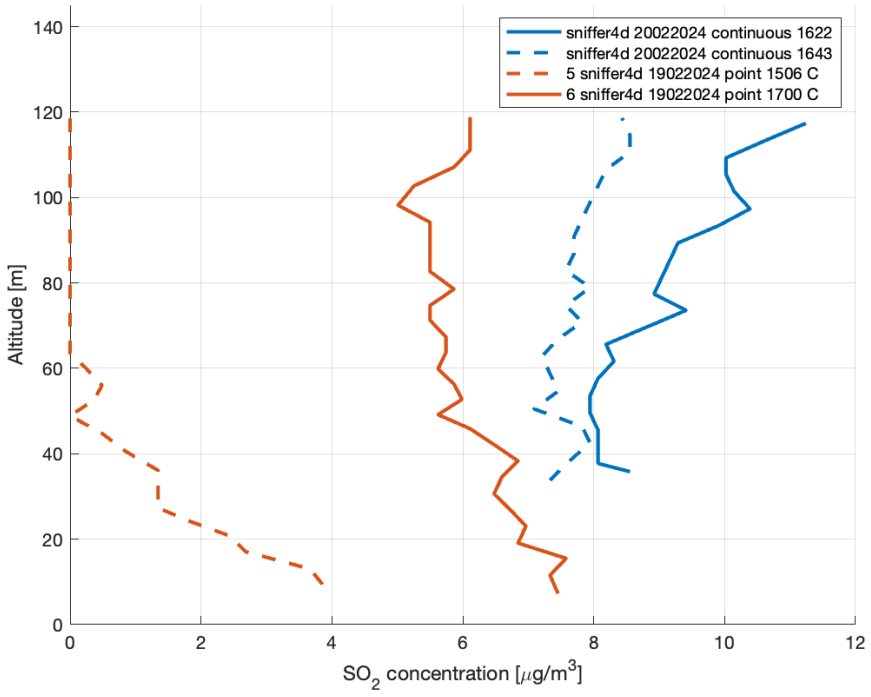

Figure 4.107: Comparison of SO_2 profile with altitude from point and continuous measurements at location C.

The SO_2 concentration decreases with the first 35 m of altitude. Since the measurements for the continuous data were carried out at a minimal altitude of 35 m, this effect cannot be found. After the first 35 m, the SO_2 concentration is quite constant. A slight increase can be found for some of the measurements. This increase is found for the continuous measurements as well. The point data does not fully match with the continuous data here, which might be the result of environmental factors such as wind.

$PM_{2.5}$ CONCENTRATION

The measured $PM_{2.5}$ concentrations against altitude at locations A, B and C can respectively be found in figure 4.108, figure 4.109 and figure 4.110.

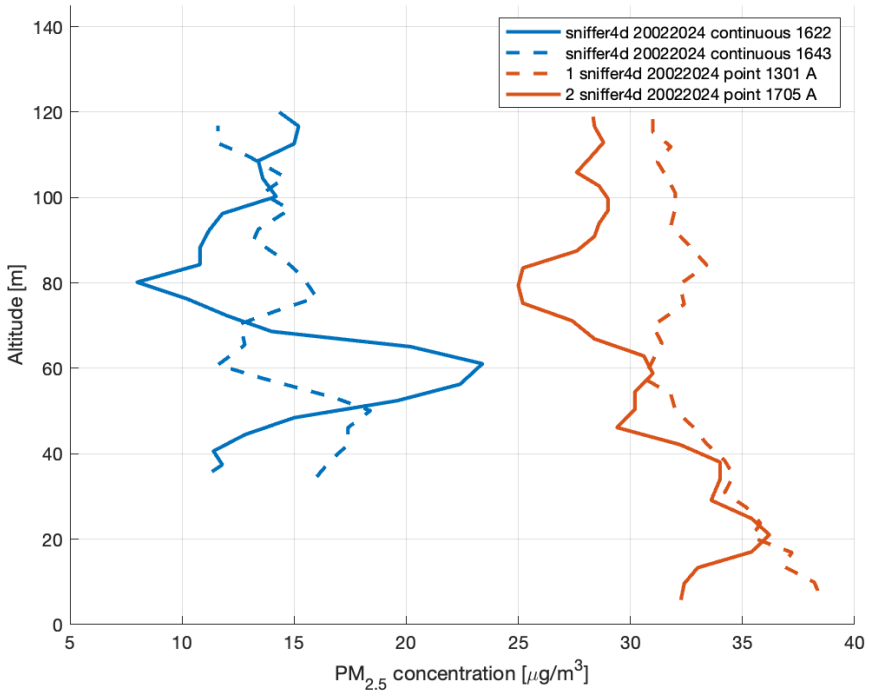

Figure 4.108: Comparison of $PM_{2.5}$ profile with altitude from point and continuous measurements at location A.

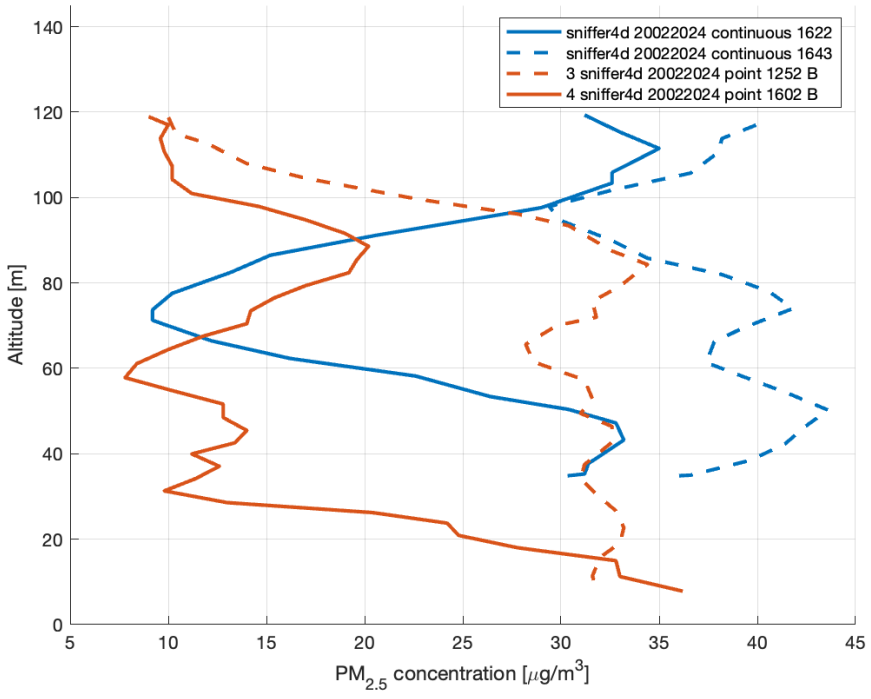

Figure 4.109: Comparison of $PM_{2.5}$ profile with altitude from point and continuous measurements at location B.

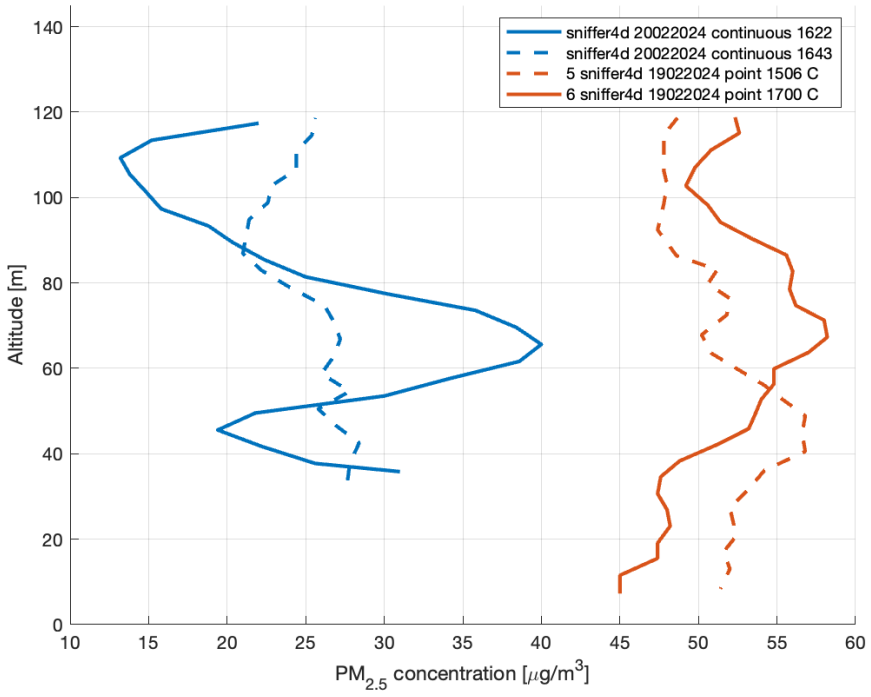

Figure 4.110: Comparison of $PM_{2.5}$ profile with altitude from point and continuous measurements at location C.

It was previously found that the $PM_{2.5}$ concentration has a high variability. It is quite constant with altitude. Sometimes, a slight increase or decrease can be found as a result of different environmental conditions. The continuous data shows the same as the point data; areas with higher concentration of $PM_{2.5}$ can be found, but no specific trend is found with increasing altitude. The results are similar for all locations.

PM_{10} CONCENTRATION

The measured PM_{10} concentrations against altitude at locations A, B and C can respectively be found in figure 4.111, figure 4.112 and figure 4.113.

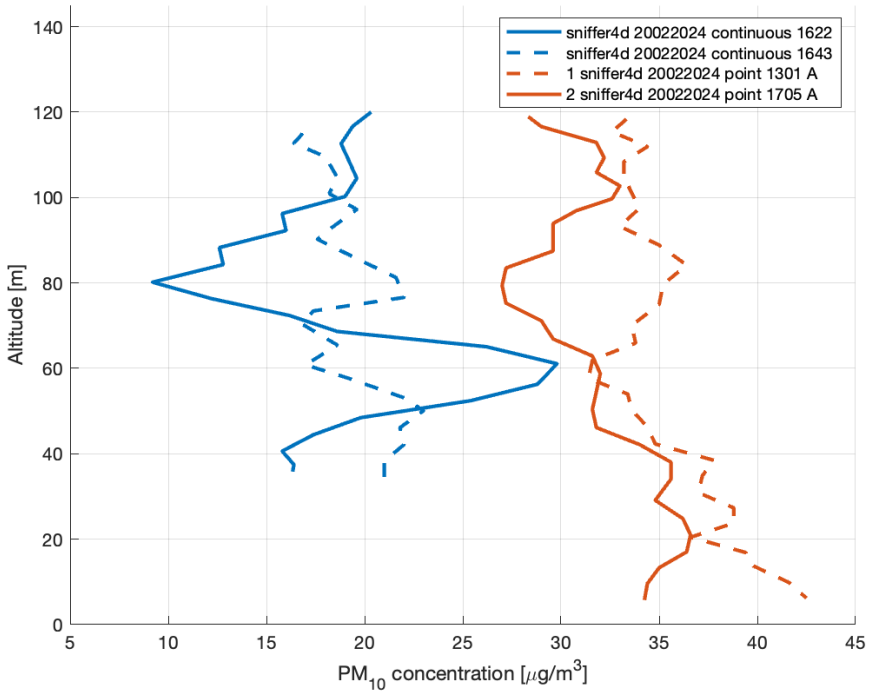

Figure 4.111: Comparison of PM_{10} profile with altitude from point and continuous measurements at location A.

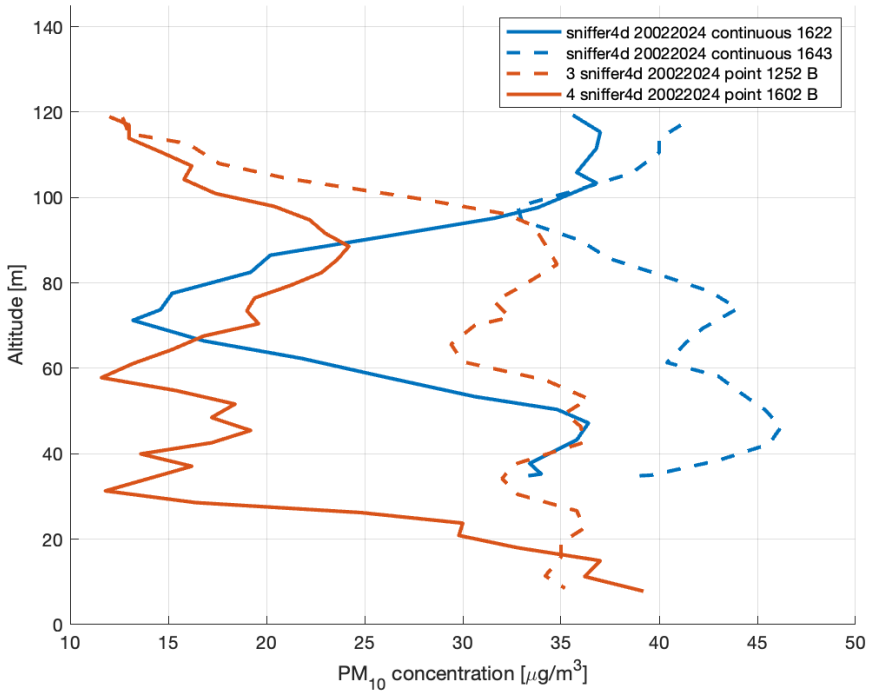

Figure 4.112: Comparison of PM_{10} profile with altitude from point and continuous measurements at location B.

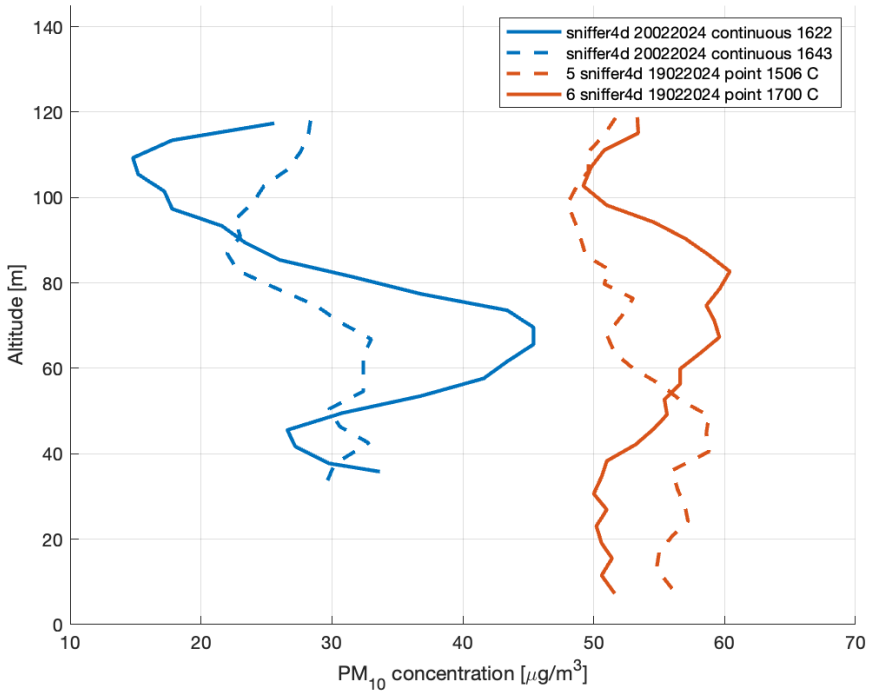

Figure 4.113: Comparison of PM_{10} profile with altitude from point and continuous measurements at location C.

The PM_{10} concentration trends are similar to the $PM_{2.5}$ ones. With an increase in altitude, there tends to be high variability. Yet, no specific trend can be found; it is overall quite constant with increasing altitude. The conclusion of the continuous data is in line with the one from the point data.

4.3.4. MAY VERSUS FEBRUARY MEASUREMENTS

Between the 14th and 16th of May 2024, a soundwalk experiment was conducted for the ImAFUSA project on drone noise. Measurements were carried out between 10.00 and 17.30. The same setup as in the February measurements was used, which consists of the DJI Mavic 3 Enterprise and Sniffer4D Mini 2. We thus also obtained new air quality data. The experiment was conducted in the same park as in February; therefore, we can look at the differences in air quality between May and February.

For the soundwalk experiment, the drone took off at one location, hovered here at a selected altitude (between 10 and 30 m), flew horizontally with a speed of circa 2 m/s to another point, hovered for some more time, and landed. Because of the sensitivity of the sensors to variation in temperature, we look at the measured concentrations when the drone is hovering. Moreover, if the temperature was still stabilising at the start of the hovering, this part is excluded.

We compare the mean air pollutant concentrations obtained from all measurements taken in February to those taken in May, within an altitude range of 10-30 m. Due to the limited number of measurements available in May, we make no distinction between time of day, location measured at and altitude. The range of the means of the individual measurements has been included as well to further analyse the differences in air pollutant concentrations between February of May. Finally, based on the earlier conducted data research in section 4.1, we include expectations on differences in air pollutant concentrations from local air quality monitoring stations in Athens.

	Expectation from monitoring stations	February measurements	May measurements
Temperature mean (range) [°C]	-	9 (7-10)	17 (14-20)
CO concentration mean (range) [mg/m^3]	May concentration ≈ **0.6** * February concentration	0.01 (0-0.12)	0.04 (0-0.18)
NO_2 concentration mean (range) [µg/m^3]	May concentration ≈ **1.0** * February concentration	66 (43-80)	45 (1-93)
O_3 concentration mean (range) [µg/m^3]	May concentration ≈ **1.8** * February concentration	34 (1-66)	104 (68-168)
SO_2 concentration mean (range) [µg/m^3]	May concentration ≈ **1.0** * February concentration	6 (2-9)	9 (2-12)
$PM_{2.5}$ concentration mean (range) [µg/m^3]	May concentration ≈ **0.7** * February concentration	43 (20-61)	8 (0-23)
PM_{10} concentration mean (range) [µg/m^3]	May concentration ≈ **0.7** * February concentration	46 (25-65)	9 (1-25)

Table 4.9: Comparison of average concentrations from February and May measurements. Range has been indicated between brackets.

The measured temperature is significantly higher in May compared to the one measured in February. For the CO concentration, no clear difference is found between the February and May concentrations. This is likely caused by the offset of the CO sensor, resulting in readings often being zero. From the local monitoring stations, a decrease was expected in May compared to February.

No significant differences between the two months can be found for the NO_2 and SO_2 concentrations, which was also expected from the earlier conducted data research. The measured NO_2 concentration is on average higher in February than May, but this can also be caused by other environmental conditions.

A strong increase is found in the O_3 concentration of May, compared to the one from February. This increase was expected from the data research, although in the actual sensor readings it is even higher. Environmental conditions could again play a role here. The significant difference found can be explained by the increased presence of sunlight in May.

Both measured $PM_{2.5}$ and PM_{10} concentrations are significantly lower in May than in February. A decrease was expected from the data research; moreover, the decrease found in the measurements is higher than the expected decrease from the data research. This decrease is likely caused by a decrease in heating and thus biomass burning. Moreover, meteorological conditions (such as temperature inversions) can have an effect here. Again, part of the difference found can be explained by other environmental conditions which changed during the measurements in February and May.

4.4. ENVIRONMENTAL IMPACT

Since most UAM configurations that are being developed nowadays have a full electric power train [16], there will be no direct emissions. However, one should not forget the indirect emissions, due to usage of electricity and its full life cycle: from production to recycling.

As mentioned by Koiwanit et al. [17], a Life Cycle Assessment (LCA) can help to identify the full environmental impact of an UAM configuration. It is used to investigate how sustainable the whole life cycle of a product is, from production to waste or recycling [48]. The most widely known LCA methods are EDIP97, Eco-indicator 99 and CLM2001 [49]; the last one has been used previously to identify the environmental impact of an UAM configuration [17].

A factor typically typically not included in a LCA analysis is noise. Acceptance of UAM is limited because of its noise profile, which is different to traditional aircraft [50]. Afonso et al. [51] showed that noise increases with an increasing MTOW of drones. Drones with a smaller MTOW typically have a higher frequency noise.

As part of our research, we looked at the environmental impact resulting from energy usage for a case of monitoring air quality with a drone. A full noise analysis or LCA has not been included in the scope of this research.

This environmental impact is calculated in different steps. Firstly, a use case is developed for measuring air quality with drones. Secondly, the route flown by the drone is determined. Thirdly, the required energy is calculated. Finally, the required energy is translated to environmental impact based on how the energy is produced.

We assume that we want to monitor the air quality in Aigaleo (Athens), where the measurements of the earlier discussed research took place. The total area of Aigaleo is 6 km^2, about 3 x 2 km. A horizontal resolution of 50 m is assumed, taken from the continuous measurements of the experiment conducted. We assume that we want to measure between 4 and 120 m altitude (116 m vertical range). A horizontal and vertical flight speed of respectively 3.0 and 0.5 m/s are used. It is assumed that the whole area is monitored twice a day for one year, equal to 730 repetitions.

The flight path is determined based on an approach by Zhao et al. [3], which optimises the flight time to reduce battery consumption. An example of this flight path can be found in figure 4.114. In horizontal and vertical direction respectively 85 000 and 197 200 m will be flown, equalling about 472 and 4 108 minutes of flight time. The combined flight time is 4 581 minutes.

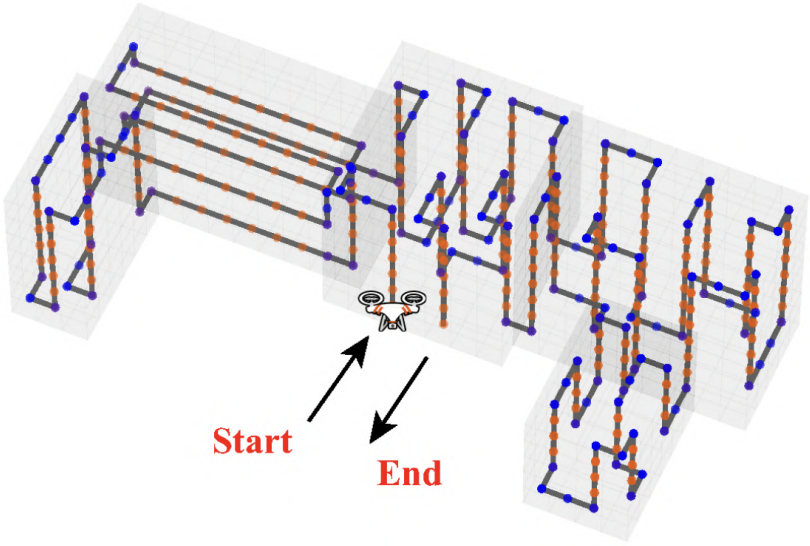

Figure 4.114: Optimised trajectory according to Zhao et al. [3].

The DJI Mavic 3 Enterprise with the Sniffer4D Mini 2 placed on top of it can fly 21 minutes [35]. Since one battery has a capacity of 77 Wh [52], we find that the energy per minute of this configuration is 3.67 W. The

energy consumption per repetition and in total are therefore respectively 17 and 12 260 kWh.

As a final step, we can translate this energy consumption into environmental impact, as can be found in table 4.10. The emissions per kWh have been calculated by Pei et al. [44] for the energy production of Greece. One remark is that the latest information available was from 2017 and it is likely the mix of energy production has changed since. Most likely, the environmental impact will be reduced for the current mix of energy production. A total emission of 8 543 kg $CO_{2,e}$ is found, which should definitely be considered when one wants to employ drones for air quality monitoring.

	Emission [g/kWh]	**Total emission [kg]**
CO_2	694.3	8512.6
$CO_{2,e}$	696.8	8543.2
CH_4	0.02	0.2
NO_x	1.2	14.9
N_2O	0.007	0.1
SO_2	3.3	41.0
$PM_{2.5}$	0.06	0.7

Table 4.10: Overview with emissions per kWh and total emissions of the use case scenario.

BIBLIOGRAPHY

[1] "Google Earth." [Online]. Available: https://earth.google.com/web/@37.99336797,23.67656426,42.9613774a,537.40230848d,35y,7.35617687h,26.64313486t,0r/data=OgMKATA

[2] "KNMI - Meetmast Cabauw." [Online]. Available: https://www.knmi.nl/kennis-en-datacentrum/uitleg/meetmast-cabauw

[3] P. Zhao, Y. Yang, Y. Zhang, K. Bian, L. Song, P. Qiao, and Z. Li, "Optimal Trajectory Planning of Drones for 3D Mobile Sensing," in *IEEE Glob. Commun. Conf., GLOBECOM - Proc.* Institute of Electrical and Electronics Engineers Inc., 2018, journal Abbreviation: IEEE Glob. Commun. Conf., GLOBECOM - Proc. [Online]. Available: https://www.scopus.com/inward/record.uri?eid=2-s2.0-85063518087&doi=10.1109%2fGLOCOM.2018.8647796&partnerID=40&md5=1192d25845c7935f3efeb21407f6c322

[4] "European Air Quality Index — European Environment Agency." [Online]. Available: https://www.eea.europa.eu/themes/air/air-quality-index/index

[5] "Air Pollution: How We're Changing the Air | Center for Science Education." [Online]. Available: https://scied.ucar.edu/learning-zone/air-quality/air-pollution

[6] P. Monks, C. Granier, S. Fuzzi, A. Stohl, M. Williams, H. Akimoto, M. Amann, A. Baklanov, U. Baltensperger, I. Bey, N. Blake, R. Blake, K. Carslaw, O. Cooper, F. Dentener, D. Fowler, E. Fragkou, G. Frost, S. Generoso, P. Ginoux, V. Grewe, A. Guenther, H. Hansson, S. Henne, J. Hjorth, A. Hofzumahaus, H. Huntrieser, I. Isaksen, M. Jenkin, J. Kaiser, M. Kanakidou, Z. Klimont, M. Kulmala, P. Laj, M. Lawrence, J. Lee, C. Liousse, M. Maione, G. McFiggans, A. Metzger, A. Mieville, N. Moussiopoulos, J. Orlando, C. O'Dowd, P. Palmer, D. Parrish, A. Petzold, U. Platt, U. Pöschl, A. Prévôt, C. Reeves, S. Reimann, Y. Rudich, K. Sellegri, R. Steinbrecher, D. Simpson, H. ten Brink, J. Theloke, G. van der Werf, R. Vautard, V. Vestreng, C. Vlachokostas, and R. von Glasow, "Atmospheric composition change - global and regional air quality," *Atmospheric Environment*, vol. 43, no. 33, pp. 5268–5350, 2009. [Online]. Available: https://www.scopus.com/inward/record.uri?eid=2-s2.0-70350036275&doi=10.1016%2fj.atmosenv.2009.08.021&partnerID=40&md5=657e6e54d7f5ade687941965f3f2b28a

[7] "Air pollution." [Online]. Available: https://www.eea.europa.eu/en/topics/in-depth/air-pollution

[8] J. Jońca, M. Pawnuk, Y. Bezyk, A. Arsen, and I. Sówka, "Drone-Assisted Monitoring of Atmospheric Pollution—A Comprehensive Review," *Sustainability (Switzerland)*, vol. 14, no. 18, 2022, publisher: MDPI. [Online]. Available: https://www.scopus.com/inward/record.uri?eid=2-s2.0-85138963579&doi=10.3390%2fsu141811516&partnerID=40&md5=da741969ab37421e637e0855d82a7400

[9] T. Zheng, B. Li, X.-B. Li, Z. Wang, S.-Y. Li, and Z.-R. Peng, "Vertical and horizontal distributions of traffic-related pollutants beside an urban arterial road based on unmanned aerial vehicle observations," *Building and Environment*, vol. 187, 2021, publisher: Elsevier Ltd. [Online]. Available: https://www.scopus.com/inward/record.uri?eid=2-s2.0-85094326874&doi=10.1016%2fj.buildenv.2020.107401&partnerID=40&md5=09276e523cde87a51f241eed3f9cd7a9

[10] A. Samad, D. Florez, I. Chourdakis, and U. Vogt, "Concept of Using an Unmanned Aerial Vehicle (UAV) for 3D Investigation of Air Quality in the Atmosphere—Example of Measurements near a Roadside," *Atmosphere*, vol. 13, no. 5, 2022, publisher: MDPI. [Online]. Available: https://www.scopus.com/inward/record.uri?eid=2-s2.0-85129403049&doi=10.3390%2fatmos13050663&partnerID=40&md5=6de3f19dccddfb26855ae9681cfd990b

[11] N. Motlagh, M. Irjala, A. Zuniga, E. Lagerspetz, V. Rantala, H. Flores, P. Nurmi, and S. Tarkoma, "Toward Blue Skies: City-Scale Air Pollution Monitoring Using UAVs," *IEEE Consumer Electronics Magazine*, vol. 12, no. 1, pp. 21–31, 2023, publisher: Institute of Electrical and Electronics Engineers Inc. [Online]. Available: https://www.scopus.com/inward/record.uri?eid=2-s2.0-85128631925&doi=10.1109%2fMCE.2022.3167800&partnerID=40&md5=d8294c2ced98908afc8fddaa75e4dc53

[12] M. Marinov, I. Topalov, B. Ganev, E. Gieva, and V. Galabov, "UAVs based particulate matter pollution monitoring," in *Int. Sci. Conf. Electron., ET - Proc.* Institute of Electrical and Electronics Engineers Inc., 2019, journal Abbreviation: Int. Sci. Conf. Electron., ET - Proc. [Online]. Available: https://www.scopus.com/inward/record.uri?eid=2-s2.0-85074953930&doi=10.1109%2fET.2019.8878586&partnerID=40&md5=e4e79b20fb451c4c828937475beb8f73

[13] C. Li, M. Liu, Y. Hu, H. Wang, Z. Xiong, W. Wu, C. Liu, C. Zhang, and Y. Du, "Investigating the vertical distribution patterns of urban air pollution based on unmanned aerial vehicle gradient monitoring," *Sustainable Cities and Society*, vol. 86, 2022, publisher: Elsevier Ltd. [Online]. Available: https://www.scopus.com/inward/record.uri?eid=2-s2.0-85136593580&doi=10.1016%2fj.scs.2022.104144&partnerID=40&md5=725dd64daaede8359888fabe3ab75a14

[14] C. Miao, A. Cui, Z. Xiong, Y. Hu, W. Chen, and X. He, "Vertical evaluation of air quality improvement by urban forest using unmanned aerial vehicles," *Frontiers in Ecology and Evolution*, vol. 10, 2022, publisher: Frontiers Media S.A. [Online]. Available: https://www.scopus.com/inward/record.uri?eid=2-s2.0-85142743811&doi=10.3389%2ffevo.2022.1045937&partnerID=40&md5=952a7c25437c8a7cc101f433caf9061c

[15] A. Chodorek, R. Chodorek, and A. Yastrebov, "The Prototype Monitoring System for Pollution Sensing and Online Visualization with the Use of a UAV and a WebRTC-Based Platform," *Sensors*, vol. 22, no. 4, 2022, publisher: MDPI. [Online]. Available: https://www.scopus.com/inward/record.uri?eid=2-s2.0-85125385838&doi=10.3390%2fs22041578&partnerID=40&md5=84c1d1ffc99d077e468e7e645d5af1c0

[16] "Study on the societal acceptance of Urban Air Mobility in Europe," McKinsey & Company, Tech. Rep., May 2021, carried out for European Union Aviation Safety Agency.

[17] J. Koiwanit, "Analysis of environmental impacts of drone delivery on an online shopping system," *Advances in Climate Change Research*, vol. 9, no. 3, pp. 201–207, 2018, publisher: National Climate Center. [Online]. Available: https://www.scopus.com/inward/record.uri?eid=2-s2.0-85054356420&doi=10.1016%2fj.accre.2018.09.001&partnerID=40&md5=eb62a99ec6c48d9e1015690e8f2fed1d

[18] S. Kim, T. Kim, K. Suh, and J. Jeon, "Energy and environmental performance of a passenger drone for an urban air mobility (UAM) policy with 3D spatial information in Seoul," *Journal of Cleaner Production*, vol. 415, p. 137683, Aug. 2023. [Online]. Available: https://www.sciencedirect.com/science/article/pii/S0959652623018413

[19] "Home | ImAFUSA - Impact and Capacity Assessment Framework for U-space Societal Acceptance." [Online]. Available: https://www.imafusa-sesar.eu/

[20] P. Sicard, E. Agathokleous, S. C. Anenberg, A. De Marco, E. Paoletti, and V. Calatayud, "Trends in urban air pollution over the last two decades: A global perspective," *Science of The Total Environment*, vol. 858, p. 160064, Feb. 2023. [Online]. Available: https://www.sciencedirect.com/science/article/pii/S0048969722071649

[21] M. Czarnecka and J. Nidzgorska-Lencewicz, "Impact of weather conditions on winter and summer air quality," *International Agrophysics*, vol. 25, no. 1, pp. 7–12, 2011. [Online]. Available: https://www.scopus.com/inward/record.uri?eid=2-s2.0-79952292126&partnerID=40&md5=f8f703329be34fe1b68be9727dbd2fe4

[22] "Ambient (outdoor) air pollution." [Online]. Available: https://www.who.int/news-room/fact-sheets/detail/ambient-(outdoor)-air-quality-and-health

[23] "Carbon monoxide | RIVM." [Online]. Available: https://www.rivm.nl/en/who-collaborating-centre-for-tobacco-product-regulation-and-control/fields-of-expertise/tobacco-contents-and-emissions/harmful-substances-in-tobacco-smoke/carbon-monoxide

[24] S. M. S. Nagendra, U. Schlink, A. Müller, and M. Khare, "Introduction to Urban Air Pollution," in *Urban air quality monitoring, modelling and human exposure assessment*, ser. Springer Transactions in Civil and Environmental Engineering, 2363-7641. Singapore: Springer, 2021, pp. 3–11. [Online]. Available: http://public.eblib.com/choice/PublicFullRecord.aspx?p=6357252

[25] I. Dedoussi, "Aircraft emissions and climate effects: Lecture 9," Mar. 2023.

[26] R. Cichowicz and M. Dobrzański, "Modeling pollutant emissions: Influence of two heat and power plants on urban air quality," *Energies*, vol. 14, no. 17, 2021, publisher: MDPI AG. [Online]. Available: https://www.scopus.com/inward/record.uri?eid=2-s2.0-85113889944&doi=10.3390%2fen14175218&partnerID=40&md5=ff02d60314b904b2b188c2cbd18423f4

[27] N. Motlagh, P. Kortoci, X. Su, L. Loven, H. Hoel, S. Haugsvaer, V. Srivastava, C. Gulbrandsen, P. Nurmi, and S. Tarkoma, "Unmanned Aerial Vehicles for Air Pollution Monitoring: A survey," *IEEE Internet of Things Journal*, pp. 1–1, 2023, publisher: Institute of Electrical and Electronics Engineers Inc. [Online]. Available: https://www.scopus.com/inward/record.uri?eid=2-s2.0-85163555231&doi=10.1109%2fJIOT.2023.3290508&partnerID=40&md5=bcfd456d86e76dec0d732252694b9bb0

[28] R. Cichowicz and M. Dobrzanski, "3D spatial analysis of particulate matter (PM_{10}, $PM_{2.5}$ and $PM_{1.0}$) and gaseous pollutants (H_2S, SO_2 and VOC) in urban areas surrounding a large heat and power plant," *Energies*, vol. 14, no. 14, 2021, publisher: MDPI AG. [Online]. Available: https://www.scopus.com/inward/record.uri?eid=2-s2.0-85110859631&doi=10.3390%2fen14144070&partnerID=40&md5=44831aed351c47aea6bbd4b95b17e2e8

[29] M. Gratsea, E. Liakakou, N. Mihalopoulos, A. Adamopoulos, E. Tsilibari, and E. Gerasopoulos, "The combined effect of reduced fossil fuel consumption and increasing biomass combustion on Athens' air quality, as inferred from long term CO measurements," *Science of the Total Environment*, vol. 592, pp. 115–123, 2017, publisher: Elsevier B.V. [Online]. Available: https://www.scopus.com/inward/record.uri?eid=2-s2.0-85015698472&doi=10.1016%2fj.scitotenv.2017.03.045&partnerID=40&md5=ba008c64b722692abeb5de5421faf780

[30] G. Grivas, E. Athanasopoulou, A. Kakouri, J. Bailey, E. Liakakou, I. Stavroulas, P. Kalkavouras, A. Bougiatioti, D. Kaskaoutis, M. Ramonet, N. Mihalopoulos, and E. Gerasopoulos, "Integrating in situ Measurements and City Scale Modelling to Assess the COVID–19 Lockdown Effects on Emissions and Air Quality in Athens, Greece," *Atmosphere*, vol. 11, no. 11, 2020, publisher: MDPI AG. [Online]. Available: https://www.scopus.com/inward/record.uri?eid=2-s2.0-85095975193&doi=10.3390%2fatmos11111174&partnerID=40&md5=6e16d1ae08e197ebbf38320b62375377

[31] A. Valavanidis, T. Vlachogianni, S. Loridas, and C. Fiotakis, "Atmospheric Pollution in Urban Areas of Greece and Economic Crisis. Trends in Air Quality and Atmospheric Pollution Data, Research and Adverse Health Effects," vol. 1, pp. 1–27, Nov. 2015. [Online]. Available: https://www.researchgate.net/publication/284415702_Atmospheric_Pollution_in_Urban_Areas_of_Greece_and_Economic_Crisis_Trends_in_Air_Quality_and_Atmospheric_Pollution_Data_Research_and_Adverse_Health_Effects

[32] E. Diapouli, M. Manousakas, S. Vratolis, V. Vasilatou, T. Maggos, D. Saraga, T. Grigoratos, G. Argyropoulos, D. Voutsa, C. Samara, and K. Eleftheriadis, "Evolution of air pollution source contributions over one decade, derived by PM_{10} and $PM_{2.5}$ source apportionment in two metropolitan urban areas in Greece," *Atmospheric Environment*, vol. 164, pp. 416–430, 2017, publisher: Elsevier Ltd. [Online]. Available: https://www.scopus.com/inward/record.uri?eid=2-s2.0-85020860322&doi=10.1016%2fj.atmosenv.2017.06.016&partnerID=40&md5=0f93614d15d885d8d7b9bd4d706c7da0

[33] M. Haugen, S. Gkantonas, I. El Helou, R. Pathania, E. Mastorakos, and A. Boies, "Measurements and modelling of the three-dimensional near-field dispersion of particulate matter emitted from passenger ships in a port environment," *Atmospheric Environment*, vol. 290, 2022, publisher: Elsevier Ltd. [Online]. Available: https://www.scopus.com/inward/record.uri?eid=2-s2.0-85138121752&doi=10.1016%2fj.atmosenv.2022.119384&partnerID=40&md5=062ca041a048d76a5c8df3cb5df8286f

[34] S. M. S. Nagendra, U. Schlink, A. Müller, and M. Khare, "Air Quality Measuring Sensors," in *Urban air quality monitoring, modelling and human exposure assessment*, ser. Springer Transactions in Civil and Environmental Engineering, 2363-7641. Singapore: Springer, 2021, pp. 89–104. [Online]. Available: http://public.eblib.com/choice/PublicFullRecord.aspx?p=6357252

[35] Soarability, "Sniffer4D Mini 2 User Manual," Tech. Rep., Sep. 2023, v1.1 2023.01.09.

[36] "Products." [Online]. Available: https://www.alphasense.com/Products

[37] "Open Category - Low Risk - Civil Drones," Sep. 2022. [Online]. Available: https://www.easa.europa.eu/en/domains/civil-drones-rpas/open-category-civil-drones

[38] "Litchi for DJI Drones." [Online]. Available: https://flylitchi.com/

[39] H. Brantley, G. Hagler, E. Kimbrough, R. Williams, S. Mukerjee, and L. Neas, "Mobile air monitoring data-processing strategies and effects on spatial air pollution trends," *Atmospheric Measurement Techniques*, vol. 7, no. 7, pp. 2169–2183, 2014, publisher: Copernicus GmbH. [Online]. Available: https://www.scopus.com/inward/record.uri?eid=2-s2.0-84904596857&doi=10.5194%2famt-7-2169-2014&partnerID=40&md5=a8df238ce0cde5129a93028eaff9cf6c

[40] "Drone Data Management and Flight Analysis | Airdata UAV." [Online]. Available: https://airdata.com/

[41] R. Cichowicz and M. Dobrzański, "Spatial analysis (Measurements at heights of 10 m and 20 m above ground level) of the concentrations of particulate matter (PM_{10}, $PM_{2.5}$, and $PM_{1.0}$) and gaseous pollutants (H_2S) on the university campus: A case study," *Atmosphere*, vol. 12, no. 1, 2021, publisher: MDPI AG. [Online]. Available: https://www.scopus.com/inward/record.uri?eid=2-s2.0-85099451795&doi=10.3390%2fatmos12010062&partnerID=40&md5=26f44726d6247853613b41d38dd90388

[42] P. Singh and P. Verma, "A comparative study of spatial interpolation technique (IDW and Kriging) for determining groundwater quality," in *GIS and Geostatistical Techniques for Groundwater Science*. Elsevier, 2019, pp. 43–56, journal Abbreviation: GIS and Geostatistical Techniques for Groundwater Science. [Online]. Available: https://www.scopus.com/inward/record.uri?eid=2-s2.0-85075714671&doi=10.1016%2fB978-0-12-815413-7.00005-5&partnerID=40&md5=e9995f13ccd252a33e53a6e545cb6c7c

[43] A. Goodchild and J. Toy, "Delivery by drone: An evaluation of unmanned aerial vehicle technology in reducing CO_2 emissions in the delivery service industry," *Transportation Research Part D: Transport and Environment*, vol. 61, pp. 58–67, 2018, publisher: Elsevier Ltd. [Online]. Available: https://www.scopus.com/inward/record.uri?eid=2-s2.0-85019651961&doi=10.1016%2fj.trd.2017.02.017&partnerID=40&md5=9e152afa48b5573bfea2f4917479e9dc

[44] G. Pei, J. Buonocore, P. Salimifard, B. Sousa, L. Ferguson, and J. G. Allen, "Assessing the climate and health impacts of energy consumption in European Union countries," Jan. 2024.

[45] "Up-to-date air quality data — European Environment Agency." [Online]. Available: https://www.eea.europa.eu/data-and-maps/explore-interactive-maps/up-to-date-air-quality-data

[46] "Luchtmeetnet.nl." [Online]. Available: https://www.luchtmeetnet.nl/

[47] "Cross Validation (Geostatistical Analyst)—ArcGIS Pro | Documentation." [Online]. Available: https://pro.arcgis.com/en/pro-app/latest/tool-reference/geostatistical-analyst/cross-validation.htm

[48] S. Mitchell, J. Steinbach, T. Flanagan, P. Ghabezi, N. Harrison, S. O'Reilly, S. Killian, and W. Finnegan, "Evaluating the sustainability of lightweight drones for delivery: towards a suitable methodology for assessment," in *ECCM - Proc. Eur. Conf. Compos. Mater.: Compos. Meet Sustain.*, Vassilopoulos A.P. and Michaud V., Eds., vol. 6. Composite Construction Laboratory (CCLab), Ecole Polytechnique Federale de Lausanne (EPFL), 2022, pp. 355–362, journal Abbreviation: ECCM - Proc. Eur. Conf. Compos. Mater.: Compos. Meet Sustain. [Online]. Available: https://www.scopus.com/inward/record.uri?eid=2-s2.0-85149369372&partnerID=40&md5=d040af6b56d465599f873f29b339bdf4

[49] L. Dreyer, A. Niemann, and M. Hauschild, "Comparison of three different LCIA methods: EDIP97, CML2001 and eco-indicator 99: Does it matter which one you choose?" *International Journal of Life Cycle Assessment*, vol. 8, no. 4, pp. 191–200, 2003, publisher: Springer Verlag. [Online]. Available: https://www.scopus.com/inward/record.uri?eid=2-s2.0-0042707657&doi=10.1007%2fBF02978471&partnerID=40&md5=841280d7d1376ff2984b1c679d21edff

[50] A. Torija and C. Clark, "A psychoacoustic approach to building knowledge about human response to noise of unmanned aerial vehicles," *International Journal of Environmental Research and Public Health*, vol. 18, no. 2, pp. 1–16, 2021, publisher: MDPI AG. [Online]. Available: https://www.scopus.com/inward/record.uri?eid=2-s2.0-85099384719&doi=10.3390%2fijerph18020682&partnerID=40&md5=3be87f2d34e9893626466641cf3b32e6

[51] F. Afonso, A. Ferreira, I. Ribeiro, F. Lau, and A. Suleman, "On the design of environmentally sustainable aircraft for urban air mobility," *Transportation Research Part D: Transport and Environment*, vol. 91, 2021, publisher: Elsevier Ltd. [Online]. Available: https://www.scopus.com/inward/record.uri?eid=2-s2.0-85099631258&doi=10.1016%2fj.trd.2020.102688&partnerID=40&md5=4932a44d2c21b2b8132d45b2f0da87cf

[52] "Specs - DJI Mavic 3 Enterprise - DJI Enterprise." [Online]. Available: https://enterprise.dji.com/mavic-3-enterprise/photo